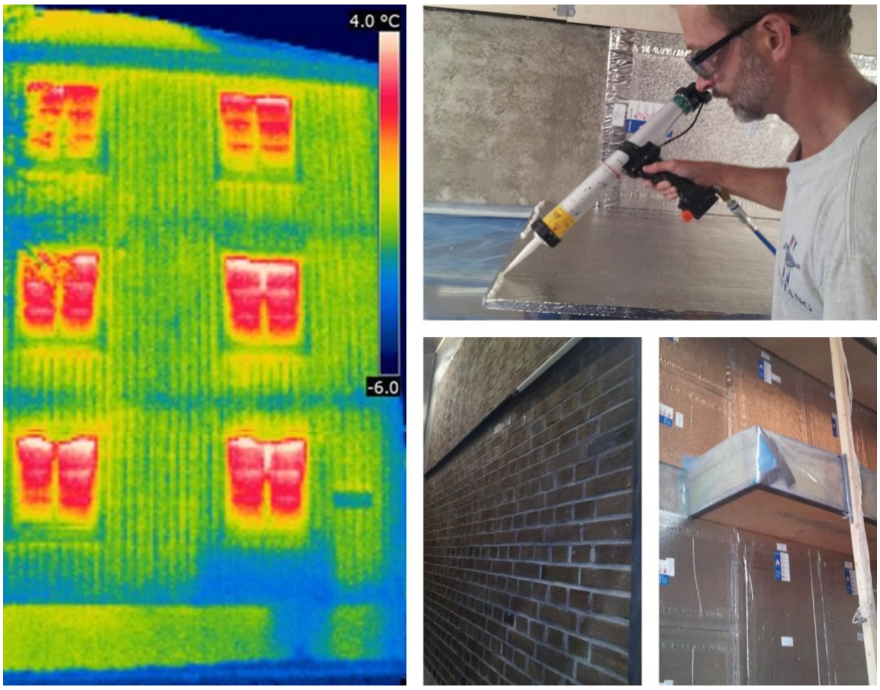

Building Retrofit using Vacuum Insulation Panels

Hygrothermal Performance and Durability

Thesis for the Degree of Doctor of Philosophy

PÄR JOHANSSON

Department of Civil and Environmental Engineering
CHALMERS UNIVERSITY OF TECHNOLOGY
Gothenburg, Sweden 2014

THESIS FOR THE DEGREE OF DOCTOR OF PHILOSOPHY

Building Retrofit using Vacuum Insulation Panels

Hygrothermal Performance and Durability

PÄR JOHANSSON

Department of Civil and Environmental Engineering

CHALMERS UNIVERSITY OF TECHNOLOGY

Gothenburg, Sweden 2014

Building Retrofit using Vacuum Insulation Panels
Hygrothermal Performance and Durability
PÄR JOHANSSON
ISBN 978-91-7385-976-9

Doktorsavhandlingar vid Chalmers tekniska högskola
Ny serie nr 3657
ISSN 0346-718X

Department of Civil and Environmental Engineering
Division of Building Technology, Building Physics
Chalmers University of Technology
SE-412 96 Gothenburg
Sweden
Telephone + 46 (0)31-772 1000

Cover:
Left: thermogram of the exterior wall of the field study building before retrofitted with vacuum insulation panels (VIPs) on the exterior (Chapter 4). Right: a brick wall built in the laboratory was covered by VIPs on the interior, glued to the surface, and investigated in a large-scale building envelope climate simulator (Chapter 5).

Chalmers Reproservice
Gothenburg, Sweden 2014

Building Retrofit using Vacuum Insulation Panels
Hygrothermal Performance and Durability
PÄR JOHANSSON
Department of Civil and Environmental Engineering
Division of Building Technology, Building Physics
Chalmers University of Technology

ABSTRACT

Many old buildings have unsatisfactory thermal performance compared to the standards of today. One way to increase the thermal performance is to add thermal insulation to the building envelope. However, many old buildings are listed and considered to be valuable for historical and esthetic reasons. This often limits the position and thickness of the additional insulation layer. Vacuum insulation panels (VIPs) present unprecedented possibilities to reduce the required thickness of the insulation layer. The aim of this work was to investigate the possibilities, limitations and risks when using VIPs in the walls of old buildings. A special focus was on the practical experiences, durability assessment and quality assurance of the VIPs from field studies. The thesis is divided into three themes where the first theme aims to investigate the applicability of the transient plane heat source (TPS) method as a tool for quality assurance of the VIPs. The conclusion is that the method is applicable in a laboratory, but the equipment is too large to perform field measurements. In the second theme, the exterior wall of a county governor's house was thermally insulated on the exterior with 20 mm thick VIPs. The calculated energy use for heating decreased with 24%. However, due to air and moisture diffusion into the VIPs, the energy use increases slightly during the service life. Temperature and relative humidity sensors were installed in the test wall and in a neighboring (non-retrofitted) wall as reference. It was concluded that the hygrothermal performance of the test wall was substantially better than of the reference wall. A deviation was found between the measured and numerically simulated relative humidity. Using numerical simulations, the deviation could be explained by air leakages in the wall. The third part of the thesis consists of a laboratory study where a brick wall with wooden beam ends was thermally insulated with VIPs on the interior. A parametric study was performed using hygrothermal numerical simulations to evaluate the influences by the climate, the thickness of the wall, and the properties of the brick and mortar on the moisture content in the wall. Based on these results, the wall was built and tested in a large-scale building envelope climate simulator. The wall was exposed to driving rain on the exterior surface and a temperature gradient. It was expected that the moisture content would increase in the wall with VIPs on the interior. However, the measurements showed that there was no significant difference between the cases with and without VIPs. Finally, it can be concluded that a substantial energy use reduction can be achieved when using VIPs in old buildings. With a careful design and construction process, the risk of damages to the old structure can be minimized.

Key words: listed building, retrofitting, exterior wall, vacuum insulation panel, transient plane heat source, measurement, numerical simulation, exterior insulation, interior insulation, brick wall, wooden beam ends, field study, laboratory

Renovering av byggnader med vakuumisoleringspaneler
Hygrotermisk prestanda och hållbarhet
PÄR JOHANSSON
Institutionen för bygg- och miljöteknik
Avdelningen för byggnadsteknologi, byggnadsfysik
Chalmers tekniska högskola

SAMMANFATTNING

Många äldre byggnader har en otillfredsställande energiprestanda jämfört med dagens normer. Ett sätt att minska energianvändningen är att tilläggisolera klimatskalet. Eftersom många av de gamla byggnaderna anses bevarandevärda för deras historiska och estetiska bidrag till stadsrummet, finns det ofta begränsningar i placeringen och tjockleken av isoleringsskiktet. Vakuumisoleringspaneler (VIP) ger stora möjligheter att minska den tjocklek som krävs för att minska byggnadens energianvändning. Syftet med detta arbete är att undersöka möjligheter, begränsningar och risker vid användandet av VIP i äldre byggnaders ytterväggar. Ett särskilt fokus riktas mot de praktiska erfarenheter, utvärderingar av beständighet och kvalitetssäkring som finns när det gäller användandet av VIP ifrån fältförsök. Avhandlingen är uppdelad i tre teman. I det första temat undersöktes användbarheten av metoden transient plane heat source (TPS) för kvalitetssäkring av VIP. Slutsatsen är att metoden är användbar i laboratorium men att utrustningen är för stor för att utföra mätningar i fält. I det andra temat isolerades en yttervägg i ett landshövdingehus med 20 mm tjock VIP på utsidan. Den beräknade energianvändningen för uppvärmning minskade med 24 %. På grund av att luft diffunderar in i VIP:arna ökar energianvändningen något under deras livslängd. Temperatur- och relativ fuktighetsmätare installerades i den tilläggsisolerade väggen och i en angränsande (oisolerad) referensvägg. Mätningarna visade att den hygrotermiska prestandan i den tilläggisolerade väggen var väsentligt bättre än i referensväggen. En avvikelse mellan den uppmätta och numeriskt simulerade relativa fuktigheten noterades vilken, genom numeriska simuleringar, kunde förklaras av luftläckage i väggen. Den tredje delen av avhandlingen handlar om en laboratoriestudie där en tegelvägg med träbalksändar tilläggsisoleras med VIP på insidan. En parameterstudie genomfördes där påverkan av klimatbelastningen, väggens tjocklek och egenskaperna på teglet och murbruket på väggens fuktinnehåll studerades genom hygrotermiska numeriska simuleringar. Baserat på dessa resultat byggdes muren och testades i en storskalig klimatskalssimulator. Det var förväntat att fuktinnehållet skulle öka när väggen tilläggsisolerades med VIP på insidan. Mätningarna visade dock ingen signifikant skillnad mellan fallen med och utan VIP. Slutligen kan konstateras att energianvändningen kan minskas substantiellt genom att använda VIP i gamla byggnader. Genom en genomtänkt design och varsamt genomförande kan risken för skador på den gamla konstruktionen minimeras.

Nyckelord: k-märkt, renovering, yttervägg, vakuumisoleringspanel, transient plane heat source, mätning, numerisk simulering, utvändig tilläggsisolering, invändig tilläggisolering, tegelvägg, träbalkar, fältförsök, laboratorium

PREFACE

The work presented in this thesis has been carried out at the Division of Building Technology, Department of Civil and Environmental Engineering at Chalmers University of Technology in Gothenburg, Sweden. The project has been financially supported by The Swedish Research Council Formas through the projects: Retrofit applications on old buildings using highly efficient novel thermal insulation materials (2009-1513) and Homes for tomorrow (2010-49).

The public housing corporation Familjebostäder i Göteborg AB contributed with a field study building and financed all material, measurement equipment and construction work. Without the fruitful cooperation and financial support from Familjebostäder this project could not have been realized to this extent. The financial support for travel expenses from the Adlerbert Research Foundation, Chalmersska forskningsfonden, Friends of Chalmers – Young Researchers, The Royal Society of Arts and Sciences in Gothenburg, Maj och Hilding Brosenius Forskningsstiftelse, and The Lars Hierta Memorial Foundation are also greatly appreciated.

The staff at the Laboratory of Building Science and Technology at Empa in Dübendorf, Switzerland, is thanked for making my visit there during January to March 2013 a memorable and pleasant experience. Especially Dr. Samuel Brunner and Dr. Karim Ghazi Wakili are thanked for making this visit possible.

The collaboration with the Norwegian University of Science and Technology (NTNU) and SINTEF Building and Infrastructure, in Trondheim, Norway, would not have been possible without the great assistance of Dr. Berit Time, Professor Bjørn Petter Jelle and Professor Stig Geving. Also, the staff in the laboratory in Trondheim is thanked for their helpfulness and positive spirit.

Last, but not least, I would like to thank all my colleagues at the Division of Building Technology for the encouraging and collaborative spirit which create an excellent working environment. A special thanks to my supervisors Professor Carl-Eric Hagentoft and Associate Professor Angela Sasic Kalagasidis who have inspired me with their cheerfulness and curiosity. I am also grateful to Dr. Simon Pallin, Senior Lecturer Bijan Adl-Zarrabi and Professor Johan Claesson for our positive and productive collaborations.

Pär Johansson

Gothenburg, February, 2014

LIST OF PUBLICATIONS

The thesis is a continuation on the licentiate thesis "Retrofitting of old Exterior Wall with Vacuum Insulation Panels: Measurements of Thermal Properties, Moisture Performance and Practical Considerations" (Lic 2012:2) and based on the following appended papers:

Theme 1: Quality assurance of VIPs, measurements of the thermal performance of VIPs using the transient plane heat source (TPS) method

I. Johansson, P., Adl-Zarrabi, B., and Hagentoft, C.-E. (2012). Using transient plane source sensor for determination of thermal properties of vacuum insulation panels. *Frontiers of Architectural Research*, *1*(4), 334-340.

II. Johansson, P. and Claesson, J. (2014). Analytical model to calculate the temperature increase in a low conductive material covered by a highly conductive layer. *Submitted to the 10th Nordic Symposium on Building Physics*. June 15-19, 2014, Lund, Sweden.

Theme 2: Exterior insulation of listed brick and wood building with VIPs, field measurements and hygrothermal numerical simulations.

III. Johansson, P. (2011). Assessment of the Risk for Mold Growth in a Wall Retrofitted with Vacuum Insulation Panels. *Proceedings of the 9th Nordic Symposium on Building Physics*. May 29-June 2, 2011, Tampere, Finland, pp. 349-356.

IV. Johansson, P., Kalagasidis, A. S., and Hagentoft, C.-E. (2014). Retrofitting of a listed brick and wood building using vacuum insulation panels on the exterior of the facade: Measurements and simulations. *Energy and Buildings*, *73*(April 2014), 92-104.

Theme 3: Interior insulation of brick buildings with VIPs, laboratory measurements and hygrothermal numerical simulations.

V. Johansson, P., Geving, S., Hagentoft, C.-E., Jelle, B. P., Rognvik, E., Sasic Kalagasidis, A., and Time, B. (2014). Interior insulation retrofit of a historical brick wall using vacuum insulation panels: Hygrothermal numerical simulations and laboratory investigations. *Submitted to Building and Environment*.

Paper I was written in cooperation with Bijan Adl-Zarrabi and Carl-Eric Hagentoft. Paper II was written by me. I did the numerical simulations and compared them to analytical solutions and my own TPS measurements. Johan Claesson developed the analytical solution presented and used in Paper II. He was also involved in the final editing of the paper.

Papers III and IV were written by me. Angela Sasic Kalagasidis provided input for which cases to simulate in Paper III. Angela Sasic Kalagasidis and Carl-Eric Hagentoft were involved in the final editing of both papers.

Papers V was written mainly by me. The hygrothermal numerical simulations were performed by me with input from Stig Geving, Carl-Eric Hagentoft, Angela Sasic Kalagasidis and Berit Time. The design of the experiment and test wall was decided based on discussions with all the co-authors. The laboratory measurements were performed in the laboratory of the Norwegian University of Science and Technology (NTNU) and SINTEF Building and Infrastructure in Trondheim, Norway, by Egil Rognvik, Øystein Holmberget and Ole Aunrønning. All co-authors were involved in the final editing of the papers.

Two reports with literature studies are important to the conclusions of this study but are not appended with the thesis:

i. Johansson, P. (2012). *Vacuum Insulation Panels in Buildings: Literature Review*. Report 2012:1. Gothenburg, Sweden: Chalmers University of Technology, Department of Civil and Environmental Engineering.

ii. Berge, A. and Johansson, P. (2012). *Literature Review of High Performance Thermal Insulation*. Report 2012:2. Gothenburg, Sweden: Chalmers University of Technology, Department of Civil and Environmental Engineering.

Other publications by the author are (in chronological order):

A. Johansson, P., Geving, S., Hagentoft, C.-E., Jelle, B. P., Rognvik, E., Sasic Kalagasidis, A., and Time, B. (2014). Retrofitting a brick wall using vacuum insulation panels: measured hygrothermal effect on the existing structure. *Accepted for publication in Proceedings of the 10th Nordic Symposium on Building Physics.* June 15-19, 2014, Lund, Sweden.

B. Johansson, P., Time, B., Geving, S., Jelle, B. P., Sasic Kalagasidis, A., Hagentoft, C.-E., and Rognvik, E. (2013). Interior Insulation Retrofit of a Brick Wall Using Vacuum Insulation Panels: Design of a Laboratory Study to Determine the Hygrothermal Effect on Existing Structure and Wooden Beam Ends. *Proceedings of the 12th International Conference on Thermal Performance of the Exterior Envelopes of Whole Buildings*. December 1-5, 2013, Clearwater Beach, Florida, USA.

C. Brunner, S., Wakili, K. G., and Johansson, P. (2013). Vacuum insulation panels (VIP) in refrigerator room, freezing room & fridge. *Proceedings of the 11th International Vacuum Insulation Symposium*. September 18-19, 2013, Dübendorf, Switzerland, pp. 25-26.

D. Johansson, P. (2012). Tilläggsisolering av gamla byggnader med vakuumisolering (Retrofitting of old buildings using vacuum insulation panels). [In Swedish]. *Bygg och teknik, 5/2012*, pp. 26-31.

E. Johansson, P., Adl-Zarrabi, B., and Hagentoft, C.-E. (2012). Using Transient Plane Source Sensor for Determination of Thermal Properties of Vacuum Insulation Panels. *Proceedings of the 5th International Building Physics Conference.* May 28-31, 2012, Kyoto, Japan, pp. 137-142.

F. Johansson, P. (2011). In situ Measurements of Façade Retrofitted with Vacuum Insulation Panels. *Proceedings of the 10th International Vacuum Insulation Symposium*. September 15-16, 2011, Ottawa, Canada, pp. 107-111.

G. Johansson, P., Adl-Zarrabi, B., and Hagentoft, C.-E. (2011). Measurements of Thermal Properties of Vacuum Insulation Panels by using Transient Plane Source Sensor. *Proceedings of the 10th International Vacuum Insulation Symposium.* September 15-16, 2011, Ottawa, Canada, pp. 18-21.

H. Pallin, S., Johansson, P., and Hagentoft, C.-E. (2011). Stochastic Modeling of Moisture Supply in Dwellings based on Moisture Production and Moisture Buffering Capacity. *Proceedings of the 12th Conference of the International Building Performance Simulation Association*. November 14-16, 2011, Sydney, Australia, pp. 366-373.

I. Johansson, P., Pallin, S., and Shahriari, M. (2011). Development of a Risk Assessment Procedure Applied on Building Physics: Part One; Model Development. *Proceedings of the 12th International Conference on Building Materials and Components*. April 12-15, 2011, Porto, Portugal, pp. 109-116.

J. Pallin, S., Johansson, P., and Shahriari, M. (2011). Development of a Risk Assessment Procedure Applied on Building Physics: Part Two; an Applicability Study. *Proceedings of the 12th International Conference on Building Materials and Components*. April 12-15, 2011, Porto, Portugal, pp. 479-486.

K. Johansson, P. (2010). Hygrothermal Conditions in Ventilated Cathedral Ceilings: Influences on Roof Ventilation and Emissivity; Field Study and Analysis. *Proceedings of the 11th International Conference on Thermal Performance of the Exterior Envelopes of Whole Buildings.* December 5-9, 2010, Clearwater Beach, Florida, USA.

Within the framework of IEA ECBCS Annex 55 Reliability of Energy Efficient Building Retrofitting - Probability Assessment of Performance and Cost (RAP-RETRO), the following reports have been presented by the author:

a. Johansson, P. (2013). Subtask 2: Comparison of different economic assessment methodologies, in relation to ST2-CE5. Unpublished Paper. *Prepared for the 7th IEA/ECBCS Annex 55 meeting*, April 17-19, 2013, Curitiba, Brazil.

b. Johansson, P. and Hagentoft, C.-E. (2012). Solution on IEA/ECBCS Annex 55 RAP-RETRO, Subtask 2, Common Exercise 5: Economic Assessment of Retrofitting Measures. Unpublished Report. *Prepared for the 6th IEA/ECBCS Annex 55 meeting*, October 29-31, 2012, Leuven, Belgium.

c. Johansson, P. (2011). Solution on IEA/ECBCS Annex 55 RAP-RETRO, Subtask 2, Common Exercise 3: Sensitivity Analysis on Hygrothermal Performance of Cold Attics. *Prepared for the 4th IEA/ECBCS Annex 55 meeting*, October 25-27, 2011, San Antonio, Texas, USA.

d. Johansson, P. (2011). Solution on IEA/ECBCS Annex 55 RAP-RETRO, Subtask 2, Common Exercise 2: Hygrothermal Analysis of Massive Wall with Interior Insulation. *Prepared for the 3rd IEA/ECBCS Annex 55 meeting*, April 18-20, 2011, Porto, Portugal.

e. Stein, J., Hagentoft, C.-E., Arfvidsson, J., Harderup, L.-E., Johansson, P., Mjörnell, K., Pallin, S., Pietrzyk, K., Kalagasidis, A. S., Ståhl, F., and Svennberg, K. (2011). Energieffektiviseringar – vilka risker finns och hur ska de hanteras? (Energy efficiency measures – what risks are there and how should they be addressed?). [In Swedish]. *Bygg och teknik, 2/2011*, pp. 30-33.

f. Johansson, P., Pallin, S., and Shahriari, M. (2010). Risk Assessment Model Applied on Building Physics: Statistical Data Acquisition and Stochastic Modeling of Indoor Moisture Supply in Swedish Multi-family Dwellings. Unpublished Report. *Prepared for the 2nd IEA/ECBCS Annex 55 meeting*, October 25-27, 2010, Copenhagen, Denmark.

CONTENTS

NOTATIONS

Roman letters

a	(m^2/s)	Thermal diffusivity
c_p	(J/(kg·K))	Specific heat capacity at constant pressure
d	(m)	Diameter or thickness
d_g	(m)	Mean diameter of a gas molecules
d_t	(m)	Time dependent penetration depth
f	(-)	Temperature factor
k_B	(J/K)	Boltzmann constant
l_{mean}	(m)	Mean free path
n	(-)	Refraction index
s_d	(m)	Vapor diffusion thickness
t	(s), (h), (years)	Time
$u_{w,eq}$	(m-%))	Equilibrium moisture content
$u_{w,initial}$	(m-%))	Initial moisture content
v	(kg/m^3)	Vapor content
A	(m^2)	Surface area
A_a	(mbar/year)	Pre-exponential factor in Arrhenius equation
E_a	(J/mol)	Activation energy in Arrhenius equation
K	(-)	Extinction coefficient
K_n	(-)	Knudsen number
L_{2D}	(W/(m·K))	Thermal coupling coefficient
P	(m)	Circumference
P_a	(mbar/year)	Annual pressure increase
P_g	(Pa) or (bar)	Gas pressure
R	(J/(mol·K))	Ideal gas constant
R_s	(m^2·K/W)	Surface heat transfer resistance
R_{se}	(m^2·K/W)	Surface heat transfer resistance on the exterior
R_{si}	(m^2·K/W)	Surface heat transfer resistance on the interior
T	(°C) or (K)	Temperature
$T_{effective}$	(K)	Weighted annual average temperature
T_{indoor}	(°C)	Indoor temperature
$T_{outdoor}$	(°C)	Weighted annual average temperature
T_{sensor}	(°C)	Temperature at the sensor position
U	(W/(m^2·K))	Thermal transmittance
Z	(s/m)	Surface vapor transfer resistance

Greek letters

α	(-)	Solar absorptivity of a surface
β	(-)	Heat transfer efficiency between gas molecule and pore wall
δ	(m)	Characteristic size of a system
δ_v	(m^2/s)	Vapor diffusion coefficient
ε	(-)	Emissivity of a surface
λ	(mW/(m·K))	Thermal conductivity
λ_{cop}	(mW/(m·K))	Thermal conductivity for the center-of-panel
λ_{eff}	(mW/(m·K))	Thermal conductivity of the VIP layer with thermal bridges
λ_{g0}	(mW/(m·K))	Gas conductivity in atmospheric pressure
μ	(-)	Vapor diffusion resistance factor
ρ	(kg/m^3)	Density
σ	($J/(K^4 \cdot m^2 \cdot s)$)	Stefan-Bolzmann constant
τ	(years)	Time for equilibrium moisture content
Ψ	(mW/(m·K))	Linear thermal transmittance

1 Introduction

The present focus on energy efficiency and reduced carbon emissions in society urges for the development of low-energy buildings and massive retrofitting measures in the built environment (IEA, 2013). The Energy Performance of Buildings Directive (EPBD) adopted by the European Union in 2010, states that the measures have to be aimed at reaching new and retrofitted “nearly zero-energy buildings” (nZEB) by the end of 2020. All new public buildings should by the end of 2018 be designed as nZEB (European Parliament, 2010). The definition of the maximum energy use of a nZEB differs in the different member countries. In Sweden, the first proposed definition meant that the current energy requirements should be kept for the nZEB. This proposal received criticism for being too soft compared to the technical potential and the intentions of the EPBD (Näringsdepartementet, 2012). Some of the consultative bodies demanded tougher demands on the energy retrofitting measures in the existing building stock. No matter what the requirements will be on new developments, energy retrofitting measures in the existing building stock are essential to reach the energy targets of a halved energy use in the building sector by 2050 compared to 1995 (Boverket, 2010).

1.1 Background

Building codes were first implemented in 1946 in Sweden (IEA, 2013). At that time the performances were specified for each part of the building envelope. The first energy use requirements were introduced in 1975 after the oil crisis in 1973-1974. The requirements were specified with maximum U-values and demands on the air tightness for different building parts. The codes have been developed during the following years, tightening the demands on the energy use. The latest performance based energy codes are aiming at reducing the energy use further by introducing the same demands on retrofitted buildings as for new developments (Boverket, 2011).

The original technical documentations and drawings of old buildings are often of bad correspondence with reality or completely lacking. The Swedish National Board of Housing, Building and Planning (Boverket) concluded that out of 1 800 investigated buildings, 40% had technical documentations and drawings that could not be used or were completely lacking them. This makes the knowledge of the energy performance of large parts of the building stock hard to evaluate. However, investigated buildings from before 1960 had an average U-value of the exterior walls of 0.58 $W/(m^2 \cdot K)$ (Boverket, 2009) while the current building regulations recommends a U-value of 0.18 $W/(m^2 \cdot K)$ (Boverket, 2011). The high thermal transmittance of the exterior walls leads to a high energy use for heating and an insufficient thermal comfort for the occupants. It should be pointed out that all buildings from the time before 1975 have to be retrofitted before 2050. This is close to two million apartments which is three times more than what will be built till 2050. To reach the energy reduction targets by 2050 in Sweden, the retrofitting measures should include measures for improved energy performance (IVA, 2012).

Many of the old buildings are considered to be of value for historical and esthetic reasons. Around 10% of the 3 100 000 Swedish buildings have some preservation value. Although the total number of specified listed buildings in Sweden is uncertain, an investigation in 8 Swedish counties in 2010 showed that it can be roughly approximated to 67 000 buildings or about 2% of the Swedish building stock. To that number around 2 600 buildings are added every year (Naturvårdsverket, 2013). The requirements on building preservation have in many cases created difficulties to energy retrofit the old building stock. In the near future, there will be a challenge to increase the thermal performance while maintaining the qualities of these buildings and historical areas of interest.

For existing buildings the energy use can be reduced by a number of measures, such as heat recovery of the ventilation air or additional thermal insulation in the building envelope (Dalenbäck *et al.*, 2005). One of the possible measures to reduce the energy use is to retrofit the exterior walls. This could be done on either the exterior or interior side. Exterior insulation is preferred from a moisture perspective since the temperature in the wall is increased, leading to a lower relative humidity in the construction. Installing interior insulation leads to the contrary, an increased risk for moisture damages in the wall. This measure reduces the temperature in the outer part of the wall, leading to an increased relative humidity. Thereby the risk for mold and dry rot fungi in organic materials increases. Also in brick walls insulated on the interior, the risk for damages increases. Freeze-thaw action in the brick and mortar could lead to damages caused by the lower temperature. However, for many listed buildings, retrofitting on the exterior side of the wall is not allowed. There the remaining solution is to add insulation on the interior. Straube *et al.* (2012) studied a number of brick buildings in the United States where interior insulation had been added and concluded that rain hitting the façade had to be addressed properly and that there was a risk that wooden beam ends in the walls were damaged. Also Künzel (1998) showed that interior insulation of brick walls needed to be combined with rain protection measures to avoid moisture induced damages.

Examples of listed buildings that have been energy retrofitted have been presented by e.g. Morelli *et al.* (2012), Weller *et al.* (2008) and Häupl *et al.* (2004). As for Sweden, an overview of four listed retrofitted buildings from the 1940s to 1960s in Gothenburg was presented by Johansson (2011). All the buildings had a brick façade and brick or aerated concrete walls. The retrofitting measures involved adding 30-50 mm glass wool on the exterior of the walls, protected by either a layer of render or a ventilated façade board. The calculated U-value was reduced from 0.83-1.73 $W/(m^2 \cdot K)$ to 0.13-0.5 $W/(m^2 \cdot K)$ after the retrofitting, depending on the existing construction and which measure that was used. Capener *et al.* (2012) also studied a brick building in Gothenburg which was retrofitted with an external thermal insulation composite (ETIC) system involving 50 mm glass wool and two layers of external render. Measurements showed a 27% reduction in energy use and reduced moisture content in the wall. Another approach was proposed by Rasmussen (2011) where 95 mm glass wool was added on the interior of a listed brick façade and 195 mm glass wool covered by render was added on the exterior of the remaining façades of a building from year 1900 in Copenhagen, Denmark.

Already today, thermal insulation layers of up to 50 cm are common in passive houses and other low energy buildings. The thickness of the additional insulation layer is an important limitation. The appearance of the façade will be changed with exterior insulation, e.g. the depth of window placements and wall to roof connection will be difficult to maintain after the retrofitting. Using interior insulation, the rentable floor area will be reduced after the retrofit which reduces the income for the building owner. Novel highly efficient thermal insulation materials such as vacuum insulation panels (VIPs) make it possible to decrease the thermal transmittance while minimizing the additional insulation thickness. The thermal conductivity of a VIP is 5-10 times lower than for conventional insulation materials (Baetens *et al.*, 2010) which decreases the needed thickness for a given thermal resistance with the same relation. Therefore it could be more appropriate to use VIPs than conventional insulation materials when retrofitting the building envelope of listed buildings.

Unlike most insulation materials, VIPs cannot be adapted on the construction site. The rigid panels have to be pre-ordered in the correct dimensions. They are sensitive to damages which could lead to puncturing and a fivefold increase in the thermal conductivity. Therefore special care has to be taken in all stages of the construction process to avoid a damaged VIP. Examples of a number of different constructions where VIPs has been used in retrofitted building envelopes have been reported in the literature. During 2002-2005, the international efforts in VIP research were assembled in the IEA/ECBCS Annex 39 High Performance Thermal Insulation (HiPTI). The project included monitoring and evaluation of 20 buildings with VIPs in floors, roofs, walls, dormer windows and other constructions (Binz *et al.*, 2005). The number of case studies where VIPs were used in façades is limited, but there exists studies of VIPs used both on the interior (Dreyer and Korjenic, 2005; Viridén, 2007) and exterior (Binz and Steinke, 2006; Kubina, 2010; Zwerger and Klein, 2005) of existing exterior walls. Some practical issues when retrofitting with VIPs on the exterior were discussed by Zwerger and Klein (2005) who investigated the use of VIPs in an ETIC system such as the one presented in Figure 1 in Paper IV. One of the conclusions from these studies is that VIPs are a feasible mean to decrease the energy use in the building stock.

1.2 Scope

The aim of this thesis is to investigate the possibilities, limitations and risks when retrofitting with VIPs in the walls of old buildings. The literature has been reviewed to gather knowledge and experiences gained during the years by various researchers. A special focus was on the practical experiences and durability assessment of the VIPs from field studies. One of the concerns regarding the use of VIPs in buildings is the quality assurance during design, transport and construction. In this thesis, the practical experiences, durability assessment and quality assurance are evaluated based on findings in the literature and by own experiments.

Today there is no standardized procedure for in situ measurement of the thermal conductivity of the VIPs before they are installed in the construction (Erbenich, 2009). A fast and inexpensive method which could be used to determine the thermal conductivity of the VIPs could be based on the transient plane heat source (TPS) method. In this thesis, a numerical simulation model and a novel analytical solution (Claesson, 2012) have been used to evaluate the applicability of the TPS method.

When new materials and solutions are introduced to the building market, there is a risk of damages caused by the changed hygrothermal state in the existing building envelope. For instance the cold attics in Swedish single family houses are more prone to moisture damages today than what was the case before they were furnished with additional thermal insulation on the attic floor. To avoid a repetition of the consequences following the previous attempts to decrease energy use, investigations with sensitivity analysis and risk assessment procedures are needed before the final retrofitting measure is determined (Day, 2003). In this thesis hygrothermal numerical simulations were used to investigate the benefits and risks by using VIPs. Two case studies were designed following the results of the hygrothermal numerical simulations:

- A three story residential building from 1930 was insulated with VIPs on the exterior of the wall. The practical applicability of the VIPs was tested and the long-term moisture performance of the wall was monitored. The wall was continuously evaluated with regard to the changed hygrothermal conditions.

- A brick wall was insulated on the interior with VIPs. It was studied in a large-scale building envelope climate simulator in the laboratory of the Norwegian University of Science and Technology (NTNU) and SINTEF Building and Infrastructure in Trondheim, Norway. Special focus was pointed to investigating the practical limitations when using VIPs on the interior. Also the influence by the retrofitting on wooden beam ends in the wall was studied. The moisture content in the wall was monitored to evaluate the risk for moisture damages.

1.3 Methods

To evaluate the state-of-the-art in VIP research, an extensive literature review was carried out where more than 180 publications were gathered and scrutinized. Papers published in conference proceedings and journals together with reports available online were included in the review. Many of the studies on durability assessment of VIPs have been published by the Swiss Federal Laboratories for Materials Science and Technology, Empa. As a guest researcher at the Laboratory of Building Science and Technology at Empa, during the period January to March 2013, the methods and findings were discussed and elaborated further in close contact with the experienced researchers.

A novel analytical solution (Claesson, 2012) was used together with three-dimensional numerical simulations to evaluate the transient plane heat source (TPS) method (Paper I and Paper II). The numerical simulation results were compared to transient measurements using the TPS sensor. Five setups were simulated and measured: EPS, EPS covered by aluminum foil and VIP laminate respectively, and the evacuated and damaged VIPs. EPS was used to simplify the measurements and to be able to vary the high conductive envelope material.

Hygrothermal one and two-dimensional numerical simulations were used to evaluate the risks and benefits by adding interior and exterior insulation to the old walls (Paper III). The risk for damages to the existing wooden structure of the field study building was evaluated in the commercial two-dimensional heat and moisture simulation software WUFI 2D (Fraunhofer IBP, 2010). Four different wall constructions were examined. The boundary conditions and material parameters were varied to perform a sensitivity analysis of the designs. The same approach was used to find the influential parameters and suitable brick and mortar for the laboratory investigations (Paper V). Hygrothermal numerical simulations were performed to investigate the appropriate testing sequence, amount of rain and temperate gradient over the wall. Also, the influence of the wall thickness, and the properties of the brick and mortar were studied by using one and two-dimensional hygrothermal numerical simulations in WUFI 2D.

The field study was performed in a three story multi-family building in Gothenburg built in 1930 (Paper IV). The owner of the building, the public housing corporation Familjebostäder i Göteborg AB, wanted to find a way to decrease the heating energy demand by retrofitting the exterior wall without changing the esthetic qualities of the building. To find suitable solutions for the design of the retrofitted wall, the literature was reviewed and two study visits were performed in southern Germany. Two VIP producers and a building with VIPs in the exterior wall were visited. The retrofit design was developed in close collaboration with the project team which was put together by Familjebostäder. The team included a project manager and project leader from Familjebostäder, two structural engineers from WSP Byggprojektering and representatives from the building contractor Tvåtumfyra AB. Questions regarding changes to esthetic qualities and hygrothermal conditions in the building caused by the retrofitting were discussed. The final retrofit design was based on a laser scanning of the existing wall which was imported to a CAD tool by WSP Byggprojektering.

The exterior wall of the field study building was equipped with 15 hygrothermal sensors which measured the temperature and relative humidity every hour on a number of different positions to study the influence of the added exterior insulation layer. Also, a neighboring façade (non-insulated) was used for reference measurements. The measurements have been monitored by SP Technical Research Institute of Sweden who also installed the sensors in the walls. Measurements of the wall before and after retrofitting using infrared thermography and blower door were also performed by SP.

The laboratory study (Paper V) was part of a research project which was run in cooperation between Chalmers University of Technology, NTNU and SINTEF Building and Infrastructure. Based on the results of the hygrothermal numerical simulations, brick and mortar was selected and a 250 mm homogenous brick wall was erected. Four wooden beam ends were installed in the brick to simulate the connection of the wooden intermediate floor. The wall was equipped with three different types of moisture sensors. Eight temperature and relative humidity sensors and eight wood moisture sensors were installed in the mortar between the bricks. In each of the wooden beams, three resistance moisture meters (pin-type) were installed. The wall was exposed to two climate cycles where the interior surface was covered with VIPs in the first sequence and exposed to the indoor climate during the second.

1.4 Limitations

There are several novel thermal insulation materials and components that have been introduced on the Swedish construction market during the last years. In this study only the use of VIPs in retrofitting is considered. The diversity of the Swedish building stock is large and there are many different types of buildings which have been constructed during different years. One of the most challenging types of buildings is those built before 1950 because of their special features that have to be preserved after a retrofitting. It is also these buildings that have the largest potential reduction in energy use for heating. Therefore this study involves the use of VIPs in retrofitting of brick buildings and of one specific type of building from before 1950. In the field study only one exterior wall has been retrofitted with VIPs on the exterior. The laboratory study only considers the hygrothermal conditions in a brick wall insulated on the interior compared to a non-insulated case. The laboratory study only considers conditions above the freezing point with a heavy rain load on the façade.

The long term durability of the VIPs themselves has not been evaluated in this study. The performance of the VIPs is influenced by diffusion of air and moisture through the envelope but these matters have not been treated in the numerical simulation study. Sufficient air tightness is an important mean to decrease the energy demand for heating of a building. The influence of lack of air tightness around e.g. windows on the energy demand and hygrothermal conditions has only been studied for the field study building. Measurement uncertainties of the hygrothermal sensors and TPS sensor are not studied in detail. There is also an economic aspect concerning the additional costs when using VIPs in buildings which has only been addressed briefly in the literature survey.

1.5 Reading guide

The thesis starts with a literature review and a description of the general heat transfer mechanisms in insulation material which are then used to describe the physical principles of the VIPs. The numerical simulations and measurements with the TPS sensor on EPS and VIPs are described in Chapter 3. In Chapter 4, the field study building in Gothenburg is described and results from the hygrothermal numerical simulations and measurements are presented. The laboratory study of the interior insulation of the brick wall is presented in Chapter 5. Conclusions, discussions and suggestions for future research topics can be found in Chapter 6 and 7.

2 Vacuum insulation panels (VIPs)

This chapter presents a summary of the literature reviews published in Report i and ii of the heat transfer mechanisms in thermal insulation materials and the use of novel thermal insulation materials available on the construction market. Novel thermal insulation materials, such as aerogel and vacuum insulation panels (VIPs), can reach lower thermal conductivities compared with common insulation materials because of their smaller pores and the reduced gas pressure in the material. VIPs have been used in some years in refrigerators and cold shipping boxes and has now started to be used in buildings. A model of the long-term durability prediction was developed at Empa in Switzerland which was investigated during the visit there.

2.1 History of VIP research

The concept of the VIP originates from a patent filed in Germany in 1930 concerning a rubber enclosed porous body. Around 20 years later a patent for an evacuated glass wool core wrapped in a steel foil was filed in the United States. The first patent of a panel with a core of a nanostructured material was filed in 1963. The development of the VIP continued with experiments of different core materials and envelope techniques. It was clear that the main difficulty was the durability and permeability of the laminate around the core. Nanostructured materials that could be used in the core were available already in the 1930s following Kistlers experiments with aerogels. However, the commercial production of aerogels was suspended in the 1970s which lead to development of alternative core materials, such as precipitated and fumed silica. Meanwhile, the increasing demands on durable laminates with low gas permeability from food packaging, pharmaceutical and electronic industries helped boosting the development of thin laminates. The low permeable laminates made it possible to use other porous materials than aerogel in the core of the VIPs with a maintained performance (Fricke *et al.*, 2008).

The VIPs seen on the construction market today (February 2014) were introduced in the early 1990s. It was considered to be a suitable component to replace the insulation materials containing chlorofluorocarbons (CFCs). These substances were banned following the enforcement of the Montreal Protocol on substances that deplete the ozone layer in 1989. The core material was at that time precipitated silica enclosed by a plastic envelope with a 12 µm thick aluminum foil. Another producer at the same time introduced a VIP with a fiber core and an envelope of 75 µm thin welded sheet steel. The products were intended for the refrigerator industry and the thermal conductivity ranged around 2-7 mW/(m·K). VIPs with a diatomite filling and a 100 µm sheet steel casing has also been tested for application in district heating pipes (Fricke *et al.*, 2008). The higher temperature in the pipes leads to a faster aging of the panels than in buildings since the driving force for gas diffusion gets larger.

During the last two decades, a large number of studies have been published concerning the use of VIPs. In this study more than 180 papers and reports have been gathered, categorized and scrutinized. The different publications have been chosen based on their availability in different scientific databases. Most of the publications were published in English or German while a smaller number were published in other languages. Conference papers have been included if they were made available online. However, not all papers presented at the biannual international vacuum insulation symposium (IVIS) in 2005 (Dübendorf, Switzerland), 2007 (Würzburg, Germany), 2009 (London, UK), 2011 (Ottawa, Canada) and 2013 (Dübendorf, Switzerland) have been included since many of these studies already were reported elsewhere. The number of publications divided by publication year is presented in Figure 2.1.

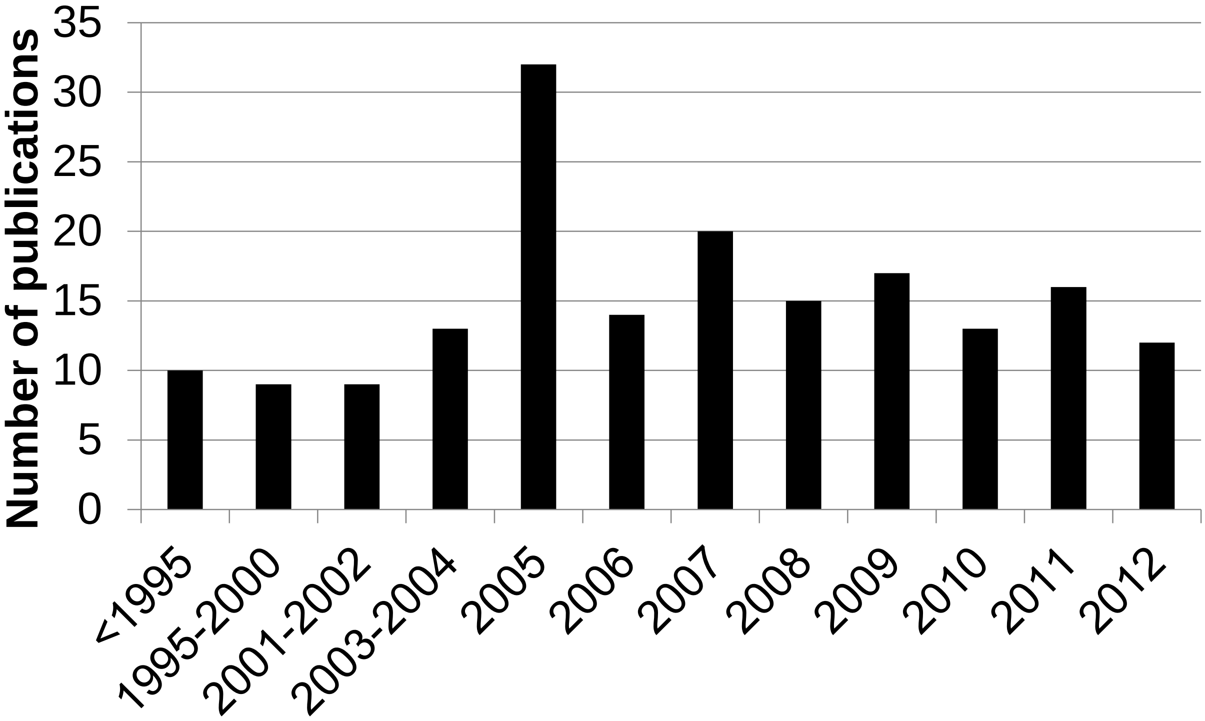

Figure 2.1. Number of publications concerning VIP research divided on the year of publication. The majority of the studies were published during 2005 following the closing of IEA/ECBCS Annex 39.

There is a clear tendency that most papers were published after year 2000. A peak is visible during 2005 when 32 studies were published. This was caused by the finalization of the international research efforts in the IEA/ECBCS Annex 39 High Performance Thermal Insulation Systems (HiPTI) which was undertaken 2002 to 2005 and lead to a large number of publications. Of the 180 publications, only 10 were published before 1995 and after 2005 the number of publications seems to be more equal every year and is stable around 15 publications per year. The earlier publications could be harder to access and are therefore not included in this study why the selection is more complete for the more recent years. Figure 2.2 presents the publications depending of the country of origin and the topic.

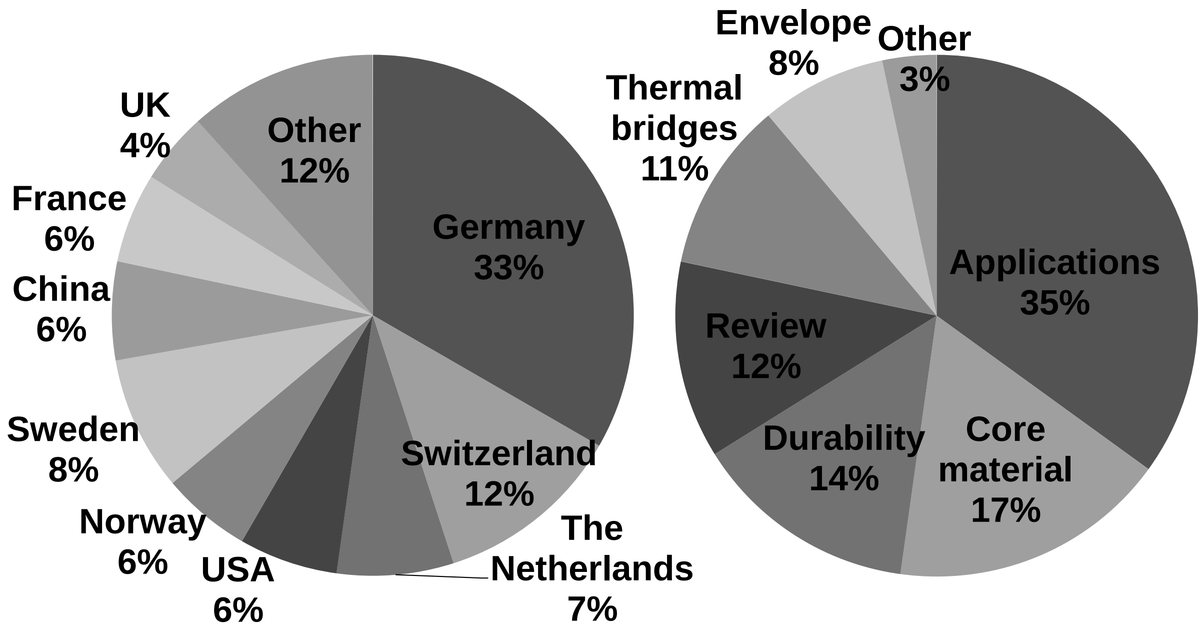

Figure 2.2. Left: share of publications concerning VIP research divided on the country of origin. Most publications originated from ZAE Bayern in Würzburg, Germany and Empa in Dübendorf, Switzerland. Right: Share of publications concerning VIP research divided on the different main topics.

The majority of the publications were from Germany and Switzerland where much of the research concerning VIPs have taken place at ZAE Bayern in Würzburg, Germany and Empa in Dübendorf, Switzerland. The most common topic found in the publications was how VIPs have been applied in buildings and in other fields. A third of the publications concerned this topic, while the studies of the different core materials and durability issues were second and third most published. Among the earlier publications, review papers were common. This could be a consequence of the relatively new field where different research institutes investigated the possible strengths and weaknesses of the VIPs.

2.2 Embodied energy in different VIPs

The environmental impact from the production of a VIP with a fumed silica core wrapped in a metalized multi-layered polymer laminate have been investigated by Institut Bauen und Umwelt e.V. (IBU) (n.d.) in Germany and by Schonhardt *et al.* (2003) in Switzerland. The analysis by Schonhardt *et al.* (2003) showed that 90% of the energy used in the VIP production derived from the core material while only 4% was used for the laminate production. With an alternative core material or a more energy efficient process, calculations showed that the environmental impact of VIPs could be decreased by 45% which would put VIPs on the same level of environmental impact as glass wool. A comparison of the primary energy demands for production of VIPs, mineral wool and expanded polystyrene (EPS) is shown in Figure 2.3.

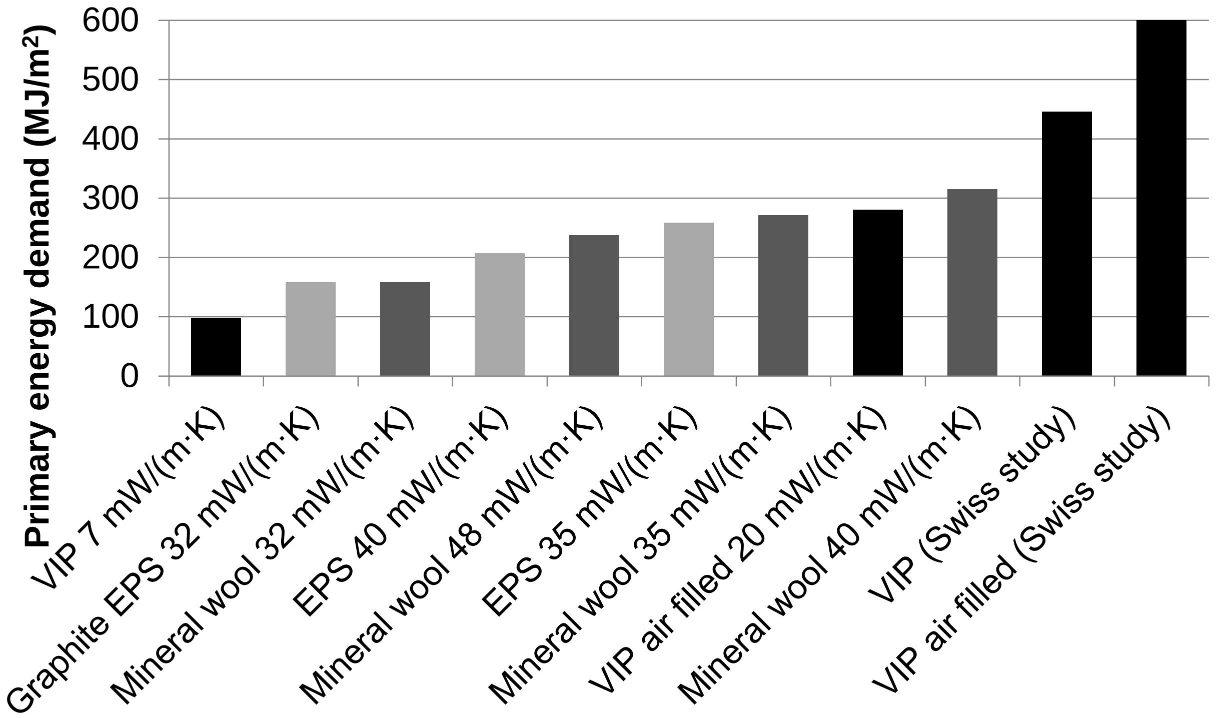

Figure 2.3. Primary energy demand for production of one m² insulation material with the same thermal resistance as 25 mm VIPs with a thermal conductivity of 7 mW/(m·K). The values represent average values for a range of products with similar thermal conductivity. The environmental product declarations were made by Institut Bauen und Umwelt e.V. (IBU) (n.d.) in all cases except for the two Swiss VIP calculations which were made by Schonhardt et al. (2003).

It is clear that there is a wide variation between the two studies. The environmental product declarations by Institut Bauen und Umwelt e.V. (IBU) (n.d.) are made during different years which influences the emissions from the energy mix used in the production of the materials. From that study it is clear that the VIP is competitive with mineral wool and EPS which ranges between 158 MJ/m^2 and 315 MJ/m^2 compared to 98 MJ/m^2 and 281 MJ/m^2 for the evacuated and air filled VIPs respectively. The substantially higher primary energy demand in the study by Schonhardt *et al.* (2003) could be caused by other energy sources and different primary energy factors for Germany and Switzerland. However, Schonhardt *et al.* (2003) compared a VIP with EPS and mineral wool and concluded that the embodied energy was 120% higher in a VIP than in glass wool production but only 12% higher than in EPS production. Some research remains to improve the certainty of the primary energy used for production of a VIP to make fair comparisons possible between the different insulation materials. However, these studies clearly show that the embodied energy for VIPs is in the same order of magnitude as for conventional insulation materials. Therefore, in many cases, the increased energy use during the production can be met by the lower energy use for heating of the buildings during the service life.

2.3 General heat transfer in insulation materials

The heat transfer through a homogenous material is described by the thermal conductivity, λ (mW/(m·K)), which can be divided in three parts:

$$\lambda = \lambda_s + \lambda_g + \lambda_r \text{ (mW/(m·K))} \tag{2.1}$$

where λ_s is the thermal conductivity through the solid, λ_g is the thermal conductivity through the gas and λ_r is the radiative thermal conductivity within the pores.

The conduction through the solid is dependent on the characteristics of the material. In metals, the heat is transferred mainly by means of the free electrons which transfer more energy from the warm to the cold side than in the opposite direction. Imperfections in the material and atomic collisions limit the heat transfer by the electrons. On the other hand, in insulation materials the number of free electrons is much lower than in metals which means that the heat is mainly transferred by lattice vibrations (Brodt, 1995). To limit the thermal conduction through the solid structure of the materials, insulation materials are manufactured to be as porous as possible.

Gas conduction is dependent on which gas is used, the size of the pores in the material and the number of gas molecules in the pores. One way to reduce the gas conduction is to use a gas with a lower conductivity, e.g. argon and krypton instead of air in windows. Another way to decrease the gas conduction is to reduce the pore sizes of the material, leading to fewer collisions between gas molecules and an increasing number of the elastic collisions between gas molecules and pore wall. This phenomenon is called the Knudsen effect which influences the gas conduction, λ_g (mW/(m·K)), according to Equation 2.2 (Baetens *et al.*, 2010):

$$\lambda_g = \frac{\lambda_{g0}}{1 + 2 \cdot \beta \cdot K_n} \text{ (mW/(m·K))} \tag{2.2}$$

where

$$K_n = \frac{l_{mean}}{\delta} \text{ (-) and } l_{mean} = \frac{k_B \cdot T}{\sqrt{2} \cdot \pi \cdot d_g^2 \cdot P_g} \text{ (m)} \tag{2.3}$$

where K_n (-) is the Knudsen number which is governed by l_{mean} (m), the mean free path of the gas molecules, and δ (m), the characteristic size of the system, i.e. the distance between two pore walls. $k_B = 1.38 \cdot 10^{-23}$ J/K is the Boltzmann constant, T (K) is the temperature, d_g (m) is the mean diameter of the gas molecules and P_g (Pa) is the gas pressure. Further on λ_{g0} (mW/(m·K)) is the gas conductivity in atmospheric pressure and β (-) a constant characterizing the efficiency of heat transfer between gas molecule and pore wall, commonly between 1.5-2.0 (Baetens *et al.*, 2011). The heat transfer by gas conduction, depending on the gas pressure and pore size, is presented in Figure 2.4.

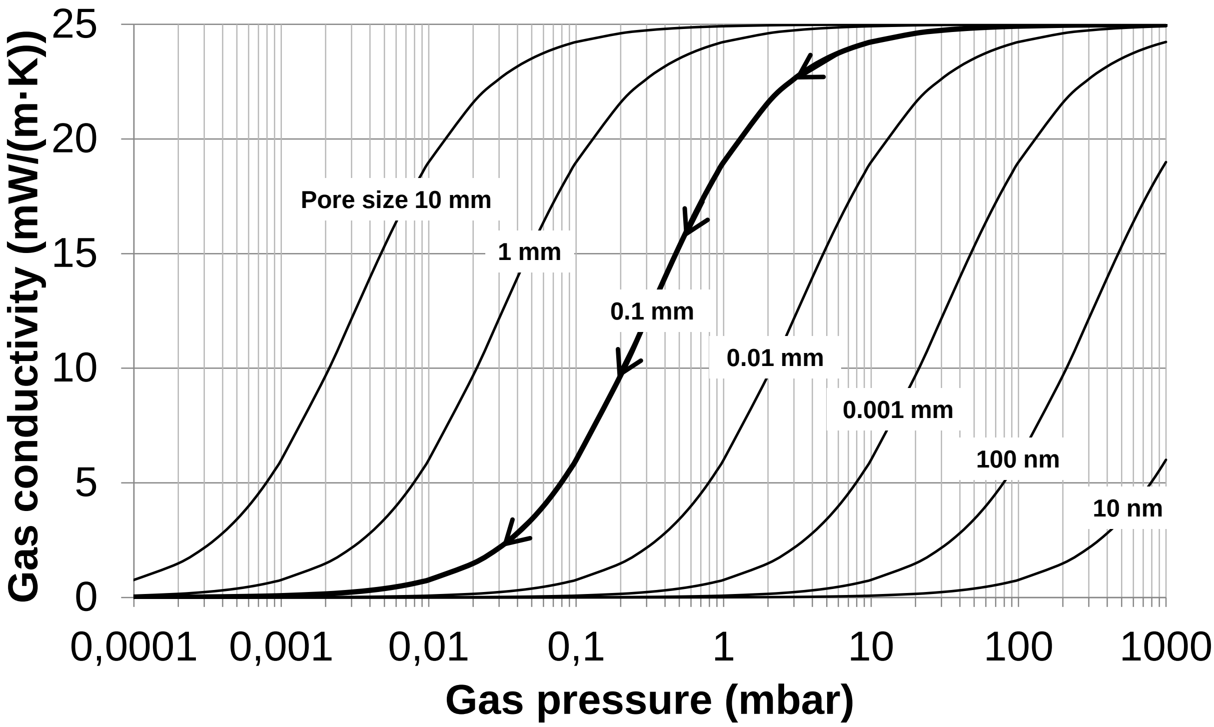

Figure 2.4. Heat transfer by gas conduction in porous materials depending on pore size and gas pressure up to atmospheric pressure at 1 000 mbar. Fumed silica, which is a material used in the VIP core, has pores in the range of 10-100 nm (Based on Simmler et al., 2005).

For a material with a pore size of e.g. 0.1 mm, there are three distinct areas as shown in Figure 2.4. The gas conductivity is constant until the gas pressure is reduced to around 20 mbar. With a decrease in gas pressure, the mean free path of the gas molecules is increased which decreases the number of collisions between the gas molecules. In this area the gas conduction is strongly influenced by the gas pressure. At a sufficiently low pressure, the gas conductivity is negligible and all heat conduction is through the solid and by radiation (Brodt, 1995).

Heat transfer by radiation is caused by the electromagnetic radiation that all surfaces emit. Inside the pores of a material, heat radiates from both the warm and the cold surfaces. The net radiation is the difference between them. The rate of the heat transfer by radiation is dependent on the temperature of the surface and can be described by:

$$\lambda_r = \frac{16 \cdot n^2 \cdot \sigma \cdot T^3}{3 \cdot K} \text{ (W/(m·K))} \tag{2.4}$$

where n (-) is the refraction index, $\sigma = 5.67 \cdot 10^{-8}$ J/(K^4·m^2·s) the Stefan-Blotzmann constant, T (K) the mean temperature of the surfaces and K (1/m) the extinction coefficient. The heat transfer by radiation can be counteracted by adding an opacifier, e.g. silicon carbide, to the material. The opacifier has a higher extinction coefficient compared with other materials which lower the heat transfer by radiation.

One of the most extreme thermal insulation materials is aerogel which typically has a thermal conductivity down to 13 mW/(m·K) at atmospheric pressure (Lu *et al.*, 1992). The density is typically around 100 kg/m^3, but researchers have been able to produce transparent aerogels with a density as low as 3 kg/m^3 (Tillotson and Hrubesh, 1992) which is close to the density of air, 1.2 kg/m^3. The material has extremely small pores with a diameter in the range of 20-40 nm. The method of producing aerogel was invented in the 1930s but the material has until now mostly been used in special applications in space industry, chemical industry and in sport equipment. The production process demands much energy and is quite complicated with production at a critical state involving elevated temperature and pressure. Therefore the pure aerogel product is still too expensive for use in buildings. A fiber material with aerogel is available on the construction market with a thermal conductivity around 13 mW/(m·K) (Baetens *et al.*, 2011) which could be compared to glass wool that have a thermal conductivity of 40 mW/(m·K).

Some other novel thermal insulation materials were described in Report ii. These materials are based on existing materials which have been improved by using some additives. The graphite EPS is such a product where graphite lowers the heat transfer by radiation in the EPS. By this measure the thermal conductivity is reduced from 36 mW/(m·K) to 31 mW/(m·K) (BASF, 2011). Another way of decreasing the thermal conductivity of the material is used in the polyisocyanurate (PIR) which is an improvement of the polyurethane (PUR) by using other substances, reactants and catalysts in the production process. The thermal conductivity of PIR is around 22 mW/(m·K) (EcoTherm, 2010).

By removing the air inside the porous core material, the initial center-of-panel thermal conductivity of a VIP with a fumed silica core is around 2-4 mW/(m·K) (Baetens *et al.*, 2010). This value increases by time due to the irreversible pressure increase in the core material due to air and moisture diffusion through the laminate. Therefore a design value of 7-8 mW/(m·K) for a fumed silica VIP should be used which corresponds to the thermal conductivity after 25 years usage (Brunner and Simmler, 2008). If the panel is damaged and filled with air, the thermal conductivity increases to 20 mW/(m·K) which is lower than stagnant air and most thermal insulation materials.

2.4 Properties of the core material

The principle behind the VIP is similar to a thermos bottle where the heat transfer is reduced by removing the air between the inner walls of the bottle. In a flat VIP it is not possible to have an empty space inside the panel since this would lead to collapse. Therefore a material is used inside the core of the panel that withstands the atmospheric pressure on the envelope when the interior is evacuated. Figure 2.5 shows two evacuated VIPs where the envelope surrounding the core material is visible and an opened VIP with the core material and laminate exposed.

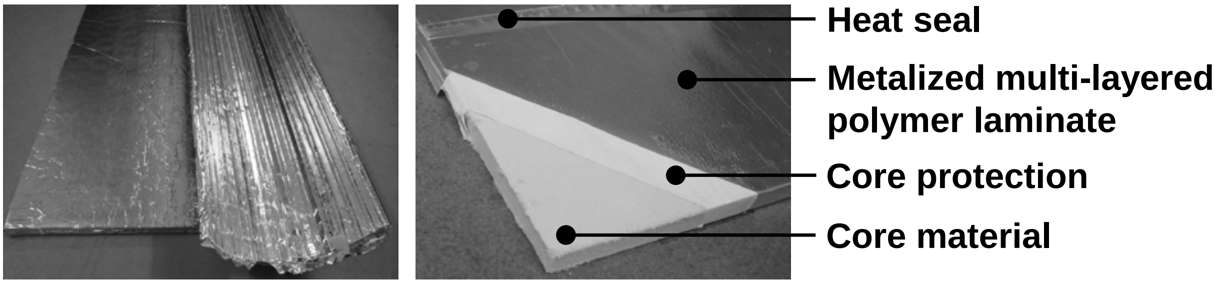

Figure 2.5. Left: flat and concave VIP for use as pipe insulation (Photo: Axel Berge). Right: the fine powder core is wrapped in a heat sealed metalized multi-layered polymer laminate (Photo: va-Q-tec AG).

The core material is a fine powder or fiber from which the air has been removed to a gas pressure of 0.2-3 mbar. There are different materials that can be used in the core of a VIP where the most common material in Europe is fumed silica. Also glass fiber and open cell polyurethane are used, but mainly for application in freezers and refrigerators. Figure 2.6 shows the relation between the internal gas pressure and the thermal conductivity of five different materials that can be used in the core of a VIP.

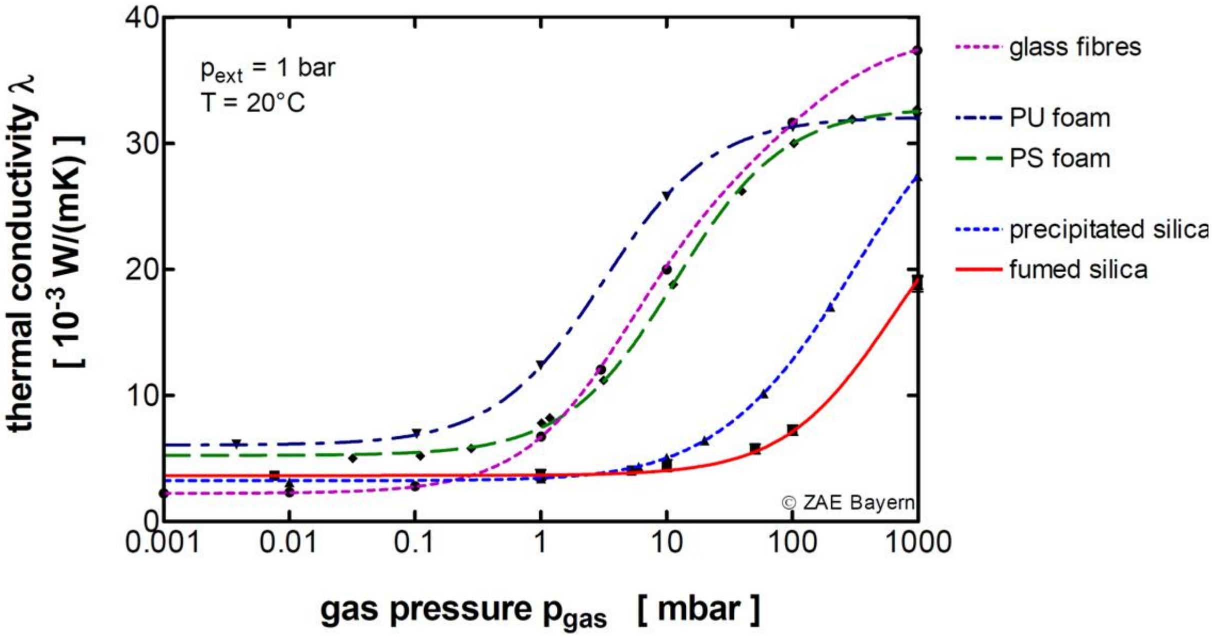

Figure 2.6. Thermal conductivity of different materials which are used in the core of VIPs as a function of the internal gas pressure. Normal atmospheric pressure is 1 000 mbar (Simmler et al., 2005).

As can be seen in Figure 2.6, the thermal conductivity at a specific pressure varies for the VIPs with different core materials. For glass fibers, the center-of-panel thermal conductivity is around 1.5-3 mW/(m·K) at a pressure below 0.1 mbar. The thermal conductivity increases then rapidly with increasing pressure. The same relation is found for the polyurethane and polystyrene foam with a thermal conductivity of 7-9 mW/(m·K) up to around 1 mbar. Another behavior is found for the fumed silica where the thermal conductivity is 4-5 mW/(m·K) up to around 10 mbar (Caps *et al.*, 2008). The pores of fumed silica are in the order of 100 nm which limits the heat transfer between the gas molecules (Fricke, 1993). The Knudsen number, described in Section 2.3, explains the low thermal conductivity at atmospheric pressure.

Inside the pores, the temperature difference is normally too low to induce gas convection. On material scale, however, there is gas convection through the open pore structure which cannot be neglected. In VIPs, the gas convection is reduced firstly by the small pore size of the core material and secondly by removing the gas from the porous core material. The internal pressure increases with time due to air and moisture diffusion through the laminate around the core. Therefore the thermal conduction through the gas in the core material will increase with time, following the curve in Figure 2.6. The required properties of the envelope around the core depend on the core material and the required service life of the VIPs. The envelope needs to be less permeable in glass fiber VIPs than in fumed silica VIPs. This was shown in Figure 2.6 where the thermal conductivity of the glass fiber increases at a lower pressure than the thermal conductivity of the fumed silica. To reduce the permeability of the envelope, the thickness of the metalized layer is increased. This leads to a higher heat flow through the envelope at the edges and thus increases the total heat flow through the VIP layer.

2.5 Thermal bridges around the perimeter of a VIP

The metalized multi-layered polymer laminate around the VIP increases the total heat flow through the VIP layer. Figure 2.7 shows the principal heat flow path through the laminate.

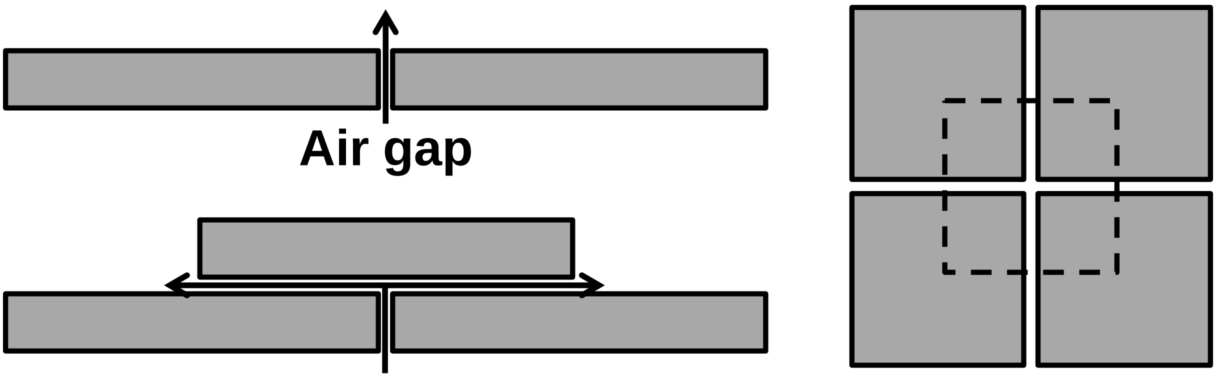

Figure 2.7. Thermal bridge around the perimeter of a VIP. The thermal bridge can be reduced by 64-72% by adding a second staggered layer of VIPs (Ghazi Wakili et al., 2011).

The additional heat flow through the laminate is quantified by the linear thermal transmittance, Ψ (mW/(m·K)). This value can be calculated numerically (Binz *et al.*, 2005; Schwab *et al.*, 2005; Sprengard and Spitzner, 2011), analytically (Tenpierik and Cauberg, 2007) or measured in guarded hot plate apparatus (Brunner *et al.*, 2012b; Ghazi Wakili *et al.*, 2004; Ghazi Wakili *et al.*, 2011). In the standard SS-EN ISO 10211, the total heat flow through a construction with two-dimensional thermal bridges is given by the thermal coupling coefficient, L_{2D} (W/(m·K)). This term is here called the effective thermal conductivity, λ_{eff} (mW/(m·K)), and is calculated by

$$\lambda_{eff} = \lambda_{cop} + \Psi \cdot d \cdot P/A \text{ (mW/(m·K))} \quad (2.5)$$

where λ_{cop} (mW/(m·K)) is the thermal conductivity through the centre-of-panel, d (m) is the thickness, P (m) is the circumference and A (m^2) is the area of the VIP. The linear thermal transmittance is dependent on the center-of-panel thermal conductivity, the thermal conductivity of the laminate, the thickness of the panel and the thermal conductivity of the surrounding materials (Binz *et al.*, 2005).

The influence on the linear thermal transmittance of the laminate around the VIPs by different boundary conditions was investigated numerically by Schwab *et al.* (2005). Between the VIPs there can be up to 1 cm wide air gaps, as shown in Figure 2.7, because of the imperfections of the shape of the VIPs. In some cases the VIPs are embedded in a protective material, e.g. EPS or polyurethane, which creates a thermal bridge between the panels. With a surface heat transfer coefficient on the interior side of 8 W/(m^2·K) and 25 W/(m^2·K) on the exterior side, the linear thermal transmittance was 2 mW/(m·K) for a 20 mm thick VIP with perfect connections. For the more true case with an air gap of 5 mm between the panels, the linear thermal transmittance increased to 12 mW/(m·K). Sprengard and Spitzner (2011) made similar calculations where they varied the thickness of the aluminum layers in the laminate, the size of the panel, the thermal conductivity and thickness of the material between and/or covering the VIPs. As could be expected, the linear thermal transmittance increased with the width of the material in the gap between the VIPs, and with the thermal conductivity of that material. For a layer of 20 mm thick VIPs with a material with a thermal conductivity of 35 mW/(m·K) in the gap between the panels, the linear thermal transmittance was 7.5 mW/(m·K) for 10 mm gap, 13 mW/(m·K) for 20 mm gap and 29 mW/(m·K) for 50 mm gap. For a wider gap between the VIPs, and for materials with higher thermal conductivity, the influence by the thermal bridge gets so large that the design should only be considered for very large VIPs. By covering the VIPs on both sides with 5 mm EPS, the linear thermal transmittance could be reduced to 2.6 mW/(m·K) compared to the original case with 3.2 mW/(m·K). The effective thermal conductivity of the VIPs decreases with the size of the panels. The thermal bridges increased the effective thermal conductivity with 26% for a 0.3 m x 0.2 m (width x height) VIP and with 4% for a 1.5 m x1.0 m VIP (Sprengard and Spitzner, 2011).

To increase the durability of VIPs, different approaches have been suggested and tested. A more robust version of the panels is the vacuum insulated sandwiches (VIS) which are covered by a stainless steel casing. The sandwich can be part of the load-bearing system and take loads without any additional protection (Tenpierik *et al.*, 2007). Gudmundsson (2009) calculated the thermal bridges created by the robust protective casing around the VIS and found that the thermal bridge could be reduced by using insulation materials adjacent to the VIS. Also, the length of the edge could be elongated to decrease the influence of the casing. Thorsell (2006) investigated a serpentine edge of the casing which showed that the thermal bridges decreased with this design. With 11 slots of 20 mm depth the influence could be minimized to a linear thermal transmittance of 11 mW/(m·K) which is comparable to the effect by the metalized multi-layered polymer laminate mentioned above. The linear thermal transmittance of the casing was 28 mW/(m·K) without any slots. Sprengard and Spitzner (2011) also compared the effect of replacing the metalized multi-layered laminate with a more durable 6-12 µm thick aluminum foil. The resulting linear thermal transmittance was 8-9 times higher for the aluminum foil compared to the metalized multi-layered laminate.

A study of the linear thermal transmittance using guarded hot plate apparatus was presented by Ghazi Wakili *et al.* (2004). They investigated the influence by different setups and compared the measurements with a numerical model of the VIP. The thermal bridge effect of the laminate on 20 mm thick VIPs of sizes 500 mm x 500 mm (width x height) and 500 mm x250 mm were studied. Two different laminates were tested, one laminate with a total aluminum thickness of 90 nm and another laminate with 300 nm aluminum. The linear thermal transmittance was 7 mW/(m·K) for the 90 nm aluminum and 9 mW/(m·K) for the 300 nm aluminum. The thermal bridge could be reduced by using double layered VIPs in the constructions, with the second layer covering the edges as shown in Figure 2.7. Measurements on different arrangements of 15-40 mm thick, 500 mm x 500 mm and 500 mm x 250 mm VIPs were presented by Ghazi Wakili *et al.* (2011). The VIPs were encapsulated in a metalized multi-layered polymer laminate with a total aluminum thickness of 300 nm. The average linear thermal transmittance was around 2.5 mW/(m·K) for these cases. Comparing this result with the study of single layer VIPs, the effect of the thermal bridge was reduced by 64-72% by adding the second layer.

2.6 Long-term durability prediction

In Europe, the declared thermal conductivity of insulation materials is given as the average performance over 25 years, e.g. SS-EN 13162. All materials change with time by the surrounding conditions, such as temperature shifts, exposure to moisture and by ultraviolet radiation. Garnier *et al.* (2011) identified a number of factors that influence the durability of the aluminum layers in the VIP laminate. Experiments on different glues in the laminate were performed to identify harmful combinations. The aluminum oxide was not stable in acidic (pH<4) or alkaline (pH>9) environments. Fluoride ions, which are present in drinking water, were identified as one of the chemical compounds that could cause degradation of the laminate. To produce durable laminates, the glue should be free of chlorides and other substances such as Ga, Tl, In, Sn, Pb which also could reduce the stability of the aluminum in the laminate.

The influence by moisture and elevated temperatures was studied by Brunner *et al.* (2008) experimentally. A number of VIPs were stored during 1 year in 65°C and 75% relative humidity (RH), which is an extreme climate compared to the actual climate in a building. After 100 days, the laminate was mechanically deformed and beginning to delaminate but still functioning. Within a year, the laminate failed and the VIPs were filled with air. In another experiment, VIPs were stored in 80°C and 80% RH for 8 h and then the climate was changed to 25°C and 50% RH for 4 h. The result was that the aluminum oxidized and transparent spots where visible on some of the panels after 26 days (Brunner *et al.*, 2008). However, these chemical changes do not necessarily mean that the service life of the VIP has ended since not all of the panels were filled with air after the experiments and also oxidized aluminum is used as a barrier material (Simmler *et al.*, 2005).

To reach a service life of 30-50 years for VIPs, the oxygen transmission rate (OTR) through the envelope has to be below 10^{-2} $cm^3/(m^2 \cdot day)$ at one bar pressure difference and the water vapor transmission rate (WVTR) has to be below 10^{-4} $g/(m^2 \cdot day)$ (Simmler *et al.*, 2005). Since the pressure inside the VIPs increase with time, also the driving potential for the oxygen and water vapor transmissions decreases with time. Therefore, the pressure increase is largest in the beginning of the service life of the VIP and decreasing with the increasing internal pressure.

It is difficult to evaluate the very low permeability of the laminate with the measurement procedures available today within a reasonable time period. The applicability of the wet cup method, defined in SS-EN ISO 12572, was investigated in the laboratory at Chalmers. For the investigations, 6 samples were cut out of a metalized polymer laminate with three aluminum layers of 100 nm each. The samples were stored in a constant climate room with 23°C and 50% RH. The WVTR was determined by weighting the samples on a scale with 0.01 g resolution. The resulting WVTR during 31 months is presented in Figure 2.8.

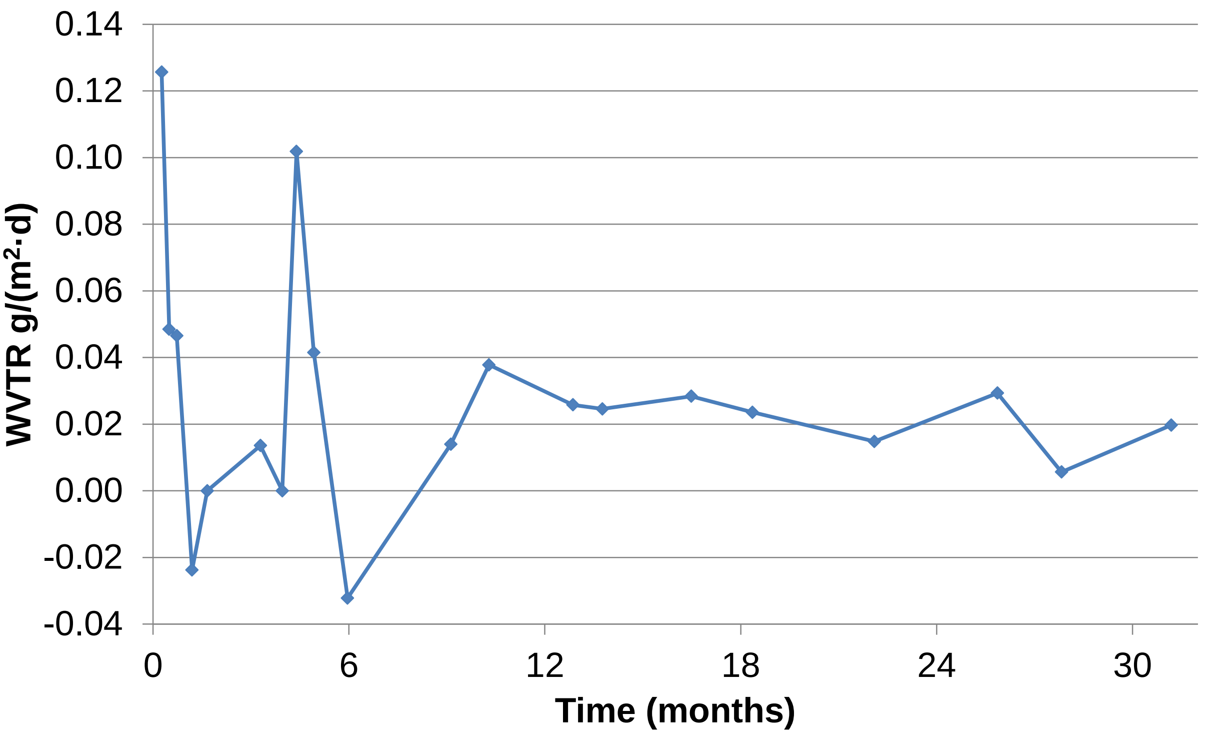

Figure 2.8. Measured average WVTR of six samples of a metalized triple-layered polymer laminate by the wet cup method in 23°C and 50% RH stored in the laboratory at Chalmers. The weight was determined on a scale with 0.01 g resolution.

The measured WVTR varied in the beginning of the measurement period but stabilized after around 9 months. It was on average $21 \cdot 10^{-3}$ $g/(m^2 \cdot d)$ after 31 months measurement with a standard deviation of $6 \cdot 10^{-3}$ $g/(m^2 \cdot d)$. The sealing of the specimens were not perfectly tight and there could have been a large leakage path through that part. However, Simmler *et al.* (2005) evaluated different permeation measurement methods on metalized multi-layered aluminum laminates. Using an electrolytic measurement process they found that the WVTR varied between $1.8 \cdot 10^{-3}$ $g/(m^2 \cdot d)$ and $130 \cdot 10^{-3}$ $g/(m^2 \cdot d)$ for a number of different triple-layered metalized laminates. This shows the difficulties to determine the WVTR with the measurement techniques available today. The wet cup method can still be used for indicative measurements to compare different laminates. The study by Simmler *et al.* (2005) also showed that the OTR and the WVTR had a strong correlation and that the OTR was around 10 times higher than the WVTR. They also found that the edges and corner effects of a VIP on the total OTR and WVTR were much lower than expected

The lack of long-term experience from using VIPs urged for accelerated aging experiments to determine the long-term durability. Simmler and Brunner (2005) investigated VIPs in constant and dynamic climate conditions. They found that the pressure and moisture increase in the VIPs was in accordance with the Arrhenius equation. Based on this finding, an aging model was developed which takes into account the air and moisture diffusion into the VIP

$$\lambda(t) = \lambda_0 + \Delta\lambda(t) \cong \lambda_0 + \frac{\delta\lambda}{\delta P_g} \cdot P_a \cdot t + \frac{\delta\lambda}{\delta u_{w,eq}} \cdot u_{w,eq} \cdot \left(1 - \exp\left(-\frac{t}{\tau}\right)\right) \text{ (mW/(m·K))} \quad (2.6)$$

where λ_0 (mW/(m·K)) is the initial thermal conductivity, $\delta\lambda / \delta P_g$ (mW/(m·K·mbar)) is the thermal conductivity increse by the annual pressure increase P_a (mbar/year) during the time t (years), $\delta\lambda / \delta u_{w,eq}$ (mW/(m·K·m-%)) is the thermal conductivity increase by the increase in mass-% moisture, $u_{w,eq}$ (m-%) is the equilibrium moisture content at 80% RH and $\tau = u_{w,eq} / u_{w,initial}$ (years) the time for moisture saturation of the core material. The pressure increase is dependent on the temperature and the duration of the temperatures. The weighted annual pressure increase P_a is calculated by

$$P_a = \frac{A_a \cdot \sum_{i=1}^{n} \exp\left(-\frac{E_a}{R \cdot T_i}\right) \cdot \Delta t_i}{8760} = A_a \cdot \exp\left(-\frac{E_a}{R \cdot T_{effective}}\right) \text{ (mbar/year)} \quad (2.7)$$

where the Arrhenius pre-exponential factor A_a (mbar/year) and the activation energy E_a (J/mol) are calculated by using empirical data and R = 8.31 J/(mol·K) is the ideal gas constant. The temperature T_i (K) during the time period Δt_i (h) is used to calculate the weighted annual average temperature, denoted the effective temperature $T_{effective}$ (K).

Simmler and Brunner (2005) investigated VIPs in different temperatures and a high RH. In the laboratory they measured the internal pressure and weight increase in a number of 250 mm x 250 mm x 20 mm (width x height x thickness) and 500 mm x 500 mm x 20 mm VIPs. The VIPs had a metalized polymer laminate of either three layers of 30 nm (MF1) or three layers of 100 nm thick aluminum (MF2). When fitting the experimental results to the Arrhenius equation, the pre-exponential factor and the activation energy could be determined. These parameters are presented in Table 3.1, calculated based on the laboratory measurements by Simmler and Brunner (2005).

Table 2.1. The pre-exponential factor and the activation energy in the Arrhenius equation based on the laboratory measurements presented by Simmler and Brunner (2005).

VIP properties (mm)	A_a (mbar/year)	E_a (J/mol)
250x250x20 MF1	$2.9 \cdot 10^9$	$4.9 \cdot 10^4$
500x500x20 MF1	$620 \cdot 10^9$	$4.0 \cdot 10^4$
250x250x20 MF2	$0.78 \cdot 10^9$	$6.1 \cdot 10^9$
500x500x20 MF2	$3.1 \cdot 10^9$	$5.3 \cdot 10^9$

The aging model was validated by Brunner and Simmler (2008) who compared it to 2 years pressure and weight increase measurements performed on VIPs installed in a flat roof of an occupied building in Switzerland. The model predicted the pressure increase with only 1.1% to 2.4% deviation while the increasing moisture content was overestimated by 67% to 80%. According to Brunner (2013) the calculated pressure increase by Brunner and Simmler (2008) was overestimated because the laminate around the VIPs in the roof had thicker aluminum layers (MF2) than what was used as input for the aging model (MF1). With the fitting parameters for MF2, the effective temperature 18.6°C on the interior of the VIP and 18.8°C on the exterior, Equation 2.7 gives a 1.1 mbar/year pressure increase. This is clearly lower than the measured pressure increase in the flat roof. The pressure in the VIPs had increased by 2.7 mbar/year on average after 2 years which is 2.5 times the calculated pressure increase. However, the new input data also gave a lower moisture increase in the VIPs. This is now only overestimated by 17% to 40%.

The same flat roof as discussed above was reopened in 2013 after 8-9 years operation. The installed VIPs were transported to a lab for measurements of the thermal conductivity (Brunner and Ghazi Wakili, 2014). It was found that the thermal conductivity indeed had increased more than could be expected based on the aging model. After 8.8 years the thermal conductivity had increased to 6.6 mW/(m·K) respective 7 mW/(m·K) while 5.6 mW/(m·K) was expected. To improve the accuracy of the aging model, Brunner and Ghazi Wakili (2014) suggested a third aging mechanism. They proposed that the interfacial contact areas between the fumed silica particles could change after long-term moisture exposure. Migration of water molecules could lead to an increased contact surface between the molecules in the fumed silica skeleton leading to an increased thermal conductivity. Morel *et al.* (2009) studied this effect and concluded that fumed silica reacts with the water molecules leading to a decreased surface area and increased rigidity of the fumed silica. The mass% moisture that was adsorbed to two different fumed silica products was 25% and 38% respectively during aging at 25°C and 94% RH for 60 days (Balard *et al.*, 2011). Work still remains to improve the aging predictions to take the moisture induced changes of the fumed silica into account. The earlier predictions may now be considered too optimistic, especially for the moist conditions which needs more investigations (Brunner, 2013). In 2013, the IEA/EBC Annex 65 Long-Term

Performance of Super-Insulation in Building Components & Systems was initiated which will study several high-performance insulation materials. The long-term performance of the VIPs is one of the focus areas which will generate new knowledge and better predictions of the long-term durability of the VIPs.

2.7 VIPs in buildings

After discussing the aging of the VIPs in laboratory with a controlled environment it is time to investigate what the VIPs will be exposed to in reality. The production of VIPs results in rigid panels of defined shape and sizes which cannot be adapted on the construction site. Each panel need to be ordered in its correct dimensions from the start. The panels have to be treated carefully in all stages of the construction since damages eventually leads to loss of vacuum and a fivefold increase in the thermal conductivity. A way to avoid unnecessary risks on the construction site is to integrate the VIPs in prefabricated constructions. (Schaffrath *et al.*, 2010) proposed to use laser scanning and automated design to make the design process more accurate and faster. They studied three different constructions and used three-dimensional laser scanning and photogrammetry to produce drawings for the prefabricated VIPs. Industrial treatment of the VIPs means they will be in a controlled environment where the staff involved in the handling of the panels can gain experience and be trained to treat the VIPs with care. Otherwise the construction site must be equipped with the right protective equipment such as protective mats and felt shoes (Binz *et al.*, 2005). As shown in Figure 2.9, it is not difficult to detect a damaged VIP when one knows what to look for.

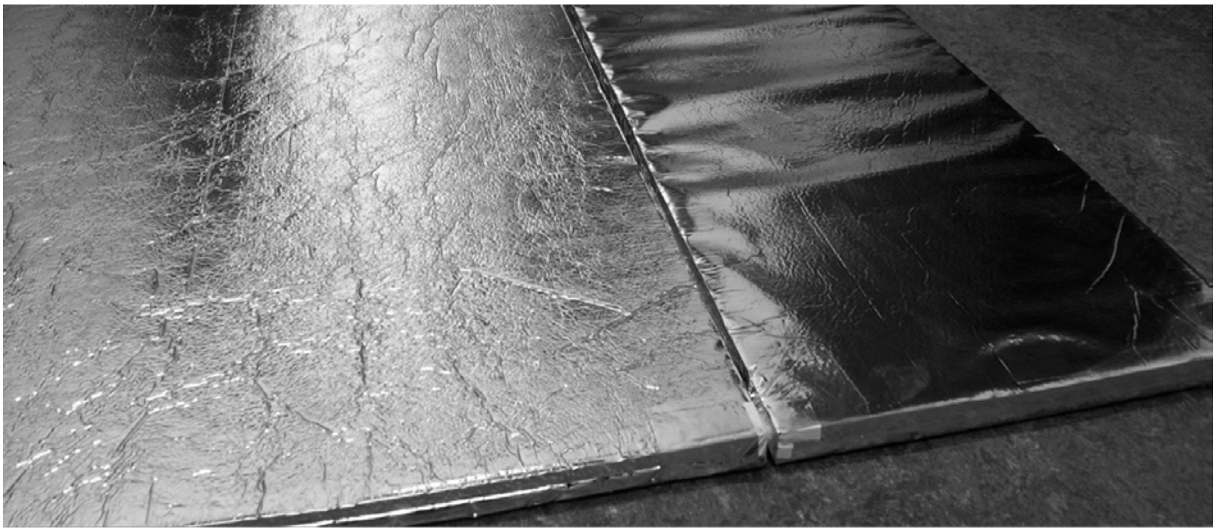

Figure 2.9. Evacuated VIP compared to the one where a laminate has been damaged. It is clear that the laminate is loose from the core in the second case (Photo: Axel Berge).

If a VIP is damaged in the construction, the heat flow through that part of the construction will increase. In the design process this has to be treated. If it has an unacceptable consequence for the energy use for heating of the building, the construction should be prepared for easy exchange of the damaged panel. In that case the construction has to be flexible and designed in a way that the VIPs are easily accessible and possible to remove. It should also be possible to detect the damaged VIP with e.g. infrared thermography, which means that the VIPs should not be covered by high conductive materials or be placed behind a ventilated air space. All attachments and joint details need to be carefully designed since brackets, window attachments and such components may harm the envelope of the VIPs. A good design can ensure this which means the designers and builders have to be aware of the special requirements of the VIPs early in the process (Binz *et al.*, 2005).

Binz *et al.* (2005) studied high performance thermal insulation components for buildings based on VIPs. In total 20 constructions built or retrofitted using VIPs were studied and the consequences on energy use, thermal bridges and moisture performance were analyzed. Based on the studies, the research team concluded that VIPs have become a feasible and important mean for designing energy efficient buildings. One of the conclusions was that there are obstacles to overcome, mainly cost and issues with durability and quality assurance of VIPs in buildings. These obstacles still remain to be solved and work is going on to evaluate and monitor VIPs in laboratory and field studies.

Heinemann and Kastner (2010) used infrared thermography to investigate 19 objects insulated with in total 3 224 m^2 VIPs, a few years after the construction finished. Three objects stood out in the investigation with more than 15% of the VIPs damaged. In one of these objects it was assumed that errors were made in the design by installing unprotected panels close to an uneven plaster surface. In another project, photos from the construction site showed that the VIPs had been stored and handled improperly by the construction workers. In some of the very first objects, an alkaline glue was used which is not recommended today since it will deteriorate the aluminum in the VIP laminate leading to a reduced service life. In the 16 objects remaining after the worst objects had been removed, 1 999 m^2 VIPs had been installed. The total percentage damaged VIPs was 4.9% in these objects. The conclusion of the study was that the percentage of damaged panels installed in a construction is low, as long as the recommendations by the producers are followed (Heinemann and Kastner, 2010). It should be noted that the study was based on infrared thermography which is a technique only possible to use when the VIPs are not covered by a highly conductive material or a ventilated air space. This is an important limitation when evaluating the thermal performance and durability of the VIPs in a finished wall.

One of the 20 constructions studied by Binz *et al.* (2005) was a listed building in Nuremberg, Germany. The retrofitting was finished in 2000 and Heinemann and Kastner (2010) investigated the building again in 2001, 2003 and 2008 with infrared thermography. The exterior of one of the gable walls was retrofitted with VIPs as shown in Figure 2.10. The 15 mm thick VIPs were secured between 35 mm thick horizontal plastic rails that were fastened in an exterior 35 mm thick layer of EPS. The VIPs were attached to the EPS with an adhesive and a vapor barrier was attached between the VIPs and the existing wall. The calculated U-value of the wall was improved from 0.7 $W/(m^2 \cdot K)$ to 0.19 $W/(m^2 \cdot K)$ which would increase to 0.32 $W/(m^2 \cdot K)$ if the panels were damaged. The infrared thermography showed a temperature difference of 0.7°C between the center-of-panel and the edge (Binz *et al.*, 2005). As can be seen in Figure 2.10 one panel underneath the two windows was damaged already in 2001. A second panel had an increased surface temperature in 2008 which indicated that it had been filled with air. The wall was overgrown with climbing plants in 2008 which made the evaluation more difficult and the thermography image less sharp. However, the remaining VIPs seem to be in good condition after 8 years of operation (Heinemann and Kastner, 2010).

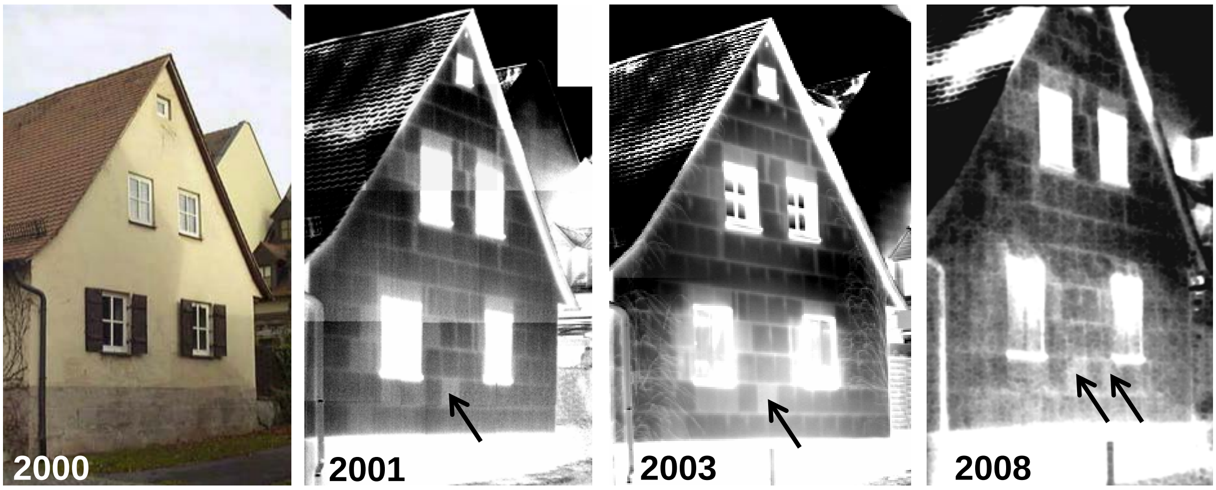

Figure 2.10. The gable of a listed building was retrofitted on the exterior with 15 mm VIPs using a special plastic rail system. The wall was afterwards investigated using thermography. From left: 2000, 2001, 2003 and 2008 (Photo: ZAE Bayern; Heinemann and Kastner (2010)).

Another façade where VIPs had been used was studied by Brunner *et al.* (2012a). The VIPs were surrounded by a layer of EPS on all sides where plaster had been applied on the exterior. One day the façade had blisters and cracks in the plaster. When the plaster was removed, 17 out of the 88 VIPs in the façade had been filled with air. The internal pressure in some of the remaining evacuated VIPs was measured and found to be above 200 mbar. Brunner *et al.* (2012a) found that the reason for the failures was that the metallization process in the production of the metalized multi-layered polymer laminate had failed. The resulting laminate had many defects in the aluminum layers resulting in a large air and moisture permeability. When solar radiation increased the temperature on the surface of the VIPs the internal pressure increased rapidly and the VIPs were blown up. This problem can be avoided in the future by careful inspection of the laminate before used as VIP envelope.

In many cases the façade of old buildings is protected for its esthetics and historical features. Using interior insulation it is possible to preserve these features. Compared to conventional insulation materials, VIPs makes it possible to reduce the thermal transmittance of the wall more with less thickness. This is beneficial from the views of the occupant and owner since the rentable floor area can be preserved. Interior insulation with VIPs was used in the retrofitting of the ground floor wall of a building from 1907 in Zurich, Switzerland. A layer of 30 mm VIPs was installed on the interior of the brick masonry wall and covered by 60 mm plaster boards. The plaster boards and VIPs were separated by a 10 mm thick air space to protect the VIPs from mechanical damages, see Figure 2.11 (Binz and Steinke, 2006; Viridén, 2007). At least one of the VIPs had been filled with air when parts of the wall were reopened. If the damage had happened during or after the construction could not be determined (Viridén *et al.*, 2004).

Figure 2.11. Interior insulation of a brick masonry wall in Zurich, Switzerland using 30 mm VIP covered by 60 mm plaster boards (Photo: Viridén + Partner AG).

In most studies of VIPs available in the literature, it was only the thermal performance of the construction that was investigated. However, also the moisture performance is important to consider since changes to existing structures will influence the risk for moisture damages. The VIP laminate is comparable to a vapor barrier in regards of vapor transfer. This may cause problems around the panels if the connection between them is insufficiently sealed. Moist air could be transported through the layer and into the cold parts of the construction. In some cases sealing tape has been used to increase the air tightness of the connections. Another option is to use an additional layer of vapor retarder to ensure a vapor tight layer.

One important issue is the resistance to fire by the VIPs since there are high demands on the resistance to burning and smoke generation for building materials. Fumed silica is nonflammable and is therefore classified A1 according to DIN-EN 13501-1 (Porextherm, 2009). On the other hand, the silica is enclosed by the metalized multi-layered polymer laminate which is highly flammable. The laminate will start decomposing at around 150°C causing production of carbon monoxide, formaldehyde and possibly other aldehydes. The laminate auto ignites at around 350°C (Microtherm, 2009) with a fast fire development. Newly developed VIPs have a 6 µm thick flame-retardant brominated acrylic copolymer coating on the outside of the laminate to increase the fire resistance. Therefore, in Germany, the VIPs are classed according to DIN 4108-10 as B2 which is the same class as for wood and other materials with normal combustibility (Porextherm, 2009).

A Norwegian investigation performed by Grynning *et al.* (2009) concluded that the building traditions in the Nordic countries are different from the traditions in central Europe. Many of the buildings with VIPs are located in Switzerland and Germany where the use of wood is less common. Norwegian single family houses are almost exclusively built using a wooden frame with a ventilated roof. This means that the conclusions from the Swiss and German studies cannot be applied directly to the Nordic countries without further studies.

When it comes to the Swedish building sector, the interest for high-performance insulation materials is huge. However, the knowledge of the materials is still poor and the cost is too high for commercial implementation on a broader scale. There have been a few Swedish demonstration projects where VIPs have been used in the construction. The increased investment cost of the VIPs can in many cases be motivated by the saved space and reduced energy use (Clase, 2010). Different retrofitting designs using high-performance insulation materials were studied by Eriksson and Svensson Tengberg (2012) in a building from the 1970s in Alingsås, Sweden. VIPs were considered as insulation of the foundation wall and slab, and underneath the floor in the bathrooms. The increased investment cost could not be motivated by the reduced energy use and improved thermal comfort for the occupants in this project. However, the VIPs could be applicable in other projects where the space for thermal insulation was more limited (Eriksson and Svensson Tengberg, 2012).

Grynning *et al.* (2009) presented a simplified economical calculation where 6 cm thick VIPs was used in an exterior wall. The thermal resistance of the VIPs was assumed to be 5 times higher than for the mineral wool with the same thickness used as reference material. At a market value of a flat or office at 17 500 NOK/m^2 (approx. EUR 2 300 per m^2) there was no additional costs for the VIPs compared to using mineral wool. In this example, the cost of the 6 cm thick VIP was 1 600 NOK/m^2 (approx. EUR 200 per m^2). Pramsten and Hedlund (2009) studied the potential of using VIPs in Swedish multi-family buildings. A wall with VIPs was compared to a wall with the same thermal transmittance using EPS. Even though they assumed that the VIPs had a 10 times higher thermal resistance than the EPS, VIPs were not found to be an economical alternative compared to EPS. Either the price of the VIPs had to decrease or the energy price had to increase to make VIPs an economical alternative for buildings. For a market value of a flat or office at 22 450 SEK/m^2 (approx. EUR 2 500 per m^2) the price of EPS and VIPs were equal. The cost of a 20 mm thick VIP was 1 800 SEK/m^2 (approx. EUR 200 per m^2). The costs of the increased design and construction times were not included in these studies.

The payback period (PBP) using VIPs in four different retrofitting scenarios was calculated by Alam *et al.* (2011). The PBP using VIPs was compared to a wall with the same thermal resistance using EPS. The thermal conductivity of the VIPs was 8 mW/(m·K) and 35 mW/(m·K) for the EPS. The PBP was 15.3 years for the case with 10 mm VIPs which decreased to 9.6 years with 25 mm VIPs. For a wall with a U-value of 0.27 W/(m^2·K), the PBP was 10 times higher for the VIPs compared to the EPS. In the fourth scenario the PBP was 6 years longer using VIPs compared to EPS. However, the EPS required 256 mm insulation thickness compared to only 60 mm thick VIPs for the same thermal resistance. The PBP was reduced significantly when the additional income from the rentable space gained by using VIPs was taken into consideration. The value of the gained space was £40/ft^2 which is approximately EUR 500 per m^2, corresponding to the average yearly rent of commercial buildings in London, UK. For a wall with a U-value of 0.24 W/(m^2·K) the increased income led to a shorter PBP using VIPs (0.8 years) than for EPS (0.9 years) (Alam *et al.*, 2011).

A life cycle cost (LCC) analysis of using VIPs in housing projects was performed by Cho *et al.* (2013). They used a thermal conductivity of the VIPs of 4.5 mW/(m·K) and a 40 year service life. Two VIP thicknesses, 20 mm and 30 mm, were studied and compared to the LCC of a wall with 75 mm conventional insulation with a thermal conductivity of 36 mW/(m·K). Despite the higher initial investment cost, both VIP thicknesses were outperforming the conventional insulation material. The 20 mm VIP reached the same cumulative LCC as for the conventional insulation material after only 3 years while the 30 mm VIP needed 4 years. After 9 years, the thicker VIP was more cost efficient than the thinner VIP (Cho *et al.*, 2013). However, as discussed in Section 2.6, a thermal conductivity of 4.5 mW/(m·K) is too optimistic for the considered service life of 40 years. Depending on the core material and envelope material, the air and moisture permeation will increase the thermal conductivity beyond 8 mW/(m·K) within 40 years which could change the conclusions of the LCC.

To make sure that the VIPs are performing according to the specifications, it is essential to control the VIPs before they are installed in the construction. A damaged VIP can be easily detected by eye, as shown in Figure 2.5. However, the performance of the VIP can be reduced well before the laminate loosens from the core. Therefore quality assurance methods have been developed to be used at the production site to detect VIPs with an internal pressure above a limit value. At the construction site there are no other methods available than visual inspection and thermography, described above. A reliable measurement method would help to evaluate the performance of the VIPs after they have been installed in the construction. The transient plane heat source (TPS) method could be a viable measurement method. The TPS method is described and evaluated in the next chapter.

3 Measuring thermal properties of VIPs

This chapter is based on the studies described in Paper I and II. Since the thermal conductivity of the VIPs is very different between the evacuated and air filled state it is important to make sure that the VIPs are undamaged when installed in the construction. The lack of fast and reliable in situ measurement methods is one of the factors that limit the applicability of VIPs on broad scale. The first section of this chapter introduces the basic properties of the tested materials and the available measurement methods. The transient plane heat source (TPS) method was tested on five different setups. The results were compared to numerical simulations and a novel analytical solution to evaluate the applicability of the measurement method based on these initial experiments.

3.1 Background and different measurement methods

The thermal properties of a material can be measured by a number of different methods. The steady-state guarded hot plate method is a common mean to determine the thermal conductivity, λ (mW/(m·K)), of a material. The method takes some time, typically several hours, since the specimen has to be in steady-state with the hot and cold plates over which the heat flow is measured.

The specific heat capacity, c_p (J/(kg·K)), of a material tells how much heat is needed to increase the temperature of a material with a given mass. It can be measured by e.g. the calorimetric method where heat is added to a specimen and the corresponding change in temperature measured. Another parameter which is important is the density, ρ (kg/m^3), of the material. The product of the specific heat capacity and density gives the volumetric heat capacity (J/(m^3·K)). These parameters together with the conductivity defines the thermal diffusivity, a (m^2/s), by

$$a = \frac{\lambda}{\rho \cdot c_p} \quad (\mathrm{m^2/s}) \tag{3.1}$$

The thermal diffusivity is a measure of how fast heat is transferred through a material. A high thermal diffusivity means that the material reacts quickly to changes in the surrounding temperature compared to a material with a low thermal diffusivity. This material parameter can be used to calculate the time dependent penetration depth, d_t (m), by

$$d_t = \sqrt{a \cdot t} \quad (\mathrm{m}) \tag{3.2}$$

where t (s) is the time after a step change in heat flow is introduced. In Table 3.1 the tabulated thermal conductivity, specific heat capacity and density of polystyrene, aluminum, fumed silica and metalized multi-layered polymer laminate (VIP laminate) are presented. The thermal diffusivity has been calculated based on these values and the penetration depths are for a measurement period of 160 s.

Table 3.1. Tabulated material properties and penetration depth after t = 160 s.

Material	λ (mW/(m·K))	ρ (kg/m^3)	c_p (J/(kg·K))	a (mm^2/s)	d_t (mm)
Aluminum	230 000	2 700	920	91	120
EPS	32	29	1 800	0.63	10
Silica (evacuated)	4	175	850	0.027	2.1
Silica (air filled)	20	175	850	0.13	4.6
VIP laminate	2 000	1 100	1 800	1.0	13

With an up to ten times higher thermal diffusivity in the VIP laminate compared to the fumed silica, direct measurement of the thermal performance is complicated. As discussed in Section 2.7, there exists measurement methods developed for the production site. Either a direct pressure measurement or an indirect indicative method can be used. Alam *et al.* (2011) summarized the different methods and discussed briefly advantages and disadvantages.

One of the available direct pressure measurement methods is the foil lift-off method where the VIPs are placed in a pressure chamber. The pressure in the chamber is reduced until the laminate separates from the core material and the internal pressure can be determined. Another direct pressure method is the spinning rotor gauge which is connected to a valve on the VIP. This is a fast and accurate method, as long as leakages around the valve can be avoided. These are simple methods but not suitable for large sets of VIPs since they require manual handling. A method that allows for monitoring of a large number of VIPs is remote sensing by active or passive chips using the RFID technique. This method also allows for follow-up measurements after the VIPs have been installed in the construction (Alam *et al.*, 2011).

Another approach is to use an indirect indicative method, i.e. by e.g. measuring the thermal conductivity of the VIP. These methods rely on the empiric relation between the internal pressure and the thermal conductivity. An indirect method was developed by Caps (2004) where a metallic disk and a fiber material are inserted in the core material. A heated sensor is placed on the surface and cooled down. The temperature decline is registered and with knowledge of the thermal conductivity at different pressure, the internal gas pressure can be determined (Caps *et al.*, 2008). The method has been used for some years and works well under well-defined conditions and for a specified VIP. However, Erbenich (2009) concluded that it does not exist a method that can be used on the construction site to measure the thermal properties of VIPs.

Forsberg and Sørensen (2012) tested an acoustic test method on two VIPs. An evacuated VIP was compared to one filled with air. The difference between the two cases is not only that the laminate loosens from the core, as shown in Figure 2.9, but also that the stiffness of the VIP is changed. The VIPs were glued to a concrete wall and a microphone recorded the sound from tapping a hammer on the surface. There was a difference between the two cases where the evacuated panels had a more even frequency distribution than the air filled VIP, where the lower frequencies were more dominating (Forsberg and Sørensen, 2012). The method is promising but requires more investigations. The difference between the evacuated and the air filled VIP might not be large enough to be detectable on a construction site and the results are very much dependent on the acoustic mass of the material behind the VIPs.

The measurement method developed by Caps (2004), which is the most used method today, is a transient measurement method. Another similar method which can be used for a wide range of materials is the TPS method which is described in the next section.

3.2 The transient plane heat source (TPS) method

The general and specific procedures of the TPS method for measurements of thermal properties are described in SS-EN ISO 22007-2. The method uses a sensor composed of a 10 μm thick double nickel spiral, sandwiched between two layers of 25 μm thick kapton (polyimide film). The spiral serves both as heat source and as electric resistance thermometer. A constant electric power is supplied through the spiral which develops heat by the electric resistance of the nickel raising the temperature of the sample. The rate of the temperature increase depends on how quickly the heat developed in the sensor is conducted away through the surrounding materials. Heating is continued for a period of time, with the voltage across the spiral being registered. As the current is held constant, the voltage changes in proportion to changes in the electric resistance of the spiral. The sensor is clamped between two samples of the material as shown in Figure 3.1. With knowledge of the temperature variation with time, i.e. the variation of voltage, and the supplied heat flow, it is possible to calculate the thermal conductivity and volumetric heat capacity of the material. The samples of the material should not be smaller than the penetration depth defined by Equation 3.2. Otherwise, the temperature in the sensor will be affected by the heat wave reaching the boundary.

Figure 3.1. Left: TPS sensor on a VIP. Right: measurement setup with the sensor clamped between two VIPs. There was a pressure of 4.7 kPa applied on the upper sample to increase the contact with the sensor. (FIG 1 in Paper II).

To study the influence of the contact heat transfer resistance, Forsberg and Sørensen (2012) studied a number of different setups with VIPs with the TPS method. The pressure created by the weight on top of the upper sample was varied and a water and glycerin based gel was tested to increase the contact with the sensor. The pressure did not have any major influence on the temperature increase in the sensor, but the gel significantly decreased the temperature increase which indicates a lower contact heat transfer resistance using the gel. They also tested an evacuated VIP and compared the temperature increase to one filled with air. The comparison is presented in Table 3.2.

Table 3.2. Comparison of the temperature increases measured with the TPS sensor on an evacuated VIP and one filled with air after different time. The temperatures are given as the average of 10 measurements with a standard deviation of the mean with a confidence interval of 68.3%. The differences are given as the percentage of the temperature difference divided by the temperature increase of the air filled VIP. There was a pressure of 3.0 kPa applied on the upper sample during the measurements.

	Temperature increase (°C)		
Time (s)	Evacuated VIP	Air filled VIP	Difference (-)
40	4.42 ± 0.04	3.12 ± 0.01	42%
80	6.06 ± 0.04	4.22 ± 0.01	44%
120	7.06 ± 0.04	4.87 ± 0.01	45%
160	7.77 ± 0.04	5.33 ± 0.01	46%

To evaluate the TPS method further, five different setups with different materials were tested. The measurements on only the VIP setup is limited to two basic cases; one evacuated and one air filled case, as investigated above. Therefore EPS, EPS covered by aluminum foil and EPS covered by VIP laminate were measured with the TPS sensor. The average dimensions of the polystyrene were about 70 mm x 70 mm x20 mm (length x width x thickness) and the VIPs were 300 mm x 300 mm x 20 mm. The measured thicknesses of the aluminum foil and metalized multi-layered polymer laminate were 10 µm and 100 µm respectively. Each setup was tested at least 3 consecutive times with a break of 20 minutes between each measurement to make sure it was cooled down to the surrounding air temperature of 20.5°C. The heat supply in the measurements was 0.02 W through a 6.4 mm radius sensor during 160 s. The measurement results are presented in Figure 3.2

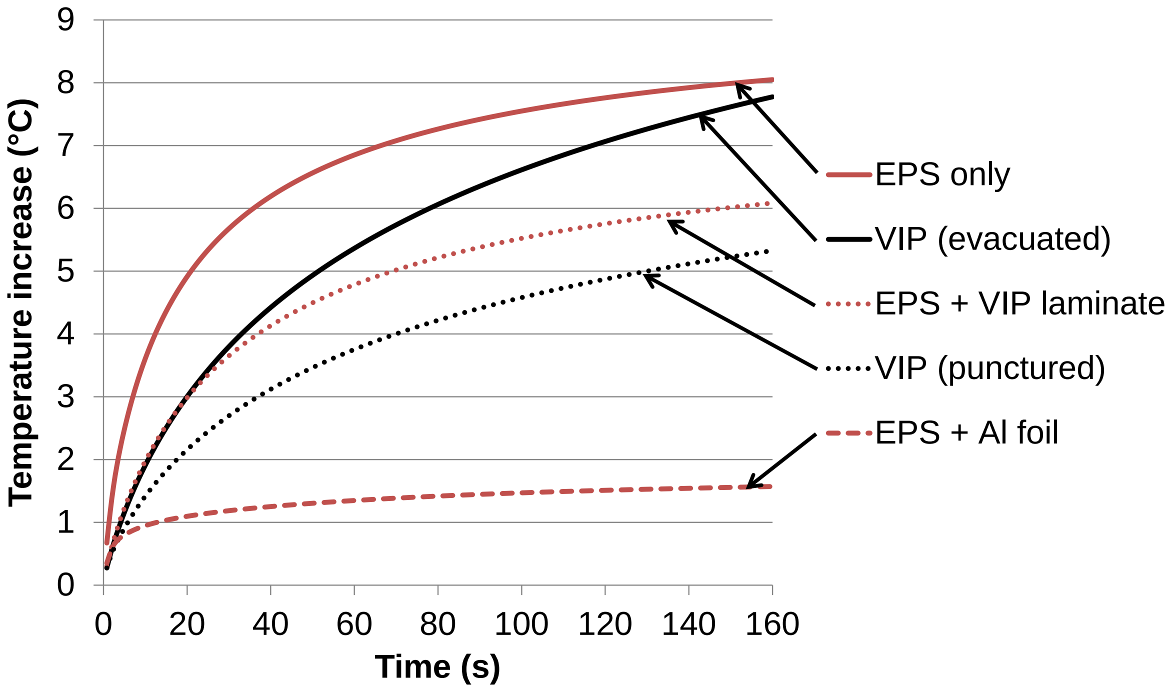

Figure 3.2. Average measured temperature increase in the five setups with a power of 20 mW supplied during 160 s in the 6.4 mm TPS sensor. All materials were measured with 4.7 kPa applied on the upper sample (FIG 3 in Paper II).

A reliable measurement procedure should have a low standard deviation for repeated measurements. One way to evaluate the reliability is by using the coefficient of variation (CV), i.e. the standard deviation divided by the average measurement result. The CV was 0.12% for the EPS setup while it was 0.79% and 0.21% for the EPS with VIP laminate and aluminum foil, respectively. For the evacuated and air filled VIP setups, the CV was 0.56% and 0.18%, respectively. The low CV indicates a good reliability and repeatability of the TPS measurements on the five setups.

The temperature increase was highest for the EPS setup. The heat was spread away from the sensor area through the highly conductive layer in the two setups where the EPS was covered by aluminum foil and VIP laminate. Even though the VIP laminate is 10 times thicker than the aluminum foil, the heat was spread faster in the latter setup which shows the substantially higher thermal conductivity in the aluminum foil than in the VIP laminate.

For the evacuated VIP and the EPS, the temperature increase only differed by 0.2°C while the thermal conductivity of the evacuated VIP was one eighth of the EPS. This discrepancy shows the importance of the laminate and the contact surface between the sensor and laminate. The rugged laminate, created by the vacuum in the VIP, gets less rugged when the VIP is filled with air. This effect increases the heat transfer through the laminate.

3.3 Comparison of measurements and simulations

To evaluate the TPS method, a numerical three-dimensional model was developed and described in Paper I and II. The numerical model was validated by comparing the results with an analytical solution for the isotropic EPS setup. In Paper II, a novel analytical solution

(Claesson, 2012) was used for the case of an isotropic material covered by a highly conductive layer. The calculated temperature increase deviated with less than 0.1% between the numerical model and the analytical solution after 160 s. Figure 3.3 shows the temperature increase measured with the TPS sensor compared to the calculated temperature increase.

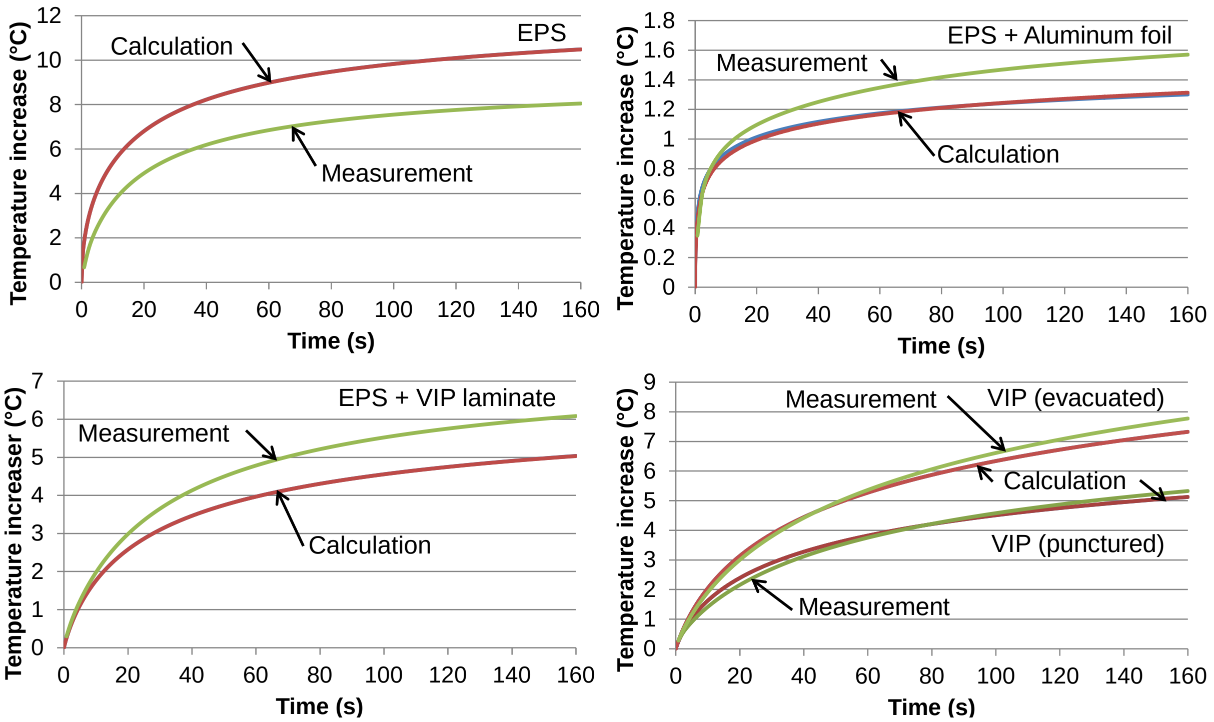

Figure 3.3. TPS measurements compared to the analytical solution for the five setups. Top left: EPS setup. Top right: EPS covered by aluminum foil. Bottom left: EPS covered by VIP laminate. Bottom right: air filled (punctured) and evacuated VIP. (FIG 4 in Paper II).

The calculated temperature increase was lower for all the cases where the isotropic material was covered by the highly conductive layer. For the isotropic EPS setup, the calculated temperature was 30% higher than what was measured with the TPS sensor. The deviation decreased to 17% when the EPS was covered by the aluminum foil and the VIP laminate. For the evacuated and air filled VIP, the temperature increases deviated with 5.8% and 3.8% respectively. The deviations between the measured and calculated temperature increases could be caused by inhomogeneity in the material. These were not taken into account in the numerical model and analytical solution.

The deviations between the measurements and calculations could also be caused by the surface properties of the materials. The contact between the sensor and the material surface is not perfect and could induce an additional contact heat transfer resistance at the surface. As mentioned above, a gel significantly decreased the temperature increase in the VIP setups which indicates a lower contact heat transfer resistance using the gel. On the other hand, the measured temperature increase of the EPS setup suggests an additional heat flow path not taken into account in the model. The properties of the contact heat transfer resistance should be investigated further using e.g. larger sensor dimension to rule out any inhomogeneity in the materials. The TPS method is applicable in the laboratory but the equipment is too large to perform field measurements. It needs further development to reduce the size and weight.

4 Field study of a wall retrofitted on the exterior

In the field study a brick and homogenous wooden wall lacking thermal insulation was insulated on the exterior with VIPs. The changed moisture performance of the existing structure and the influence by thermal bridges were analyzed and compared to a non-insulated reference wall. A pre-study where the retrofit design was investigated using a hygrothermal simulation tool was presented in Paper III. The numerically simulated temperature and relative humidity (RH) was compared to the 2.5 years measurements in the retrofitted wall in Paper IV. The numerical simulations were refined using the measured indoor and outdoor climate together with more accurate material data and air flow through the wall to explain the deviations between the simulated and measured hygrothermal performance.

4.1 Description of the field study building

The building chosen for the field study is a county governor’s house (landshövdingehus) from 1930, see Figure 4.1. This is a typical historical building for the city of Gothenburg on the Swedish west coast. Most of them were constructed during 1876-1936 following an approval by the county administrative board to build two wooden floors on top of a brick or stone masonry ground floor in order to circumvent the fire regulations that limited the height of wooden buildings to two floors. At that time Gothenburg experienced severe lack of housing due to the massive migration of people from the rural areas surrounding the city. During the period 1880-1940 the population of Gothenburg more than tripled from around 100 000 to 300 000 inhabitants, creating a high demand on affordable housing. Today, there are approximately 1 400 buildings left of this type around the city. However, the original stock was larger but due to the very low technical standards of the apartments in the buildings many of them were demolished in the 1960s and 1970s (Larsson, 1973).

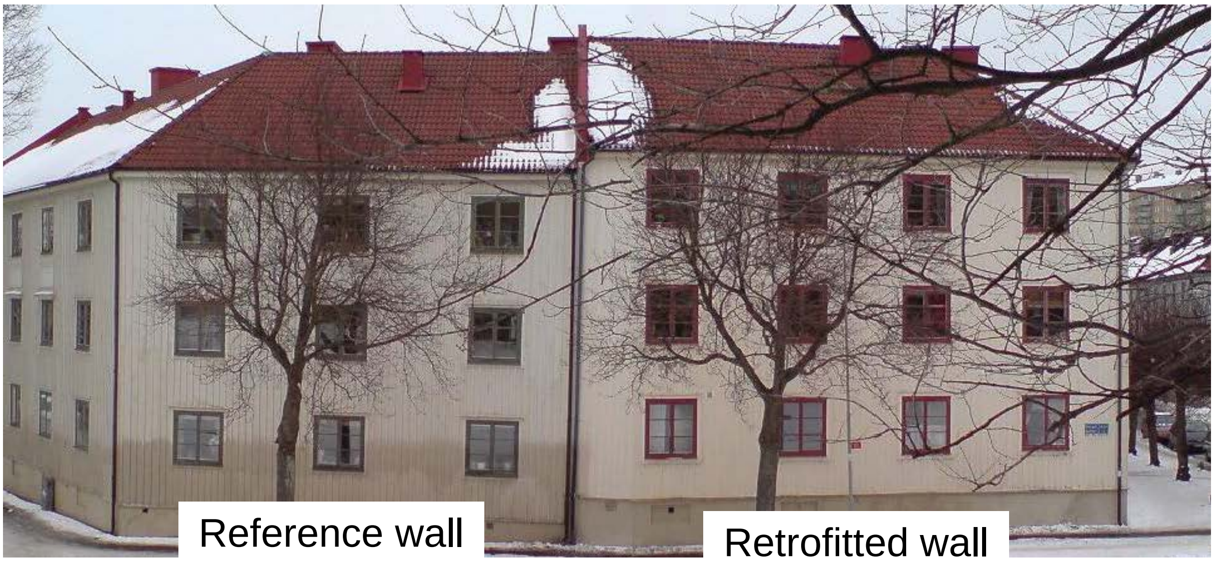

Figure 4.1. The three story county governor’s house from 1930 chosen for the field study. The right part of the façade was retrofitted with vacuum insulation panels while the left part only had the wooden cover boards replaced and worked as reference wall (FIG 1 in Paper III).

The building was built in 1930 when it was common that the ground floor was built in 1.5 stone brick masonry which gave a thickness of approximately 340 mm. The two wooden floors have walls of 80 mm standing wooden planks in three layers with flax between the boards to increase the air tightness. On the exterior a 22 mm thick vertical wooden cover board with rib flanges was mounted on top of a wind and waterproof tar paper. The interior side of the walls were originally covered with plaster on reed and wooden battens (Larsson and Lönnroth, 1972).

The moisture content in the wall was measured in June 2010 when holes in the wooden cover board were drilled and the moisture quotient measured with a resistance moisture meters (pin-type). The moisture quotient was approximately 9% close to the surface of the wooden planks while it was around 8% a few cm into the construction. In the brick grout, wooden laths were found which had a moisture quotient of 12% at the surface and 9.5% further in. The critical moisture quotient for mold growth on a wooden surface is around 20%. Figure 4.2 shows the condition of one of the window frames and the materials behind the wooden cover board.

Figure 4.2. At a visit to the buildings, holes were drilled through the wooden cover board to investigate the condition of the materials behind. The worst places were around windows (left) and in the wooden laths found in the grout between the bricks (middle). The wooden planks had flax between the planks (right) to increase the air tightness of the wall.

The two different structural materials, brick on the ground floor and wooden planks on the two upper floors, have different critical moisture levels. Wood is susceptible to moisture and a RH above 75-80% together with a temperature above 0°C during a consecutive time period could initiate mold growth on the wooden surface. Brick, on the other hand, is vulnerable to freeze-thaw action on the exterior surface which may cause cracks in the brick. These problems would increase with a retrofit solution where the insulation is placed on the interior side of the wall. Choosing a solution with insulation on the exterior, the existing materials get a better protection from the surrounding weather such as driving rain. The old structure is exposed to higher temperatures and with unchanged moisture conditions in the wall the RH should decrease.

4.2 Retrofit design

Depending on which U-value that is targeted for the wall after retrofitting, the thickness of the VIPs can be varied. Because of the listing of the building, the exterior appearance cannot be changed. This limits the overall thickness of the wall and thereby the achievable U-value. The wall thickness is limited by the connection between the wall and the roof, and it should remain as it was before. Also the connection between the wall and a fire wall which separates the building from the wall of the next building, see Figure 7 in Paper IV, should be kept. Discussions in the design team and with the building owner Familjebostäder i Göteborg AB resulted in an allowed additional thickness of 80 mm without risking the original features of the façade. This solution demanded that the old windows were moved 80 mm outwards, to be in line with the new façade. A protection layer of 30 mm glass wool boards was proposed to be installed over the entire VIP surface. The thickness of the VIPs was decided to be 20 mm. With the 30 mm thick layer of glass wool on the exterior of the VIPs, 30 mm remained. An air space, 28 mm wide, was added to the façade, see Figure 4.3, to allow for drying of possible moisture entering through the wooden cover board. One difficult detail of the design was the attachment of the wooden cover board on the façade. The chosen solution, presented in Figure 4.3, shows strips of glass wool boards, 50 mm wide and 20 mm thick, between the VIPs that allows for the wooden cover board to be attached without damaging the VIPs. Another difficult detail was the insulation around the windows. The irregularities of the old wall made it impossible to use VIPs here. Therefore glass wool boards were used to fill the space between the VIPs and windows.

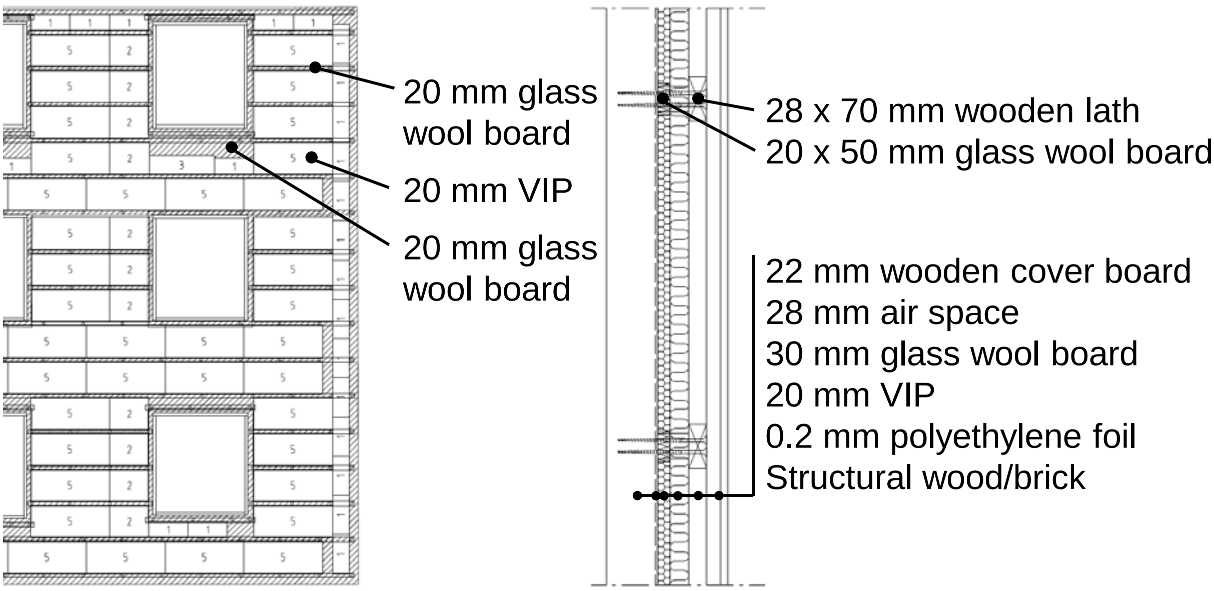

Figure 4.3. Wall layout after retrofitting with 20 mm VIP and 30 mm glass wool boards. (Figure 5 in Paper IV).

If the wall had been insulated with a continuous layer of 20 mm VIPs, the theoretical U-value was 0.22 W/(m^2·K), as shown in Figure 4 in Paper IV. However, in the final retrofit design 62% of the façade is covered by VIPs, 17% is covered with glass wool boards and the remaining 21% are windows. The parts of the façade with glass wool boards create thermal bridges through the VIP layer which are described more in detail in next section. Also the metalized multi-layered polymer laminate around the VIPs contributes to a higher heat flow. With these thermal bridges taken into account, the average U-value of the wall increased to 0.40 W/(m^2·K) which is 82% higher than of the wall with a continuous VIP layer. However, the calculated U-value of the wall after the retrofitting was reduced to 36% of the U-value before retrofitting, which is a substantial improvement.

During the reconstruction phase of the façade it proved to be difficult to follow the new technical drawings of the façade. Although great concern had been given to the design of the wall to follow the original measurements, the laser scanning had been based on a point in the lower left corner of the façade which was removed when the old wooden cover board was torn down. This meant that the required number of VIPs of specified sizes did not match the drawings. The problem was solved by rearranging the original layout and by ordering additional panels, 10% of each size. At the end only minor changes had to be done to the original design. Of the 180 panels installed in the wall three panels (1.7%) had a loose laminate which meant they had been punctured or damaged before they reached the construction site or during construction. These VIPs were exchanged to panels without visibly detectable damages.

4.3 Energy calculation

It was not possible to measure the energy use for heating and domestic hot water in the building since the heat was supplied to a larger block of buildings by district heating. The measured energy use for a similar building from 1930 in Gothenburg was 129 kWh/m^2 annually (Nilsson, 2009). A county governor's house with a measured annual energy use of 126 kWh/m^2 was studied by Molander and Olofsson (2012) who investigated different ways to reduce the peak heating power demand of the building. The simulation model adapted to their study was used here to calculate the expected reduction in energy use after the retrofitting. The model was developed in Matlab and Simulink (MathWorks, 2011) and validated by (Mata *et al.*, 2013). The energy use is calculated by an energy balance for the building where one thermal zone is modeled on hourly resolution. The thermal inertia of the building is represented by its effective internal heat capacity. The temperature of the indoor air and all the interior surfaces are assumed to be the same. The energy use for heating is defined as the heating power required to maintain a given indoor temperature using a heating system with finite power and response time (Mata *et al.*, 2013). Internal heat gains from people and appliances, solar radiation, air leakages and natural ventilation are included in the simulation model (Molander and Olofsson, 2012).

Based on the technical drawings of the field study building, it was estimated that 21% of the façade was covered by windows with a U-value of 3 W/(m^2·K) which were kept after the retrofitting. The U-value of the roof and floor were estimated to be 0.5 W/(m^2·K) and 0.9 W/(m^2·K) respectively. The U-value of the wall was calculated with regard to the thermal bridges created by the glass wool between the VIPs and around the windows, and the laminate around the VIPs. The U-values and the linear thermal transmittance were calculated using the finite difference calculation software HEAT2 (Blocon, 2000). The surface heat transfer resistance, R_s (m^2·K/W), is due to the combined effect of heat transfer by convection and radiation. Here, the standard values for the surface heat transfer resistance on the interior, R_{si} = 0.13 m^2·K/W, and exterior, R_{se} = 0.04 m^2·K/W, were used respectively. The thermal conductivity and thicknesses of the materials in the calculations are presented in Table 4.1.

Table 4.1. Thermal conductivity, λ (mW/(m·K)), and thickness, d (mm), of the materials in the U-value calculations for the wall construction in Figure 4.3. The values are generic values from HEAT2 (Blocon, 2000) except for the values of the VIP (Tenpierik and Cauberg, 2007). The x- and y-directions are defined by the heat flow which is mainly in the x-direction.

Material	Thickness d (mm)	Thermal conductivity λ (mW/(m·K))	
		x-direction	y-direction
Wood	80	140	90
Brick	340	600	600
VIP core	19.8	5	5
VIP laminate	0.1	540	200 000
Glass wool board	30	40	40
Air space	38*	180	180
Wooden cover board	22	140	90

*Should be 28 mm, a mistake in the numerical model. Less than 1% influence on the U-value.

The size of the calculation domain was determined by finding the location in the wall with the thermal bridge where the temperature was deviating less than 1% compared to the wall without any thermal bridge. The U-values were compared and the difference was divided with the width of the thermal bridge to calculate the linear thermal transmittance as discussed in Section 2.5. The calculated linear thermal transmittances are presented in Table 4.2

Table 4.2. Calculated linear thermal transmittance, Ψ (mW/(m·K)), for the two different arrangements with only a VIP laminate between the VIPs and for the case with 50 mm wide glass wool strips between the VIPs. The calculations were performed in HEAT2 (Blocon, 2000).

Thermal bridge	Linear thermal transmittance Ψ (mW/(m·K))	
	Wood	Brick
Laminate between the VIPs	67.8	75.9
Glass wool strips between the VIPs	80.2	88.7

The values in Table 4.2 can be compared to the linear thermal transmittance found in the literature and presented in Section 2.5. The linear thermal transmittance was 2-12 mW/(m·K) depending on the width of the gap between the panels (Schwab *et al.*, 2005), while the guarded hot plate measurements showed 9 mW/(m·K) (Ghazi Wakili *et al.*, 2004). By separating the VIPs with a 50 mm wide insulation material of 35 mW/(m·K), the linear thermal transmittance for a 20 mm thick VIP was 29 mW/(m·K) (Sprengard and Spitzner, 2011). These are substantially lower values than the calculations presented in Table 4.2 which were 3-7 times higher. This deviation is caused by the very high thermal conductivity of the VIP laminate which is here considered to be more similar to aluminum than what is the case in reality. In the following, the higher values for the linear thermal transmittance will be used since these are more conservative.

The calculated U-value before the retrofitting was 1.1 W/(m^2·K) for both the brick and wood wall. The calculated U-value of a wall with a continuous layer of 20 mm VIPs with a thermal conductivity of 5 mW/(m·K) was 0.17 W/(m^2·K). After 25 years, when the thermal conductivity of the VIPs increases to 7 mW/(m·K), the U-value was 0.22 W/(m^2·K). The thermal bridges created by the VIP laminate, presented in Table 4.2, also increased the U-value from 0.17 W/(m^2·K) to 0.22 W/(m^2·K). The glass wool strips added to an even higher heat transfer with a total U-value of 0.4 W/(m^2·K). Using the values from the literature for the thermal bridges, the U-value increased to 0.18 W/(m^2·K) and 0.28 W/(m^2·K) for the VIP laminate and VIP laminate and glass wool strips, respectively. Consequently the U-value increases by 43% if the calculated linear thermal transmittances in Table 4.2 are used. The calculated U-values are summarized in Table 4.3 in next section.

In the energy calculations, the total average U-value was increased by 5% to include the effect of the additional thermal bridges between building elements. The interior temperature was set to 21°C. The energy use was calculated for 2011 when the average outdoor temperature was 9.6°C with a maximum temperature of 21.5°C and minimum of -12.7°C. The natural ventilation of the building was assumed to be 0.28 l/(s·m^2), corresponding to 0.37 1/h. This is slightly lower than the 0.4 1/h measured by Boverket (2010) in buildings with natural ventilation. The air leakages were at maximum 1 l/(s·m^2) which depends on the air velocity on the building envelope. Internal heat gains from people, appliances and solar radiation, were also included in the simulation model (Molander and Olofsson, 2012). Figure 4.4 shows the heat losses distributed on the transmission through the walls, windows, floor and roof, and through the ventilation and air leakages before and after the retrofitting.

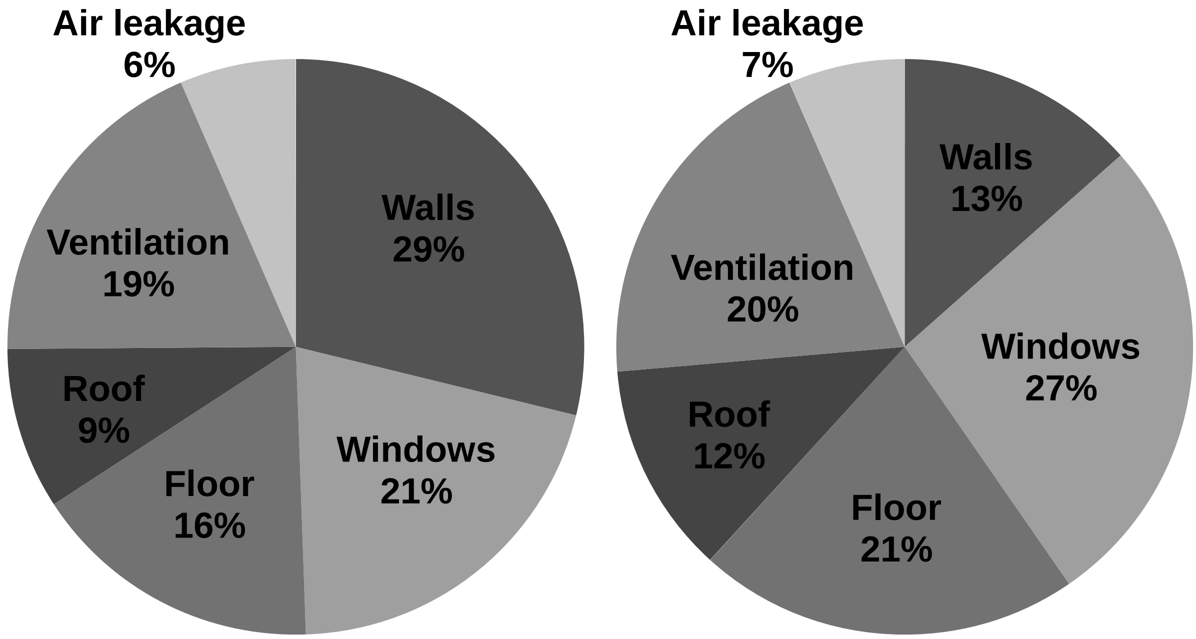

Figure 4.4. Distribution of the heat losses by transmission through the walls, windows, floor and roof, and by the ventilation and air leakages. Left: before the retrofitting. Right: After the retrofitting.

The calculated annual energy use before retrofitting was 158.7 kWh/m^2 for heating and domestic hot water. The internal heat gains from solar radiation and people and appliances as well as the losses due to ventilation and air leakages were the same after the retrofitting. The transmission losses through the walls were reduced by 23% after the retrofitting which led to a reduced need for heating by 24%. With the domestic hot water taken into account the calculated energy use after the retrofitting was 127.5 kWh/m^2. This is 20% less than the energy use before the retrofitting. As a comparison, changing the windows to windows with a U-value of 1 W/(m^2·K) gave an energy use reduction of 15% and the combination of changing windows and installing VIPs gave an energy use reduction of 34%.

The influence by the thermal bridges between the panels was also studied for the energy use. If the thermal bridges could be totally eliminated, the energy use would be 118.3 kWh/m^2 which is a 25% reduction compared to the case before retrofitting. Using the lower linear thermal transmittance from the literature, the energy use was reduced by 23% to 122 kWh/m^2. This means between 3-7% of the total energy use was caused by the thermal bridges between the VIPs. Therefore it is clear that the retrofit solution has to be designed in a way that minimizes the effect by the thermal bridges. This could be done by e.g. adding a second layer of VIPs which reduces the thermal bridges with 64-72% (Ghazi Wakili *et al.*, 2011) or by covering the VIPs on both sides with another thermal insulation material.

With time the VIPs will be filled with air due to the irreversible air and moisture diffusion through the VIP laminate. The consequences by the different percentages of air filled VIPs on the total energy use are presented in Figure 4.5.

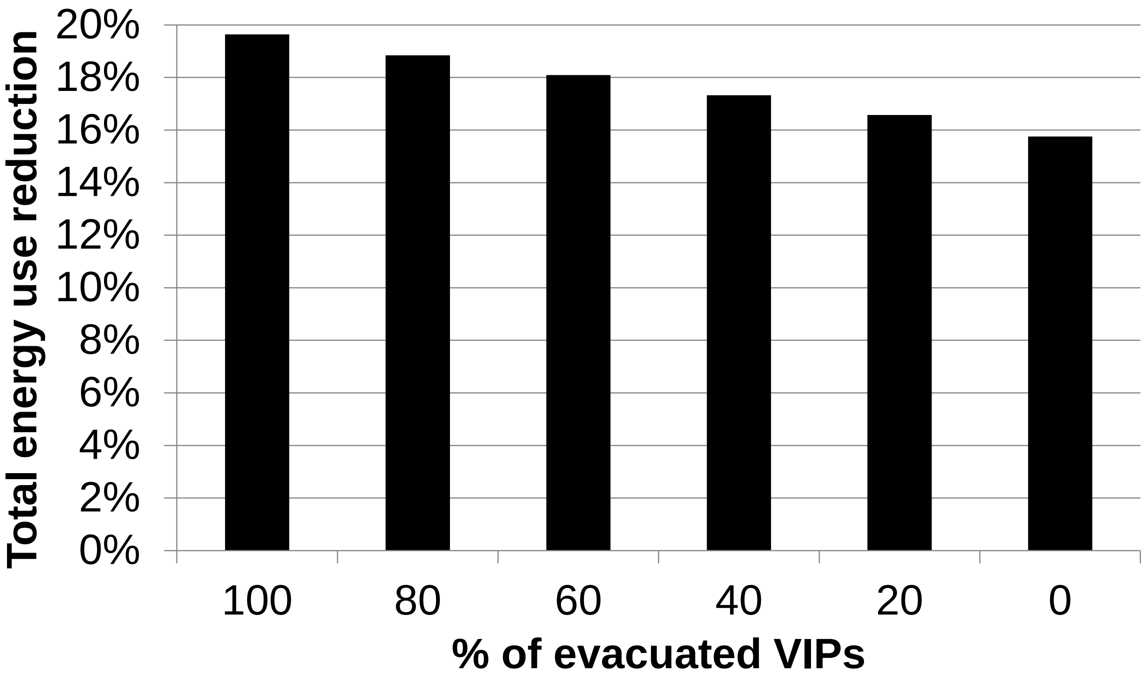

Figure 4.5. Reduction in energy use for different scenarios of the amount of air filled VIPs. The energy use is shown as the reduction of the energy use divided by the energy use before the retrofitting

The total energy use was reduced with more than 25% for the case with a continuous VIP layer without any thermal bridges. With regard to the thermal bridges in the façade, the reduction became 20% with all the VIPs evacuated. The energy use will increase with time and after the service life of the VIPs, when they are all air filled, the energy use was 133.7 kWh/m^2. Therefore the energy use of the building will increase by 5% during the service life of the VIPs. This still means a 16% energy use reduction, equal to 25 kWh/m^2 annual energy savings compared to the energy use before the retrofitting.

4.4 Infrared thermography and air tightness

There were complaints from the occupants on an insufficient thermal comfort in the building due to draft and low surface temperatures. One of the few means available to evaluate the improved thermal performance of the retrofitted wall is by infrared thermography. The building was investigated before and after the retrofitting finished by SP Technical Research Institute of Sweden. They also used the blower door method to evaluate the air tightness of the building. The aim was firstly to quantify how much the internal wall temperatures had increased and secondly to investigate how much the thermal transmittance of the wall had improved. It was discovered that the indoor air temperature varied between 21-25°C in the apartments while the wall surface temperature was around 1.5-2.4°C lower. After the retrofitting, the wall surface temperature was only around 0.3-0.8°C lower than the indoor air temperature which is a substantial improvement. Any clear conclusions of changed air tightness after the retrofitting could not be made based on the blower door measurements. The air leakage paths were dominated by leakages around the windows, at the connections between the interior and exterior wall and along the floor. The results and measurement procedure were discussed more deeply in Paper IV.

The infrared thermography results could also be used to calculate an approximate U-value of the wall before and after the retrofitting. These U-values are not at all accurate and only show an indication of how much the wall was improved after the retrofitting. The calculated U-values based on the thermography are presented in Table 4.3 and compared to the U-values which were calculated using HEAT2 (Blocon, 2000).

Table 4.3. Calculated based on the infrared thermography compared to the U-values calculated with HEAT2 (Blocon, 2000) and the values in Table 4.1.

<table>
<tr><td colspan="2" rowspan="2"></td><td colspan="2">U-value (W/(m^2·K))</td></tr>
<tr><td>Before</td><td>After</td></tr>
<tr><td colspan="2">Infrared thermography</td><td>0.67-0.98</td><td>0.12-0.36</td></tr>
<tr><td rowspan="7">Calculated with HEAT2</td><td>No thermal bridges</td><td>1.1</td><td>0.17</td></tr>
<tr><td>No thermal bridges
λ_{VIP} = 7 mW/(m·K)</td><td></td><td>0.22</td></tr>
<tr><td>Linear thermal transmittance in Table 4.2
(only the VIP laminate)</td><td></td><td>0.22</td></tr>
<tr><td>Linear thermal transmittance in the literature
(only the VIP laminate)</td><td></td><td>0.18</td></tr>
<tr><td>Linear thermal transmittance in Table 4.2</td><td></td><td>0.40</td></tr>
<tr><td>Linear thermal transmittance in the literature</td><td></td><td>0.28</td></tr>
<tr><td>All VIPs filled with air and the linear
thermal transmittance in Table 4.2
λ_{VIP} = 20 mW/(m·K)</td><td></td><td>0.54</td></tr>
</table>

It is clear that the U-value of the wall was improved after the retrofitting. However, it is difficult to quantify the improvement based on the temperatures measured with the infrared thermography. Most of the calculated U-values for the case after the retrofitting are within the measured U-value span. The variations of the local heat flow created by the thermal bridges were not visible on the thermograms. It was also investigated if any potentially damaged panels could be detected using the infrared thermography from the exterior, as was exemplified in Figure 2.10. Also the case before and after the retrofitting were compared. These thermograms are presented in Figure 4.6.

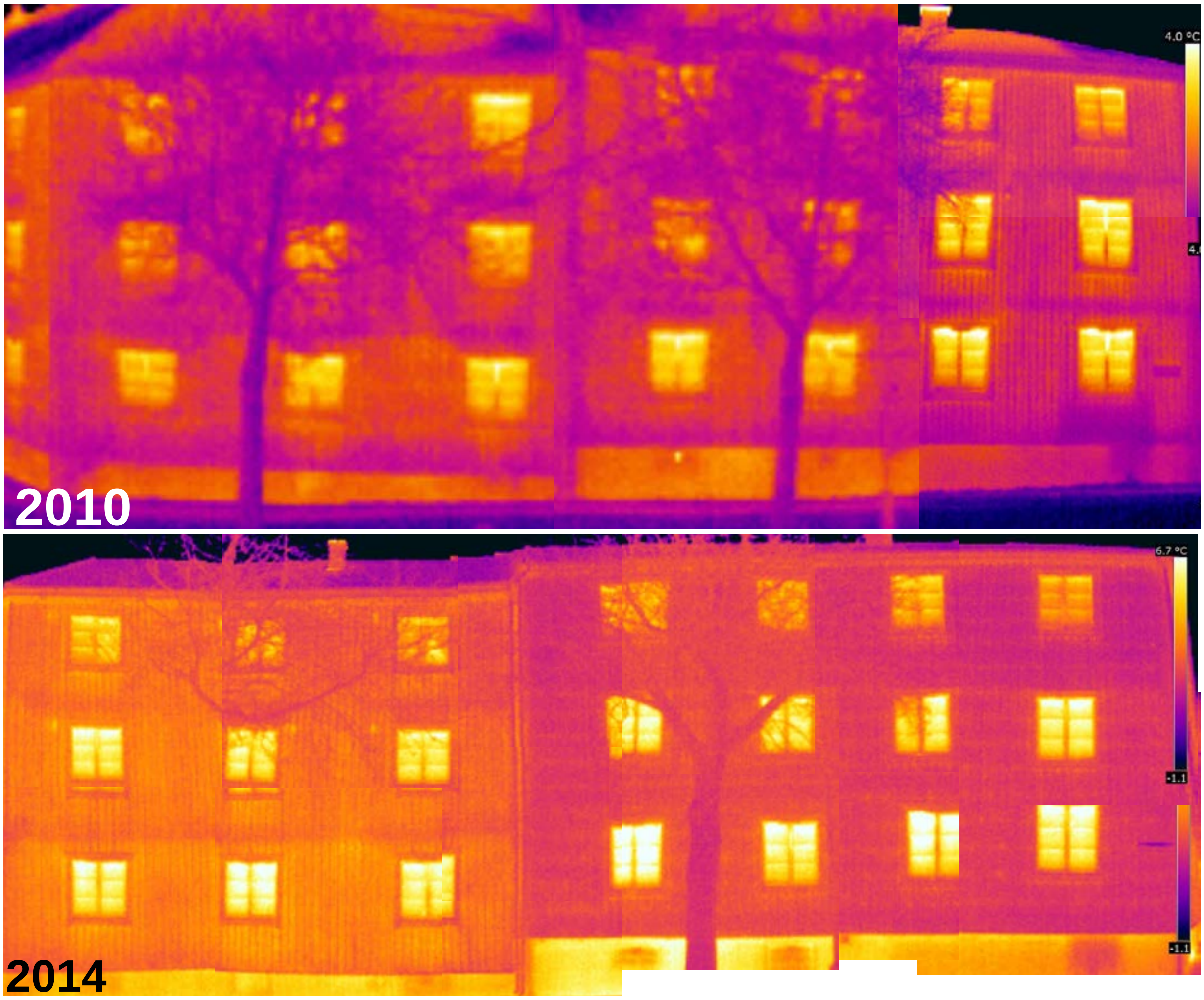

Figure 4.6. Thermograms of the exterior of the wall taken before (top) and after (bottom) the retrofitting. The figure is created by using multiple thermograms. The 12 windows (orange to yellow color) on the right of the wall belong to the retrofitted wall, while the 9 windows on the left of the wall belong to the reference wall.

The thermogram of the wall before the retrofitting was taken on February 15, 2010, and the termogram after the retrofitting was taken on February 11, 2014. Both days were cloudy with around -4°C and 3°C outdoor, respectively. It is clear that the wall surface temperatures were more similar between the two parts of the wall before the retrofitting with the intermediate floor clearly visible. After the retrofitting, the surface temperature was around 1°C lower on the retrofitted wall compared to on the reference wall. The surface temperature is more even and it is not possible to detect the intermediate floor anymore. It is also impossible to detect any areas on the retrofitted wall with higher surface temperatures that could be expected from air filled VIPs. The façade is ventilated and the glass wool covering the VIPs contributes to even out the potential temperature differences. Therefore, the infrared thermography cannot be used to detect thermal bridges around the VIPs and any air filled VIPs in this wall.

4.5 Hygrothermal measurements

To evaluate the hygrothermal performance of the retrofitted wall, temperature and RH sensors were installed in the wall and monitored for 2.5 years. The sensor positions are presented in

Figure 7 and 8 in Paper IV. In total 15 wireless temperature and RH sensors were installed in the retrofitted and reference wall. Four sensors were installed in the retrofitted brick and wood wall each. In the wood wall, one sensor was located behind the center-of-panel, VIP-VIP connection, glass wool strip and window frame on the interior of the polyethylene foil. The intention was to have an identical layout in the brick wall, but the exact position behind the VIP-VIP connection was missed and the sensor was located too low which meant two sensors monitored the glass wool strip. In the reference façade, two sensors were located behind the wooden cover board, as shown in Figure 7 in Paper IV, one in the brick and wood wall, respectively. Furthermore, one sensor was located in the kitchen of each of the four apartments closest to the monitored part of the wall to obtain the indoor conditions. The final sensor monitored the outdoor temperature and RH at the building site. It was located in a perforated plastic box placed underneath the roof eave facing southwest. Solar radiation influences the measurements and therefore it was not the air temperature that was measured, but an effective (solar-air) temperature of the wall. The sensor was protected from rain and the whole box was ventilated through a number of holes drilled in its bottom.

The sensors were driven by a battery with approximately 15 years lifetime. The signals from the sensors were collected through a wireless connection every hour by a gateway located on the attic of the building. The sensors were 60 mm x 40 mm x 28 mm (length x width x height) and measured the temperature and RH of the air in the void where the sensor was installed. The measurement accuracy of the sensors was ±2.5% for RH in the range of 10% to 90% and ±0.5°C at 25°C. The temperature could be measured between -40°C to 85°C (GE Sensing, 2007). The sensors were tested and calibrated by SP Technical Research Institute of Sweden before they were installed in the wall.

After some initial problems with the sensors, described in Section 3.5 in Paper IV, there is now more than 2.5 years of data available for the hygrothermal analysis. The measurements were started in October 2010, but the data before January 2011 are too incomplete to be included in the analysis. There were some hours with missing data also later during the measurement period. These short gaps were filled by linear interpolation. In Paper IV, the measurement results for the period between January 2011 and February 2013 were presented and analyzed. The temperature variation in the wall was much lower in the retrofitted wall than in the reference wall as shown in Figure 11 in Paper IV. Also the average RH was lower in the retrofitted wall, 35.4% compared to 60.3% in the reference wall on the ground floor, and 38.1% compared to 62% on the 2nd floor. The average indoor moisture excess, presented in Table 1 in Paper IV, varied between 1.2 g/m^3 and 3.2 g/m^3 between the apartments during this period. The indoor moisture excess was not influenced by the retrofitting since the variation was similar between the apartments in the retrofitted and reference wall, respectively.

The vapor content, v (g/m^3), in the walls was calculated using the measured temperature and RH. In the reference ground floor wall the vapor content was on average 7.2 g/m^3 and in the retrofitted wall 6.9 g/m^3. In the reference wall on the 2nd floor it was on average 8.3 g/m^3 compared to 7.2 g/m^3 in the retrofitted wall. In the reference wall, vapor can be transferred both to the interior and exterior side of the wall, while the exterior vapor transfer is blocked by the vapor barrier and VIP in the retrofitted wall. However, the lower vapor contents in the retrofitted wall indicated a dryer wall after the retrofitting which means the drying capacity is sufficient. This is beneficial from a moisture perspective since the risk for mold growth and dry rot fungi is higher in constructions with high moisture contents.

To evaluate the influence of the thermal bridges created by the VIP laminate and the glass wool strips, the temperature difference between these positions and behind the center-of-panel were calculated. In Table 2 in Paper IV, the resulting temperature differences are presented. It is clear that the temperature was highest behind the center-of-panel in most cases. There was one exception where the temperature in January 2013 behind the VIP-VIP connection on the 2nd floor was higher than behind the center-of-panel position. The temperature was lower behind the glass wool strips, than at the VIP-VIP connection, where the thermal bridge was smaller. The lowest temperature in the retrofitted wall was found at the window frame where there was less insulation.

The temperature at the sensor position in the reference and retrofitted walls can be expressed in a dimensionless form. In the standard SS-EN ISO 10211 this is denoted the temperature factor, f (-), which is here defined as

$$f = \frac{T_{indoor} - T_{sensor}}{T_{indoor} - T_{outdoor}} \text{ (-)} \tag{4.1}$$

where T_{indoor} (°C) is the indoor temperature, T_{sensor} (°C) is the temperature at the sensor position and $T_{outdoor}$ (°C) is the outdoor temperature. The temperature factor is 0 on the interior side and 1 on the exterior side of the wall. The temperature factor for the period between January 2011 and February 2013 is plotted in Figure 4.7.

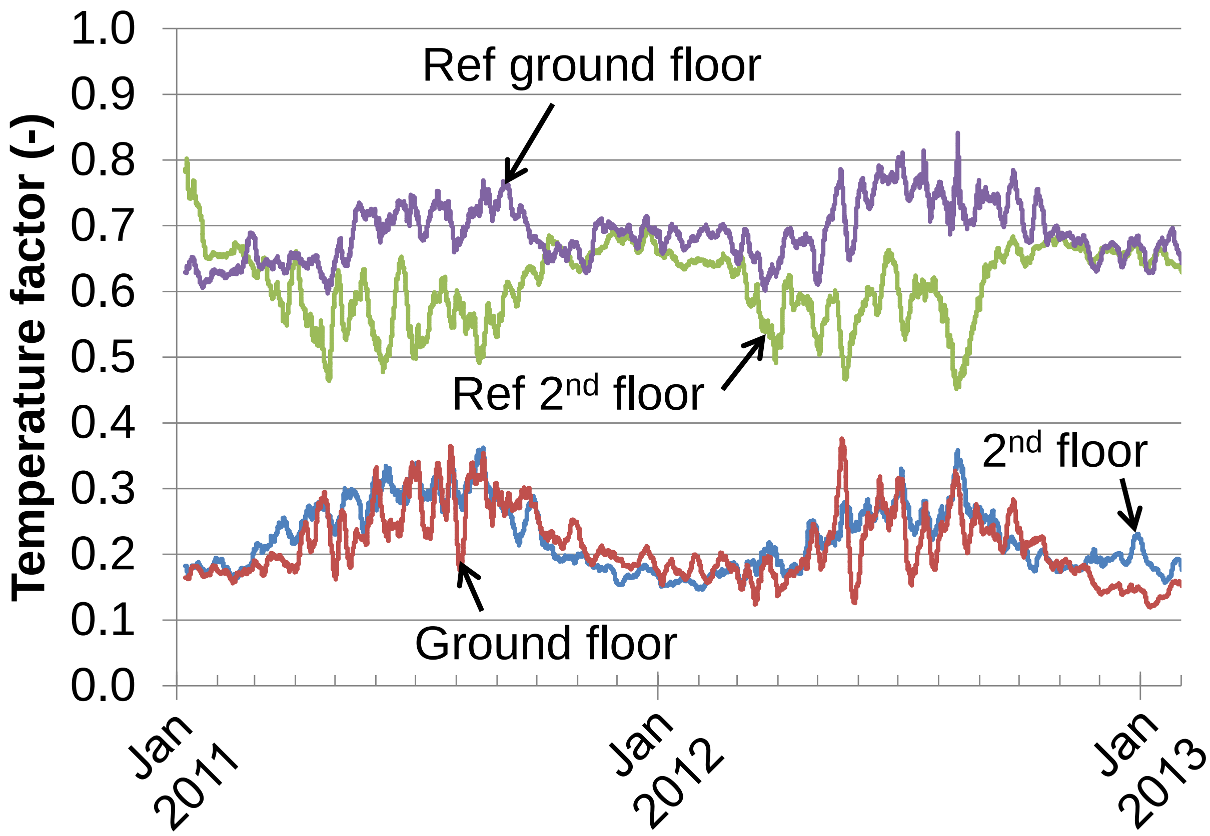

Figure 4.7. Weekly averaged temperature factor over the part of the wall on the interior of the sensor during 2011, 2012 and January 2013.

The temperature factor gives the share of the temperature drop over the part of the wall on the interior of the sensor. The lower the temperature factor is, the higher the thermal insulation on the exterior of the sensor is. It is clear that the thermal resistance of the wall on the exterior of the sensor has been substantially improved after the retrofitting. The average of the temperature factor during January 2011, 2012 and 2013 are presented in Table 3 in Paper IV. Here the temperature factor was called the relative temperature difference. In the reference wall, 63% of the temperature drop was over the non-insulated brick and wooden parts. After the retrofitting only 17% of the temperature drop was over that part of the wall. The tendency was most clear during winter time since the solar radiation during summer sometimes increased the temperature in the wall above the outdoor temperature, giving a negative value for the temperature factor. The same situation was reached when the outdoor temperature exceeded the indoor temperature. The stable temperature factors during the three winters for both the reference and retrofitted walls showed that the thermal performance of the walls were roughly the same during these periods.

In Section 4.5 in Paper IV, the expected temperature factors were calculated based on the standard thermal conductivity for the materials in the wall. The calculations for the reference wall agreed well with the measured temperatures when a higher exterior surface heat transfer resistance was used. The calculated temperature factor in the retrofitted wall agreed well with the measured temperatures. With an effective thermal conductivity of the VIP and glass wool layer of 9-10 mW/(m·K), the measured temperature factor was reached. However, based on the linear thermal transmittances in Table 4.2, the expected effective thermal conductivity was 0.15-0.16 mW/(m·K) while it was 0.13-0.14 mW/(m·K) using the linear thermal transmittance found in the literature. Therefore there are other factors that also influence the thermal performance of the wall.

Hygrothermal numerical simulations of the conditions in the wall after the retrofitting were performed before the final retrofit solution was chosen. The results from this pre-study were presented in Paper III and summarized in the next section.

4.6 Hygrothermal numerical simulations

By adding insulation to an existing wall the temperature field in the wall changes which, with an unchanged moisture load, leads to a changed moisture performance. The risk of damages to the existing wall by the retrofit measure has to be assessed to make sure the hygrothermal conditions in the wall are on the safe side. The steady-state Glaser method can be used to identify possible problems with condensation and high moisture content in materials by one dimensional heat and vapor flows. More advanced methods involving dynamic boundary conditions, capillary suction and vapor diffusion can be used to incorporate the wetting and drying of surfaces to take the buffering capacities of the different materials into account.

The vapor diffusion resistance of a surface can be defined as the thickness of a stagnant air layer with the same vapor resistance. This vapor diffusion thickness is referred to as the s_d-value (m). For instance, the s_d-value for a vapor barrier is 1 000 m and for a plaster board it is around 0.1 m. A way of describing the vapor resistance of a material is by the water vapor diffusion resistance factor, μ (-), which is defined as the ratio between the water vapor diffusion coefficient, δ_v (m^2/s), in stagnant air and in a material. The value is constant for every material and increases with a decreasing vapor diffusion coefficient, i.e. vapor permeable materials (e.g. glass wool) have a lower water vapor diffusion resistance factor compared to less permeable materials (e.g. spruce).

Surfaces are exposed to short- and long-wave radiation where the short-wave radiation is connected to the solar radiation and the long-wave radiation (infrared spectrum) is dependent on the temperature of the surrounding surfaces. The short-wave absorptivity, α (-), is defined by the fraction of solar radiation absorbed by the surface, i.e. the reflected and transmitted parts are subtracted from the total solar radiation hitting the surface. Long-wave radiation exchange is dependent on the emissivity, ε (-), of the surface which is defined as the fraction of heat radiated from the surface compared to a black body. Materials with a high emissivity are e.g. brick and concrete while metals and galvanized materials have a low emissivity.

The surface heat transfer resistance, R_s (m^2K/W), of a surface is due to the combined effect of heat transfer by convection and radiation to and from the surface. Normally the standard values used for the surface heat transfer resistance are R_{si} = 0.13 $m^2 \cdot K/W$ on the interior and R_{se} = 0.04 $m^2 \cdot K/W$ on the exterior. There is also a surface vapor resistance, Z (s/m), dependent on the air layer and convection at the surface. These standard values are 360 s/m and 60 s/m, respectively, for interior and exterior surfaces.

On the interior of the reference and retrofitted wall, a plaster board was covered by wallpapers of unknown thickness. Therefore an interior s_d-value of 0.1 m was added to the standard surface vapor resistance and the interior surface heat transfer resistance was 0.13 $m^2 \cdot K/W$. There was a layer of paint on the exterior of the wooden cover boards which has unknown vapor properties. Therefore the standard value for the surface vapor resistance was added with an s_d-value of 0.3 m. The heat transfer resistance of the exterior surface was considered to be dependent on the wind speed. The solar absorptivity of the exterior surface was 0.3 and the emissivity was 0.94.

Because the façade is exposed to the surrounding climate and located in the dominant wind direction, in this case south west, driving rain hits the virtually unsheltered surface. The air space between the wooden cover board and glass wool boards effectively stop all penetrating water in the numerical simulation model of the retrofitted wall. Although the exposure of the façade means that also wind will have an influence on the hygrothermal performance, the air leakage through the façade was neglected in the numerical simulations. The ventilated air space was treated as a non-ventilated air space, but with a somewhat higher thermal conductivity than stagnant air. This could be modeled as a real ventilated air space in later versions of WUFI 2D (Fraunhofer IBP, 2010), but was not available in the version used in these numerical simulations.

The outdoor climate used in the numerical simulations was the Gothenburg climate supplied with WUFI 2D (Fraunhofer IBP, 2010). In the numerical simulations, the outdoor temperature ranged between -12.2°C and 27.8°C with an average of 8.8°C. The outdoor RH was on average 74.5% and ranged between 19% and 100%. The indoor climate was based on measurements in two apartments in the field study building during June to August 2010. At that time the indoor temperature ranged between 23.7°C and 28.1°C with an average of 26°C. The measured indoor RH ranged between 41.9% and 62.7% with an average of 52.8%. It was observed that the indoor moisture excess was different in the two apartments. Therefore two moisture load scenarios were numerically simulated. One scenario had an indoor moisture excess of 2.3 g/m^3 and the second scenario had an indoor moisture excess of 3.9 g/m^3. In the scenario with the lower indoor moisture excess, the average indoor temperature was 21.1°C and the average RH was 48.8%. The scenario with the higher moisture excess resulted in an average indoor temperature and RH of 22.2°C and 53.3%.

Almost all the material data used in the numerical simulations were derived directly from the WUFI 2D material database (Fraunhofer IBP, 2010). Only the hygrothermal properties of the VIPs were gathered from other sources. The VIPs were modeled as two separate materials where the core was an 18 mm thick panel of fumed silica surrounded by the 1 mm thick VIP laminate. The thermal conductivity of the metalized multi-layered polymer laminate in the direction perpendicular to the laminate was based on the weighted arithmetic mean value of the different layers. In the direction parallel to the laminate it was assumed to have the same thermal conductivity as pure aluminum foil. The properties of the different materials are presented in Table 4.4.

Table 4.4. Material data used in the numerical simulations based on data from WUFI 2D material database (Fraunhofer IBP, 2010) and the values for VIP used by Tenpierik and Cauberg (2007).

Material	*d (mm)*	λ (mW/(m·K))	ρ (kg/m^3)	c_p (J/(kg·K))	μ (-)
Gypsum board	20	200	625	850	8.33
Spruce, tangential	80	140	430	1600	83.3
Spruce, radial	80	90	455	1500	130
Tar paper	1	10 000	909	1500	$2.1 \cdot 10^3$
PE membrane	0.2	1 650	130	2200	$8.7 \cdot 10^4$
Glass wool	-	40	60	850	1.3
Glass wool board	20/30	43	115	850	3.4
Air layer	30	180	1.3	1000	0.46
Evacuated VIP core	18	5	200	850	1.3
Air filled VIP core	18	20	200	850	1.3
VIP laminate, tangential	1	540	189	134	Inf.
VIP laminate, radial	1	200 000	189	134	Inf.

During the work with this thesis it became clear that the model could have been further refined. For instance, the VIP laminate was in reality only 0.1 mm but modeled 10 times thicker since the software did not allow thinner layers. Furthermore, the thermal conductivity of the VIP laminate was modeled by using values which Tenpierik and Cauberg (2007) used in their model of thermal bridges around the VIP perimeter. For instance, Ghazi Wakili *et al.* (2011) have shown that the apparent thermal conductivity of the laminate in fact is much higher, up to 10 000 mW/(m·K). This coincides with own modeling and measurement efforts described in Chapter 3 where a thermal conductivity of the VIP laminate of 2 000 mW/(m·K) was used. However, the effect by the uncertainty of the thermal conductivity of the laminate is small in comparison with other uncertainties, such as the boundary conditions and surface coefficients.

The hygrothermal numerical simulations showed that the RH in the wall was expected to decrease during the first five years that were simulated. In FIG 4 in Paper III, the numerical simulations of the original wall were compared to four retrofit alternatives. For all retrofit alternatives, the RH at the sensor position decreased from the starting value of 70%. The impact by the indoor moisture excess was presented in FIG. 5 in Paper III. It was concluded that the scenario with the higher indoor moisture excess would also lead to a decreasing RH in the wall. Also the risk for mold growth if a moist material would be built into the wall was investigated. It was shown that the moisture was allowed to dry out and after 2 years, the mold growth potential did not exceed 0.8 where values above 1 means there is a risk for mold growth in the construction. If the VIPs would be filled with air, the thermal conductivity would increase fivefold leading to a decreased temperature in the wall. If the moisture conditions are the same, the RH would increase in the wall. The numerical simulations showed that the impact by the air filled VIPs would be small for the both indoor moisture excess scenarios. For the lower indoor moisture excess the RH was around 1 percentage point higher and the difference was even smaller for the scenario with the higher indoor moisture excess (Johansson, 2012). In the next section the numerical simulations are compared to the 2.5 years measurements.

4.7 Measured temperature and relative humidity compared to numerical simulations

The hygrothermal numerical simulations of the wooden wall were compared to the measured temperature and RH in Section 4.6 in Paper IV. It was clear that the measurements deviated significantly from the numerically simulated temperature and RH. In Figure 12 in Paper IV, the measurements for the period January 7, 2011, and April 3, 2013, were compared to the numerical simulations. The numerically simulated temperature and RH at the sensor position in the wall was on average 17.3°C and 73.2% for the high moisture excess scenario and 17.4°C and 69.2% for the low moisture excess scenario while the measured temperature and RH was 21.3°C and 37.8% on average. The measured indoor temperature was 24.4°C which is 2.3-3.4°C higher than what was used in the two numerically simulated scenarios while the measured RH was 37.4% which is 11-15.6 percentage points lower than in the numerical simulations. The measured outdoor solar-air temperature was 9.2°C and the outdoor RH was 75.1% which is 0.7 percentage points higher than the climate in the WUFI 2D database (Fraunhofer IBP, 2010). The resulting measured moisture excess was 1.3 g/m^3, which is half to one third of the levels of moisture excess used in the numerical simulations.

The first step to find the parameters that made the numerical simulations diverge from the measurements was to use the measured indoor and outdoor temperature and RH. When also the initial conditions in the wall was changed to 10°C and 30% RH, the accuracy of the numerical simulation was improved, as shown in Figure 13 in Paper IV. The average simulated temperature and RH at the sensor position in the wall was 19.3°C and 36.9% while the measurements gave 21.5°C and 38.6% on average during 2011 and 2012. It was noted that the vapor content was on average 1.2 g/m^3 higher in the numerical simulations than in the measurements. This suggested that there was an additional drying process in the wall. As described earlier, the sensor was located in an air filled void in the wood, measuring the temperature and RH of the air closest to the sensor. The high fluctuation in the measured RH indicated a leaky construction with air leakage from the interior or exterior side of the vapor barrier into the wood construction. In the real wall, air could enter e.g. through details around windows and be transported along the interior of the vapor barrier to the sensor position. The wall was designed to be as air tight as possible, but it is hard to make every connection and detail perfectly air tight. Therefore, an air exchange with the outdoor air was added to the model between the vapor barrier and wood. The resulting temperature and RH is presented in Figure 14 in Paper IV.

With an increasing air exchange rate of the outdoor air through the wall, the simulated RH fluctuated more and the average RH was closer to the measured RH. However the temperature in the wall still deviated from the measured temperature. One of the remaining uncertainties in the model was the thermal conductivity of the materials in the wall. Therefore the thermal conductivity of the air layer, glass wool and wood were changed to the values in Table 4.5.

Table 4.5. Thermal conductivity used in the numerical simulation model after the revision.

Material	λ (mW/(m·K))
Air layer	25
Glass wool	33
Spruce, tangential	200
Spruce, radial	200

After the thermal conductivities of the materials were changed and an air exchange rate of 40 1/h was used, the simulated average temperature was 21.2°C. This is close to the measured average temperature 21.5°C. The simulated average RH was 38.3% which is close to the measured average RH 38.6%. Also the simulated variations during the year corresponded well with the measurements as shown in Figure 15 in Paper IV. The most important parameter for the RH was the air exchange rate while the thermal conductivity of the materials had larger influence on the temperature in the wall. Other parameters that were not investigated here but could influence the numerical simulation results are the moisture storage functions and water vapor diffusion resistance factors in the WUFI 2D database (Fraunhofer IBP, 2010) which could differ from the real materials. Also small air gaps in the walls could influence the moisture transfer through the wall. A perfect connection is assumed between the materials in the numerical simulation. This is not the case in reality. However, the good agreement between the numerical simulations and measurements shows that it is possible to predict the future hygrothermal performance of the wall which is improved after the retrofitting.

5 Interior insulation of a brick wall in the laboratory

The aim of the laboratory study was to investigate a brick wall with wooden beam ends insulated on the interior with VIPs. For that purpose, a brick wall was built in the laboratory of the Norwegian University of Science and Technology (NTNU) and SINTEF Building and Infrastructure in Trondheim, Norway. A pre-study using hygrothermal numerical simulations was presented in Paper V. Based on the conclusions of the numerical simulations, the wall was built and tested in a large-scale building envelope climate simulator. The results of the laboratory investigation of the wall with and without interior VIPs were presented in Paper V.

5.1 Background and motivation

Brick was commonly used in the construction of buildings from the time before 1960. Thus, brick is today, together with plaster, the most common façade material in multi-family buildings in Sweden. Around 40 million m^2 façade area are covered with brick and plaster, respectively (Boverket, 2009). It is not known how many of these buildings that have load-bearing brick masonry walls. However, a large part of these buildings have walls with a low thermal resistance compared to current standards and requirements. This leads to a large energy use for heating of these buildings compared to newer ones. A factor that makes it difficult to perform energy retrofitting measures in many of these buildings, particularly in buildings from the late 1800s to early 1900s, is that they have listed façades. Two examples of listed buildings are presented in Figure 5.1. These buildings are listed because of their special exterior expression and values added to the city scape. Therefore, the exterior appearance should not be changed. If the walls are to be retrofitted, interior insulation is the only adequate solution. This leads to a reduced rentable internal floor area in the building, due to the thicker walls, which limits the achievable energy use reduction. Using VIPs, the thermal resistance can be improved heavily without reducing the internal floor area as much as when using conventional insulation materials. Therefore it could be more appropriate to use VIPs when retrofitting the building envelope of listed buildings.

Figure 5.1. Left and middle: Brick buildings in Torpa in Gothenburg, built in 1948. The area is listed as an area of national interest (Photo: Angela Sasic Kalagasidis). Right: Lyckholms brewery in Gothenburg built in the late 1880s. This building is listed for its characteristic exterior expression.

Buildings in Gothenburg, situated on the west coast of Sweden, are exposed to large amounts of driving rain. The water that is sucked into the buildings with brick façades does, in some cases, not have time to dry out before a new rain event occurs. In winter, freeze-thaw action in the surface of the brick leads to cracks and damages in the brick and mortar which increases the water flow even more. This was noted e.g. in the residential area Torpa in Gothenburg, where the upper part of many brick façades has been covered by corrugated steel for protection (Danielsson *et al.*, 2013).

In buildings from around the 1900s, wooden beams were used to carry the intermediate floors. When interior insulation has been added to the wall, the temperature in the wall decreases and consequently the relative humidity (RH) increases. This is expected to lead to an increased RH in the wooden beam ends. With increasing RH, the risk for moisture damages by mold growth and dry rot fungi increases. The consequences could be an unhealthy indoor environment and in worst case structural failure. Straube *et al.* (2012) concluded that rain and water leakage issues have to be addressed properly when a brick building is insulated on the interior. They also found that the wooden beam ends were exposed to higher moisture contents after the retrofitting which increases the risk of damages. If the wall was already before the retrofitting exposed to moist conditions, the lower temperature caused by the interior insulation led to a slower drying of the wall. Künzel (1998) showed that to make a successful interior insulation of brick walls, rain protection measures are needed. Otherwise the risk for moisture induced damages increases after the retrofitting.

In this study, hygrothermal numerical simulations were used to design a full-scale laboratory experiment where a brick wall, insulated on the interior with VIPs, was exposed to driving rain and a temperature gradient. The moisture content in the brick and wooden beam ends in the wall was measured and evaluated. The aim was to investigate the influence by the interior VIPs on the risk for moisture damages in the brick and wooden beam ends.

5.2 Design of a laboratory study based on hygrothermal numerical simulations

The hygrothermal numerical simulations were presented in Paper V. The one- and two-dimensional numerical simulations were performed in WUFI 2D (Fraunhofer IBP, 2010). The same approach as described in Section 4.6, for the field study building, was used in these numerical simulations. The climate in Gothenburg and Bergen, Norway, were compared by simulating the hygrothermal performance of a brick wall on these respective locations. It was found that the climate in Bergen increased the RH and moisture content in the wall more than the climate in Gothenburg did, see Figure 4 in Paper V. In case the wall was unprotected from driving rain, the moisture content in the middle of the wall would be very high, also in the brick wall without interior insulation. However, it is expected that the lower temperature in the wall after the retrofitting increases the moisture content even further.

The thickness of the homogenous brick walls considered as reference for this study is commonly around 380 mm. The thickness of the wall built in the laboratory is limited by the weight that could be lifted by a crane, and the time for wetting and drying of the wall. A climate sequence with driving rain, solar radiation and varying temperature was defined based on the real climate in Gothenburg and the HAMSTAD benchmark project (Hagentoft *et al.*, 2004). The climate sequence used in the numerical simulations is presented in Figure 5 in Paper V. From the numerical simulations it was concluded that the wall thickness could be reduced to 250 mm. This reduction made it more practical to construct the wall, as the weight and curing time could be reduced, and thus, the time required for the experiments could be reduced. Meanwhile, the same conclusions could be made with the thinner wall since the same water inflows were registered in the numerical simulations.

The moisture content in the wall is highly influenced by the hygrothermal properties of the brick and mortar. The modern brick types are formed by dry-pressing, molding or extruding the clay to form the wanted size and shape (Brick Industry Association, 2006), giving other properties to the bricks than what manual production methods that were used in the late 1800s to the early 1900s did. Therefore, a brick with similar properties as the ones used in Sweden and Norway during that time should be used in the laboratory experiment. This means a brick which is highly capillary active with a high liquid transport coefficient and a high moisture buffering capacity. In the numerical simulations, two main groups of bricks were investigated where “hand-formed brick” and “historical brick” had similar properties while “masonry brick” and “extruded brick” had similar properties. In this part of the study, the position 60 mm from the interior surface of the brick was chosen as the monitoring position. The time before the walls were saturated with moisture at this position differed with a factor of 6 between the least and most permeable bricks which shows the importance of selecting the type of brick with the desired properties.

In the early 1900s, hydraulic lime mortar was used in masonry buildings. While appreciated for its large tolerance to movements caused by temperature and moisture fluctuations, one of the disadvantages is the longer curing time required compared to mixtures of lime and cement mortar. In the laboratory study, one of the limitations is the time for the construction of the wall. Therefore, a mortar with a short curing and adhesion time is desired, but with similar hygrothermal properties as the hydraulic lime mortar. The numerical simulations showed that the type of mortar influenced the drying of the wall. The mortar that gave the lowest drying rate was a pure cement mortar while a mixture of lime and cement gave a lower drying rate than a hydraulic lime mortar. The difference between using a lime mortar and a lime cement mortar was not substantial, thus a lime cement mortar could be used in the laboratory experiment.

The influence by the properties of the interior insulation material was also investigated with numerical simulations. The insulation material showed to have a lesser influence on the moisture accumulation rate than the type of brick and mortar had. In the numerical simulations, the rain load was found to be the dominating factor determining the vapor and water transport in the wall. The rain load in the laboratory experiment should be limited so that the effect of the added interior VIPs on the brick wall and wooden beam ends is visible. With a vapor open insulation material, moisture transfer towards the interior side of the wall was possible which lowered the moisture accumulation rate slightly. VIPs on the other hand, are vapor tight which means moisture transfer through the interior wall surface will be prevented. Therefore the climate on the interior side only influences the moisture content on places where the VIPs could not be used, such as around the wooden beams, at the intermediate floor to wall attachment, and at the inner wall to exterior wall attachment.

5.3 Results from laboratory measurements

Based on the results of the numerical simulations, brick and mortar was selected and a 250 mm homogenous brick wall was built in the laboratory. Four wooden beam ends (spruce) were installed in the brick to simulate the connection of the wooden intermediate floor, see Figure 9 in Paper V. The wall was equipped with three different types of moisture sensors: 10 temperature and RH sensors (E+E Elektronik EE060), 8 Sahlén sensors (wood moisture sensors) and 12 resistance moisture meters (pin-type). The sensor positions are shown in Figure 5.2. The RH sensors and the Sahlén sensors were located in the mortar between the bricks. The two types of sensors were used because it was uncertain how well the RH sensors would perform in the high moisture conditions in the wall. The Sahlén sensors measure the weight percentage moisture in a piece of birch around the sensor which makes them resistant to high moisture contents. The resistance moisture meters were made of two insulated (except at the tip) metal pins located 25 mm apart, and installed at three different positions in the wooden beams as shown in Figure 5.2.

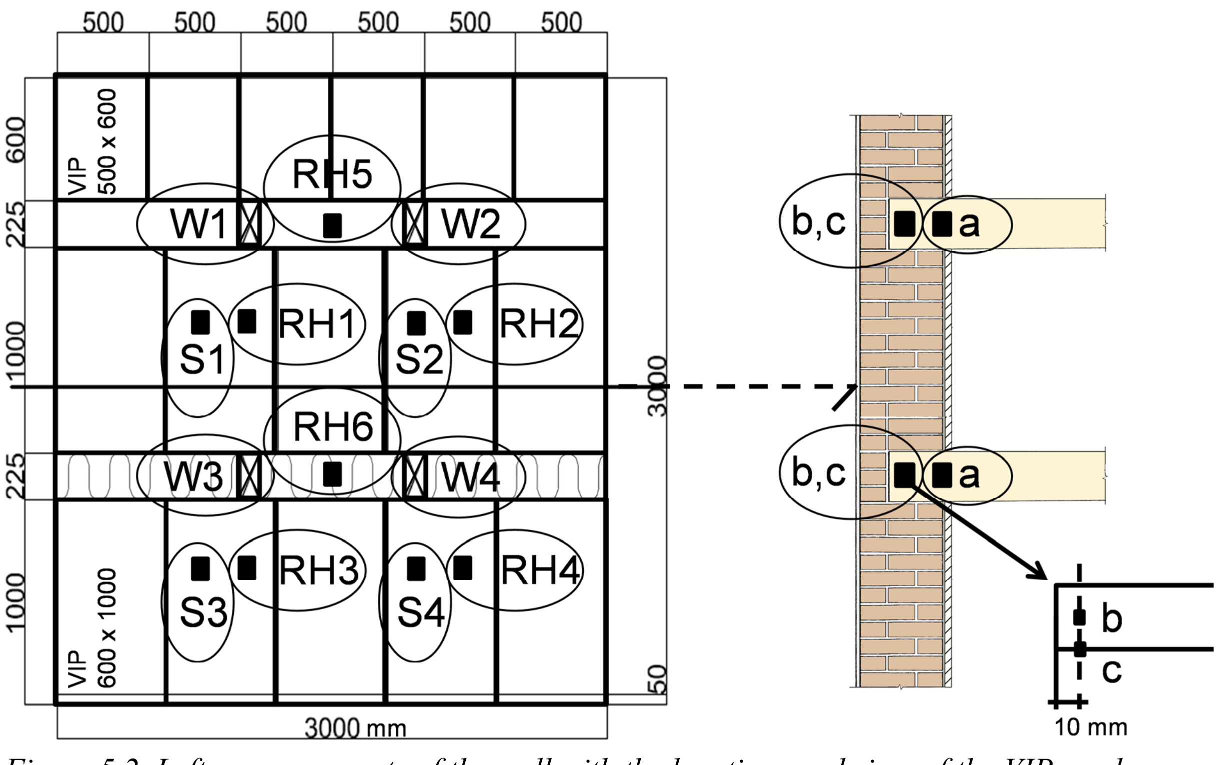

Figure 5.2. Left: measurements of the wall with the locations and sizes of the VIPs and sensor positions. RH = RH sensors, S = Salén sensors and W = resistance moisture meters. A layer of glass wool was located around the two lower wooden beams. The horizontal dashed black line shows the symmetry line of the wall where a rubber strip was installed on the exterior surface of the wall to break the water run-off. Right: the sensor positions in the wooden beams (spruce) at different depths of the wall, indicated by a, b and c. (Figure 10 in Paper V).

The wall was exposed to a climate cycle in the large-scale building envelope climate simulator in the laboratory of NTNU and SINTEF Building and Infrastructure. The climate was constantly 25°C and 40% RH on the interior side and 10°C and 90% RH on the exterior side. The interior surface was covered with VIPs in the first sequence and exposed to the indoor climate during the second. In the beginning of the experiment 2 rain events were applied on the exterior of the wall during the first sequence with interior VIPs and 3 rain events during the second sequence without VIPs. The rain events each lasted for 30 minutes with a 23.5 hour drying period before the next rain event. The rain load was measured to be approximately 5 mm/h, i.e. 5 $dm^3/(m^2 \cdot h)$ during the rain event. This was twice the amount that was assumed in the numerical simulations where a rain event of 2-3 mm/h, i.e. 2-3 $dm^3/(m^2 \cdot h)$, was simulated. Compared to measured rain events in Gothenburg during 2004, the exposure was quite extreme. On exposed façades, the measured average driving rain intensity was 1.9 mm/h, i.e. 1.9 $dm^3/(m^2 \cdot h)$, and the maximum exposure was 7 mm/h, i.e. 7 $dm^3/(m^2 \cdot h)$.

The results of the laboratory measurements of the wall, with and without interior VIPs, were presented and analyzed in Paper V. It was found that the RH in the wall increased substantially when exposed to driving rain. As expected from the numerical simulations, the moisture increased faster in the mortar in the middle of the wall compared to in the mortar on the interior surface of the brick. However, it was also found that the brick and mortar were more capillary active than expected since the moisture content increased more than in the numerical simulations. The lower part of the wall had a higher RH than the upper part of the wall in both the sequence with and without interior VIPs. The difference between the upper and lower part of the wall could be caused by the force of gravity, acting on the liquid water flow. It could also be caused by an uneven rain distribution on the wall surface.

The numerical simulations predicted that the RH increased to 100% after approximately 950 h in the wall without VIPs and after 700 h in the wall with interior VIPs. The measurements showed that, in the upper part of the wall without VIPs, one of the RH sensors was at 100% already after 30 h which is the same as for the wall with VIPs. In the lower part of the wall without VIPs all RH sensors had reached 100% RH after 38 h which is 10 h earlier than in the wall with interior VIPs. Also the Sahlén sensors gave similar results, but with some delay since the birch needs to absorb the moisture before the sensor registers the increasing moisture content. Therefore the time before the sensors in the wall showed 100% RH was longer than for the RH sensors. For the lower part of the wall without interior VIPs the Sahlén sensors reached 100% after 170 h while it took 180 h for the wall with VIPs. Based on the numerical simulations, a proportional relation between the square root of the time of saturation and the thickness of the wall on the exterior of the monitored position was developed. The relation was presented in Section 2.4 in Paper V. With this relation, the time for saturation became 70-130 h in the middle of the wall and 120-320 h on the interior surface of the brick, depending on the type of brick. This is in quite good agreement with the measured RH with the Sahlén sensor, but around twice the time which was measured with the RH sensors.

In the wooden beams, the moisture content increased more in the end of the beam than close to the interior surface of the brick, as was expected. There was no significant difference between the RH in the wooden beam ends in the case with and without VIPs. However, it was found that the temperature effect leads to a higher RH in the wooden beam close to the interior part of the brick and in the center of the beam end. During an experiment prolonged over a longer time period with a more moderate rain load, this difference could be studied more in detail since the beam ends did not reach moisture equilibrium with the surrounding brick and mortar during these investigations.

As could be expected, the temperature was higher both in the middle of the wall and at the interior surface of the brick in the wall without the interior VIPs. The measured temperatures were compared to the calculated steady-state temperature in the wall with good agreement for the wall with interior VIPs. For the wall without VIPs, the temperatures deviated from what was expected. The deviation could be caused by different surface boundary conditions than was assumed in the calculations. For instance, the interior heat transfer coefficient was 22% of the total thermal resistance in the wall without VIPs.

It was difficult to predict all the uncertainties in the laboratory measurements using the hygrothermal numerical simulations. However, the cost of the experiments necessitates good preparations to minimize the number of uncertainties to control the influential parameters. Although the numerical simulation and laboratory measurement results did not converge, much has been learnt on how to plan and conduct these types of large-scale building envelope laboratory studies.

6 Conclusions

Vacuum insulation panels (VIPs) are interesting for application in new and old buildings. However, the VIPs are easily damaged and should be handled with care at the construction site. The exact location and dimensions of each VIP have to be decided in the design phase of the construction project. All surfaces in contact with the VIPs need to be flat and checked for details that could puncture the laminate. In case a VIP is filled with air, the thermal conductivity increases by a factor of five. The rigidity of the panel is changed when it is filled with air and the laminate loosens from the core. Therefore it is easy to detect and separate air filled VIPs from evacuated ones. However, there is a lack of tools to be used to detect VIPs which are partly filled with air. The air space in the wall of the field study building made it impossible to identify the different VIPs by thermography. Only indirect methods, like the evaluation of the measured temperatures in the wall, could be used to investigate the long-term performance of the VIPs. The only way to be certain that the panels in the wall are not filled with air is to take the outer parts down to make the panels accessible for manual checking.

The transient plane heat source (TPS) method could be used to detect VIPs with a thermal conductivity above a limit value. The difference between the measured temperature increase on an evacuated and air filled VIP was 46% after 160s. There was also a low variation among the repeated measurements on the same setup which indicates a good reliability and a great potential of the method. However, the analytical solution showed that there were still some effects that have not yet been fully investigated. The contact heat transfer resistance between the sensor and VIP surface and the impact of the changed ruggedness of the VIP surface when the VIP is filled with air needs more investigations.

The field study showed that exterior insulation of an old exterior wall is an efficient mean to ensure a safe hygrothermal performance of the construction in the future. However, care has to be taken to ensure the wall still has the possibility to dry out in case moisture penetrates the construction. VIPs are not vapor permeable and therefore acts as a vapor barrier which could entrap moisture in the construction on the interior of the VIPs. In this study it was proven that the VIPs did not increase the moisture content in the wall after the retrofitting.

It was demonstrated that the calculated total energy use could be reduced with more than 25% using a continuous 20 mm thick VIP layer on the exterior of the wall. However, with regard to the thermal bridges caused by the laminate around the VIPs and the glass wool between the VIPs in the façade, the reduction became 20%. The thermal bridges stood for between 3-7% of the total energy use. These could have been reduced by e.g. covering the VIPs on both sides with another insulation material.

During the service life of the VIPs, the thermal conductivity increases as the VIPs are filled with air. This leads to an increased energy use for heating of the building which, in the field study building, was 5% which means the reduction is 16% compared to the energy use before retrofitting. In other words, the energy use does not change dramatically if some of the VIPs would be filled with air before the end of service life.

The measured relative humidity (RH) in the wall in the field study building fluctuated more than was expected from the numerical simulations. The higher fluctuations could be explained by adding an air exchange with the outdoor air on the interior of the VIPs to the numerical simulation model. The numerically simulated temperature at the sensor position was not influenced by the air exchange. Thus, to make predictions of the long-term performance of a construction based on hygrothermal simulations, knowledge of the air permeability and air flow paths through the construction is crucial.

The laboratory study of the brick wall was prepared by performing a parametric study using numerical simulations. The numerical simulations showed that the wall could be damaged by freeze-thaw action in the exterior brick surface. The risk was highest for the wall located in Bergen, since the degree of saturation was close to the critical degree of saturation. In Gothenburg, the wall did not reach as high degree of saturation but the number of freeze-thaw cycles was substantially higher.

The numerical simulations showed that the moisture content in the brick wall was highly influenced by the properties of the brick and mortar. The time before the wall was saturated differed with a factor of 6 between the wall with the least and most permeable bricks. The mortar that gave the lowest drying rate was the pure cement mortar while the mixture of lime and cement gave a lower drying rate than pure lime mortar. The properties of the interior insulation material had a lesser influence on the moisture accumulation rate. The rain load was the dominating factor determining the vapor and water transport in the wall. Having the possibility of inward drying decreased the moisture accumulation rate slightly. However, during dry periods with less rain, the VIPs reduce the drying capacity of the wall.

The investigations in the large-scale building envelope climate simulator in the laboratory of the Norwegian University of Science and Technology (NTNU) and SINTEF Building and Infrastructure showed that the RH in the brick wall increased substantially when exposed to driving rain. As expected, the moisture increased faster in the mortar in the middle of the wall compared to on the interior surface of the brick. The brick and mortar were more capillary active than expected from the results of the numerical simulations. The lower part of the wall had a higher RH than the upper part which could be caused by the force of gravity acting on the liquid water flow or a non-uniform rain load on the wall. The different sensors gave consistent laboratory measurement results, although the Sahlén sensor had a slower response to the increasing moisture content in the wall than the RH sensors had.

In the wooden beams, the moisture content increased more in the end of the beam than close to the interior surface of the brick, as was expected. There was no significant difference between the RH in the wooden beam ends in the case with and without VIPs. However, it was found that the temperature effect led to a higher RH in the wooden beam close to the interior surface of the brick and in the center of the beam end with interior VIPs. From these investigations it could not be concluded whether the interior VIPs increased the risk for moisture damages in the wooden beam ends in the wall or not, only that the reduced temperature in the wall increases the RH in the beam ends.

7 Outlook and future research

Preliminary results from the study by (Forsberg and Sørensen, 2012) showed that an acoustic measurement procedure could be developed as a quality assurance method for VIPs. A number of uncertainties regarding the influence by the surrounding materials and boundary conditions have to be investigated further before this procedure can be proposed as a quality assurance method.

It was shown that different studies of the embodied energy of the VIPs reached different results. To conclude the potential impact by using VIPs on the total energy use in the building sector, the embodied energy needs to be further investigated. In the studies available in the literature, different methods and assumptions are used which make comparisons of VIPs with other materials difficult. Also, future production methods of the VIPs could change the energy use in the production phase which leads to a changed embodied energy.

In the exterior wall of the field study building, retrofitted on the exterior with VIPs, it was not possible to detect any damaged VIPs with infrared thermography. However, the temperature measurements showed that the temperature factor at the sensor position in the wall had not changed during the 2.5 years presented here. A continued evaluation of the temperature and relative humidity in the wall is needed to assure that the retrofitting measure has a maintained hygrothermal performance throughout the entire service life of the VIPs. The only way to investigate the long-term performance of the VIPs in the field study building with complete certainty is to expose the VIP surface by removing the wooden cover boards and glass wool boards on the exterior of the VIPs.

In the laboratory, it was shown that the moisture content in the wooden beam ends in a brick wall with interior VIPs increased compared to the case without interior insulation. To protect the beam ends from high moisture contents protective measures are needed. For instance impregnation of the façade on the exterior with a water repellant surface treatment could reduce the moisture content. Another solution could be to use a local heat source around the beam ends. This measure increases the temperature locally and could thereby reduce the risk for moisture damages in the beam ends. These measures should be studied further in the laboratory and by field studies to ensure that the risk for moisture damages are minimized after the interior insulation is added to the wall.

8 References

Alam, M., Singh, H., and Limbachiya, M. C. (2011). Vacuum Insulation Panels (VIPs) for building construction industry - A review of the contemporary developments and future directions. *Applied Energy, 88*(11), 3592–3602.

Baetens, R., Jelle, B. P., and Gustavsen, A. (2011). Aerogel insulation for building applications: A state-of-the-art review. *Energy and Buildings, 43*(4), 761-769.

Baetens, R., Jelle, B. P., Thue, J. V., Tenpierik, M. J., Grynning, S., Uvsløkk, S., and Gustavsen, A. (2010). Vacuum insulation panels for building applications: A review and beyond. *Energy and Buildings*, *42*(2), 147-172.

Balard, H., Donnet, J. B., Oulanti, H., Gottschalk-Gaudig, T., and Barthel, H. (2011). Study of aging of pyrogenic silicas by gravimetry and microcalorimetry. *Colloids and Surfaces A: Physicochemical and Engineering Aspects, 378*(1–3), 38-43.

BASF. (2011). Neopor Wall Insulation. Ludwigshafen, Germany: BASF SE.

Binz, A., Moosmann, A., Steinke, G., Schonhardt, U., Fregnan, F., Simmler, H., Brunner, S., Ghazi, K., Bundi, R., Heinemann, U., Schwab, H., Cauberg, J. J. M., Tenpierik, M. J., Jóhannesson, G. A., Thorsell, T. I., Erb, M., and Nussbaumer, B. (2005). *Vacuum Insulation in the Building Sector. Systems and Applications (Subtask B)*: IEA/ECBCS Annex 39 High Performance Thermal Insulation (HiPTI).

Binz, A. and Steinke, G. (2006). Fassadendämmung mit Vakuum (Facade insulation with vacuum). [In German]. *applica, 113*(6), 22-30.

Blocon. (2000). HEAT2. A PC-program for heat transfer in two dimensions. Manual with brief theory and examples.

Boverket. (2009). *Så mår våra hus - redovisning av regeringsuppdrag beträffande byggnaders tekniska utformning m.m. (The state of our buildings - report of governmental mission on the technical design of buildings etc.).* [In Swedish]. Karlskrona, Sweden: Boverket. Retrieved from: http://www.boverket.se.

Boverket. (2010). *Energi i bebyggelsen - tekniska egenskaper och beräkningar - resultat från projektet BETSI (Energy in the built environment - technical properties and calculations - results from the BETSI study).* [In Swedish]. Karlskrona, Sweden: Boverket. Retrieved from: http://www.boverket.se.

Boverket. (2011). *Regelsamling för byggande, BBR 2012 (Regulations for construction, BBR 2012).* [In Swedish]. Karlskrona, Sweden: Boverket. Retrieved from: http://www.boverket.se.

Brick Industry Association. (2006). *Manufactoring of Brick*. Reston, Virginia, USA: The Brick Industry Association.

Brodt, K. H. (1995). *Thermal insulation: CFC-alternatives and vacuum insulation.* (Dissertation). Delft, The Netherlands: Delft University of Technology, Faculty of Applied Physics.

Brunner, S. (2013). Discussions on the long-term durability prediction of VIP. (E-mail correspondence, June 2013 and November 2013). Dübendorf, Switzerland: Empa, Swiss Federal Laboratories for Materials Science and Technology.

Brunner, S. and Ghazi Wakili, K. (2014). Hints for an additional aging factor regarding the thermal performance of vacuum insulation panels with pyrogenic silica core. *Vacuum, 100*(0), 4-6.

Brunner, S. and Simmler, H. (2008). In situ performance assessment of vacuum insulation panels in a flat roof construction. *Vacuum, 82*(7), 700-707.

Brunner, S., Stahl, T., and Ghazi Wakili, K. (2012a). An example of deteriorated vacuum insulation panels in a building façade. *Energy and Buildings, 54*(0), 278-282.

Brunner, S., Stahl, T., and Ghazi Wakili, K. (2012b). Single and double layered vacuum insulation panels of same thickness in comparison. *Proceedings of the Building Enclosure Science & Technology Conference, BEST 3: High Performance Buildings - Combining Field Experience with Innovation*, April 2-4, 2012, Atlanta, GA, USA.

Brunner, S., Tharian, P. J., Simmler, H., and Ghazi Wakili, K. (2008). Focused ion beam (FIB) etching to investigate aluminium-coated polymer laminates subjected to heat and moisture loads. *Surface and Coatings Technology, 202*(24), 6054-6063.

Capener, C.-M., Sandin, K., Molnár, M., and Jönsson, J. (2012). Energy efficient retrofitting of a 1950-ies multi-dwelling block house considering hygrothermal properties – field measurements and simulation. *Proceedings of the 5th International Building Physics Conference*, May 28-31, 2012, Kyoto, Japan.

Caps, R. (2004). *Determination of the Gas Pressure in an Evacuated Thermal Insulating Board (Vacuum Panel) by using a Heat Sink and Test Layer that are Integrated therin.* US Patent 7400999 B2.

Caps, R., Beyrichen, H., Kraus, D., and Weismann, S. (2008). Quality control of vacuum insulation panels: Methods of measuring gas pressure. *Vacuum, 82*(7), 691-699.

Cho, K., Hong, Y., and Seo, J. (2013). Assessment of the economic performance of vacuum insulation panels for housing projects. *Energy and Buildings, 70*(February 2014), 45-51.

Claesson, J. (2012). *Mathematical report: heated disk in contact with insulation material covered by thin highly conductive layer* (Report 2012:11). Gothenburg, Sweden: Chalmers University of Technology, Department of Civil and Environmental Engineering.

Clase, M. (2010). *Inventering och Utvärdering av Högpresterande Isolering SBUF Projekt 12315 (Inventory and Evaluation of High-Performance Insulation).* [In Swedish]. Gothenburg, Sweden: SBUF/FoU Väst. Retrieved from: http://www.sbuf.se.

Dalenbäck, J.-O., Göransson, A., Jagemar, L., Nilsson, A., Olsson, D., and Pettersson, B. (2005). *Åtgärder för ökad energieffektivisering i bebyggelse - Underlagsmaterial till Boverkets regeringsuppdrag beträffande energieffektivisering i byggnader (M2004/4246/Kb) (Measures to increase the energy efficiency in buildings - background report to Boverkets governmental mission concerning energy efficiency in buildings).* [In Swedish]. Gothenburg, Sweden: Chalmers University of Technology, Chalmers EnergiCentrum (CEC). Retrieved from: http://www.boverket.se.

Danielsson, A., Wannerskog, A. S., and Thuvander, L. (2013). *Case Torpa (Report)*. Gothenburg, Sweden: Chalmers University of Technology, Department of Architecture.

Day, K. C. (2003). Risk management of moisture in exterior wall systems. *Proceedings of the 2nd International Building Physics Conference*, September 14-18, 2003, Leuven, Belgium. pp. 535-544.

DIN 4108-10:2008-06 Wärmeschutz und Energie-Einsparung in Gebäuden - Teil 10: Anwendungsbezogene Anforderungen an Wärmedämmstoffe - Werkmäßig hergestellte Wärmedämmstoffe (Thermal insulation and energy economy in buildings - Part 10: Application-related requirements for thermal insulation materials - Factory made products). [In German]. Berlin, Germany: Beuth-Verlag.

DIN-EN 13501-1:2010-01 Klassifizierung von Bauprodukten und Bauarten zu ihrem Brandverhalten - Teil 1: Klassifizierung mit den Ergebnissen aus den Prüfungen zum Brandverhalten von Bauprodukten (Fire classification of construction products and building elements - Part 1: Classification using test data from reaction to fire tests). [In German]. Brussels, Belgium: European Committee for Standardization (CEN).

Dreyer, J. and Korjenic, A. (2005). Investigation of the hygrical-thermal suitability of vacuum insulation boards for refurbishing of Viennese “Gründerzeit”-buildings. *Proceedings of the 7th International Vacuum Insulation Symposium*, September 28-29, 2005, Dübendorf/Zurich, Switzerland. pp. 139-144.

EcoTherm. (2010). Eco-Cavity COSHH Hazard Datasheet. Basildon, UK: EcoTherm® Insulation (UK) Ltd.

Erbenich, G. (2009). How to Identify a High Quality VIP: Methods and Techniques to Guarantee High Quality Production and Application. *Proceedings of the 9th International Vacuum Insulation Symposium*, September 18-19, 2009, London, UK.

Eriksson, E. and Svensson Tengberg, C. (2012). *Praktiska tillämpningar av högpresterande värmeisolering i ombyggnadsprojekt. SBUF Projekt 12455 (Practical applications of high-performance insulation materials in retrofit projects).* [In Swedish]. Göteborg: SBUF/FoU Väst. Retrieved from: http://www.sbuf.se.

European Parliament. (2010). *Directive 2010/31/EU of the European Parliament and of the Council of 19 May 2010 on the Energy Performance of Buildings (recast)*. Strasbourg, France: European Parliament. Retrieved from: http://eur-lex.europa.eu.

Forsberg, J. and Sørensen, R. (2012). *VIP-paneler och högeffektiva isoleringsmaterial - Analys och mätningar av Vakuumisoleringspaneler (VIP-panels and high-efficient insulation materials - Analysis and measurements on vacuum insulation panels).* [In Swedish]. (Bachelor's thesis 2012:122). Gothenburg, Sweden: Chalmers University of Technology, Department of Civil and Environmental Engineering.

Fraunhofer IBP. (2010). WUFI 2D Transient Heat and Moisture Transport Version 3.3.2 (Computer Program). Holzkirchen, Germany: Fraunhofer IBP.

Fricke, J. (1993). Material research for the optimization of thermal insulations. *High Temperatures - High Pressures*, *25*(4), 379-390.

Fricke, J., Heinemann, U., and Ebert, H. P. (2008). Vacuum insulation panels - From research to market. *Vacuum*, *82*(7), 680-690.

Garnier, G., Marouani, S., Yrieix, B., Pompeo, C., Chauvois, M., Flandin, L., and Brechet, Y. (2011). Interest and durability of multilayers: from model films to complex films. *Polymers for Advanced Technologies*, *22*(6), 847-856.

GE Sensing. (2007). Protimeter HygroTrac Remote Wireless Monitoring System: Instruction Manual. Billerica, MA, USA: GE Sensing.

Ghazi Wakili, K., Bundi, R., and Binder, B. (2004). Effective thermal conductivity of vacuum insulation panels. *Building Research and Information*, *32*(4), 293-299.

Ghazi Wakili, K., Stahl, T., and Brunner, S. (2011). Effective thermal conductivity of a staggered double layer of vacuum insulation panels. *Energy and Buildings*, *43*(6), 1241-1246.

Grynning, S., Baetens, R., Jelle, B., Gustavsen, A., Uvsløkk, S., and Meløysund, V. (2009). *Vakuumisolasjonspaneler for bruk i bygninger – Egenskaper, krav og muligheter. Prosjektrapport 31-2009 (Vacuum insulation panels for building applications – Properties, requirements and possibilities).* [In Norwegian]. Oslo, Norway: SINTEF Building and Infrastruture.

Gudmundsson, K. (2009). A Parametric Study of a Metal Sandwich VIP. *Proceedings of the 9th International Vacuum Insulation Symposium*, September 18-19, 2009, London, UK.

Hagentoft, C.-E., Kalagasidis, A. S., Adl-Zarrabi, B., Roels, S., Carmeliet, J., Hens, H., Grunewald, J., Funk, M., Becker, R., Shamir, D., Adan, O., Brocken, H., Kumaran, K., and Djebbar, R. (2004). Assessment Method of Numerical Prediction Models for Combined Heat, Air and Moisture Transfer in Building Components: Benchmarks for

One-dimensional Cases. *Journal of Thermal Envelope and Building Science, 27*(4), 327-352.

Heinemann, U. and Kastner, R. (2010). *VIP-PROVE: Vakuumisolationspaneele - Bewährung in der Baupraxis. Wissenschaftliche Begleitforschung. Schlussbericht Energieoptimiertes Bauen, ViBau Report ZAE 2-1210-11 (2010) (VIP-PROVE: Vacuum insulation panels - Testing in construction practice. Scientific evaluation. Final report energy optimized construction).* [In German]. Würzburg, Germany: Bayerisches Zentrum für Angewandte Energieforschung e.V. ZAE Bayern. Retrieved from: http://www.vip-bau.de.

Häupl, P., Fechner, H., and Petzold, H. (2004). Interior Retrofit of Masonry Wall to Reduce Energy and Eliminate Moisture Damage: Comparison of Modeling and Field Performance. *Proceedings of the Thermal Performance of the Exterior Envelopes of Whole Buildings XI*, December 5-9, 2010, Clearwater Beach, FL, USA.

IEA. (2013). *Policy Pathway: Modernising Building Energy Codes*. Paris, France: OECD/IEA and New York, NY, USA: United Nations Development Programme (UNDP). Retrieved from: http://www.iea.org.

Institut Bauen und Umwelt e.V. (IBU). (n.d.). *IBU Umwelt-Produktdeklarationen (EPDs) (IBU Environmental Product Declarations).* [In German]. Berlin, Germany: Institut Bauen und Umwelt e.V. (IBU) [Accessed September 12, 2013] Available at: http://bau-umwelt.de/hp6253/EPDs.htm.

IVA. (2012). *Energieffektivisering av Sveriges flerbostadshus: Hinder och möjligheter att nå en halverad energianvändning till 2050 (Energy efficiency in the Swedish multi-family building stock: obstacles and possibilities to reach a halved energy use by 2050).* [In Swedish]. Stockholm, Sweden: Kungl. Ingenjörsvetenskapsakademien (IVA). Retrieved from: http://www.iva.se.

Johansson, H. (2011). *Tilläggsisolering av tegelfasader på flerbostadshus från 1940- till 1960-talet (Brick facade refurbishments of buildings from the 1940s to 1960s).* [In Swedish]. (Bachelor's thesis). Luleå, Sweden: Luleå University of Technology, Department of Civil, Environmental and Natural resources engineering.

Johansson, P. (2012). *Retrofitting of old Exterior Wall with Vacuum Insulation Panels: Meaurements of Thermal Properties, Moisture Performance and Practical Considerations*. (Licentiate thesis 2012:2). Gothenburg, Sweden: Chalmers University of Technology, Department of Civil and Environmental Engineering.

Kubina, L. (2010). Etics with Integrated Vacuum Insulation Panels. *Proceedings of the International Conference Central Europe towards Sustainable Building CESB*, June 30-July 2, 2010, Prague, Czech Republic.

Künzel, H. (1998). Effect of interior and exterior insulation on the hygrothermal behaviour of exposed walls. *Materials and Structures, 31*(2), 99-103.

Larsson, U. (1973). *Landshövdingehusen i Göteborg: en studie i klassbosättning (County governor's houses in Gothenburg: a study in the class settlement).* [In Swedish]. (Dissertation). Gothenburg, Sweden: Chalmers Tekniska Högskola, Sektionen för Arkitektur.

Larsson, U. and Lönnroth, G. (1972). Landshövdingehus och trähus i Göteborg (County governor's houses and wooden houses in Gothenburg). [In Swedish]. *Den nordiske træstad*(28).

Lu, X., Arduini-Schuster, M. C., Kuhn, J., Nilsson, O., Fricke, J., and Pekala, R. W. (1992). Thermal Conductivity of Monolithic Organic Aerogels. *Science, 255*(5047), 971-972.

Mata, É., Sasic Kalagasidis, A., and Johnsson, F. (2013). A modelling strategy for energy, carbon, and cost assessments of building stocks. *Energy and Buildings, 56*(January 2013), 100-108.

MathWorks. (2011). MATLAB Version R2011b. Natick, MA, USA: The MathWorks, Inc.

Microtherm. (2009). SlimVac Safety Data Sheet. Sint-Niklaas, Belgium: Microtherm N V.

Molander, C. and Olofsson, M. (2012). *Methods and Potentials to Reduce Peaks in Heating Power Demand - in Residential Building*. (Master's thesis 2012:105). Gothenburg, Sweden: Chalmers University of Technology, Department of Civil and Environmental Engineering.

Morel, B., Autissier, L., Autissier, D., Lemordant, D., Yrieix, B., and Quenard, D. (2009). Pyrogenic silica ageing under humid atmosphere. *Powder Technology, 190*(1-2), 225-229.

Morelli, M., Rønby, L., Mikkelsen, S. E., Minzari, M. G., Kildemoes, T., and Tommerup, H. M. (2012). Energy retrofitting of a typical old Danish multi-family building to a “nearly-zero” energy building based on experiences from a test apartment. *Energy and Buildings, 54*(0), 395-406.

Naturvårdsverket. (2013, 2013-03-21). *Miljömål, God bebyggd miljö, q-märkt (Environmental Objectives, A Good Built Environment, q mark).* [In Swedish]. [Accessed June 28, 2013] Available at: http://www.miljomal.nu.

Nilsson, T. (2009). *Energideklaration för Kungsladugård 35:12, Göteborg (Energy certificate for Kungsladugård 35:12, Gothenburg).* [In Swedish]. Gothenburg, Sweden: Agera VVS-Design AB.

Näringsdepartementet. (2012). *Regeringens skrivelse 2011/12:131. Vägen till nära-nollenergibyggnader (Government missive 2011/12:131. The route towards nearly zero-energy buildings).* [In Swedish]. Stockholm, Sweden: Regeringskansliet. Retrieved from: http://www.regeringen.se.

Porextherm. (2009). Vacupor NT-B2 Version 1.01 / 12-22-09. Kempten, Germany: Porextherm Dämmstoff GmbH.

Pramsten, E. and Hedlund, M. (2009). *Ekonomisk analys av vakuumisoleringspaneler i ytterväggar (Economical analysis of vacuum insulation panels in exterior walls).* [In Swedish]. (Master's thesis 388). Stockholm, Sweden: Royal Institute of Technology, Department of Civil and Architectural Engineering.

Rasmussen, T. V. (2011). Retrofitting Listed Buildings: Measures, Savings and Requirements. *The Open Construction and Building Technology Journal, 5*, 174-181.

Schaffrath, J., Henke, K., and Winter, S. (2010). Vorfertigung für das Bauen im Bestand am Beispiel maßgefertigter Vakuum-Dämmelemente (Prefabrication in reference to existing buildings using the example of tailor-made vacuum insulations panels). [In German]. *Bauingenieur, 85*(12), 505-512.

Schonhardt, U., Binz, A., Wohler, M., and Dott, R. (2003). *Ökobilanz eines Vakuum-Isolations-Paneels (VIP) (Life cycle assessment of a vacuum insulation panel (VIP)).* [In German]. Muttenz, Switzerland: Fachhochschule beider Basel, Institut für Energie.

Schwab, H., Stark, C., Wachtel, J., Ebert, H.-P., and Fricke, J. (2005). Thermal Bridges in Vacuum-insulated Building Façades. *Journal of Thermal Envelope & Building Science, 28*(4), 345-355.

Simmler, H. and Brunner, S. (2005). Vacuum insulation panels for building application: Basic properties, aging mechanisms and service life. *Energy and Buildings, 37*(11 SPEC. ISS.), 1122-1131.

Simmler, H., Brunner, S., Heinemann, U., Schwab, H., Kumaran, K., Mukhopadhyaya, P., Quénard, D., Sallée, H., Noller, K., Kücükpinar-Niarchos, E., Stramm, C., Tenpierik, M. J., Cauberg, J. J. M., and Erb, M. (2005). *Vacuum Insulation Panels. Study on VIP-components and Panels for Service Life Prediction of VIP in Building Applications (Subtask A)*: IEA/ECBCS Annex 39 High Performance Thermal Insulation (HiPTI).

Sprengard, C. and Spitzner, M. H. (2011). Untersuchungen zu Alterung und Wärmebrücken bei Vakuum-Isolations-Paneelen (VIP) für Bauanwendungen (Investigations into Ageing and Thermal Bridging in Vacuum Insulation Panels (VIP) for Construction Applications). [In German]. *Bauphysik, 33*(4), 234-242.

Straube, J., Ueno, K., and Schumacher, C. (2012). *Internal Insulation of Masonry Walls: Final Measure Guideline*. Somerville, MA, USA: Prepared for U.S. Department of Energy, Office of Energy Efficiency and Renewable Energy.

SS-EN 13165:2012. Thermal insulation products for buildings. Factory made rigid polyurethane foam (PU) products. Specification. Brussels, Belgium: European Committee for Standardization (CEN).

SS-EN ISO 10211:2007. Thermal bridges in buildings construction - Heat flow and surface temperatures - Detailed calculations. Geneva, Switzerland: International Organization for Standardization (ISO).

SS-EN ISO 12572:2001. Hygrothermal performance of building materials and products - Determination of water vapour transmission properties. Geneva, Switzerland: International Organization for Standardization (ISO).

SS-EN ISO 22007-2:2008. Plastics - Determination of thermal conductivity and thermal diffusivity - Part 2: Transient plane heat source (hot disc) method. Geneva, Switzerland: International Organization for Standardization (ISO).

Tenpierik, M. and Cauberg, H. (2007). Analytical models for calculating thermal bridge effects caused by thin high barrier envelopes around vacuum insulation panels. *Journal of Building Physics*, *30*(3), 185-215.

Tenpierik, M. J., Cauberg, J. J. M., and Thorsell, T. I. (2007). Integrating vacuum insulation panels in building constructions: an integral perspective. *Construction Innovation, 7*(1), 38-53.

Thorsell, T. I. (2006). Edge loss minimization in vacuum insulation panels. *Research in Building Physics and Building Engineering*, 251-256.

Tillotson, T. M. and Hrubesh, L. W. (1992). Transparent ultralow-density silica aerogels prepared by a two-step sol-gel process. *Journal of Non-Crystalline Solids, 145*(0), 44-50.

Weller, B., Rexroth, S., and Jakubetz, S. (2008). *Denkmal und Energie - Technologien und Systeminnovationen zur Energieversorgung und -einsparung bei Baudenkmalen (Monuments and energy - Technologies and system innovations for energy supply and conservation in historical buildings).* [In German]. Dresden, Germany: Technische Universität Dresden, Institut für Baukonstruktion.

Viridén, K. (2007). Retrofit Buildings close to Passive House Standard. *Proceedings of the International Conference Central Europe towards Sustainable Building CESB*, September 24-26, 2007, Prague, Czech Republic. pp. 411-415.

Viridén, K., Ammann, T., and Büsser, A. (2004). *Herausforderung Gebäudehülle bei Passivhäusern im Umbau Erfahrungen aus realisierten P+D-Projekten*. Paper presented at the 13. Schweizerisches Status-Seminar 2004 "Energie- und Umweltforschung im Bauwesen".

Zwerger, M. and Klein, H. (2005). Integration of VIP's into external wall insulation systems. *Proceedings of the 7th International Vacuum Insulation Symposium*, September 28-29, 2005, Duebendorf/Zurich, Switzerland. pp. 173-179.